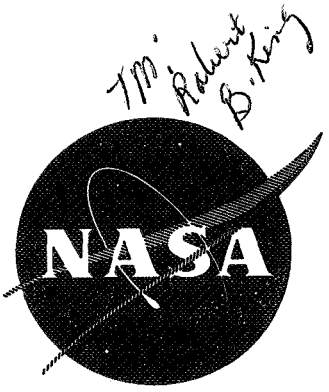

STUDY OF FUEL CELLS USING STORABLE ROCKET PROPELLANTS

by

Roger F. Drake
et al.

MONSANTO RESEARCH CORPORATION

prepared for

NATIONAL AERONAUTICS AND SPACE ADMINISTRATION

NASA Lewis Research Center

Contract NAS3-6476

Robert B. King, Technical Manager

NOTICE

This report was prepared as an account of Government-sponsored work. Neither the United States, nor the National Aeronautics and Space Administration (NASA), nor any person acting on behalf of NASA:

A.) Makes any warranty or representation, expressed or implied, with respect to the accuracy, completeness, or usefulness of the information contained in this report, or that the use of any information, apparatus, method, or process disclosed in this report may not infringe privately-owned rights; or

B.) Assumes any liabilities with respect to the use of, or for damages resulting from the use of, any information, apparatus, method or process disclosed in this report.

As used above, "person acting on behalf of NASA" includes any employee or contractor of NASA, or employee of such contractor, to the extent that such employee or contractor of NASA or employee of such contractor prepares, disseminates, or provides access to any information pursuant to his employment or contract with NASA, or his employment with such contractor.

Requests for copies of this report should be referred to

National Aeronautics and Space Administration
Scientific and Technical Information Facility
P.O. Box 33
College Park, Md. 20740

MRB5009F

FINAL REPORT

STUDY OF FUEL CELLS USING STORABLE ROCKET PROPELLANTS

18 August 1965 - 23 June 1969

Prepared for

NATIONAL AERONAUTICS AND SPACE ADMINISTRATION

February 1970

CONTRACT NAS3-6476

R. F. Drake, Project Leader

C. N. Satterfield, Consultant

J. O. Smith	B. M. Fabuss
J. C. Orth	C. H. Lu
L. F. Athearn	S. Messinger
R. E. Chute	W. R. Smith
M. C. Deibert	P. L. Terry

MONSANTO RESEARCH CORPORATION

Technical Management
NASA Lewis Research Center
Cleveland, Ohio
Space Power Systems Division
Robert B. King, Technical Manager

TABLE OF CONTENTS

TABLE OF CONTENTS (cont'd -2)

TABLE OF CONTENTS (cont'd -3)

TABLE OF CONTENTS (cont'd - 4)

LIST OF FIGURES

LIST OF FIGURES (cont'd -2)

LIST OF TABLES

LIST OF TABLES (cont'd -2)

LIST OF TABLES (cont'd -3)

I. SUMMARY

This report describes work done in the third stage of an investigation, the objective of which was to develop a capability for fuel cell operation on storable rocket propellents. The system is attractive because of the excellent long-term storage properties of the reactants as well as the possibility of utilizing propellent tank residuals to produce electric power on space missions.

Work has been completed on four major tasks in this program.

The objective of the first task is to produce a hydrogen-rich fuel cell feed stream in a simple catalytic flow reactor from Aerozine-50 (50 wt % N_2H_4, 50 wt % UDMH*). Five systems representing tradeoffs in simplicity, operating temperatures, and hydrogen production efficiencies were investigated. Based on the results of these tests, three systems were chosen for long-term testing: (1) a low temperature (30-50°C), liquid phase decomposer, (2) an intermediate temperature steam reformer (300-500°C) and (3) a high temperature (700-800°C) steam reformer with a CO shift reactor.

The results with the liquid phase reactor were not promising because of the low efficiency experienced even with the best catalysts tested. A feasible system for this application may depend upon a periodic regeneration of the catalyst (e.g., a periodic flush with H_2O), and the development of a physically stronger catalyst.

The intermediate temperature steam reformer was promising on initial tests; the best hydrogen efficiencies were about 30%. However, the performance dropped sharply on long-term tests because of carbon deposition on the catalyst; hydrogen efficiency was about 11% after 1000 hours.

We have demonstrated a combined steam reforming CO shift reactor system that produced (for over 1000 hours) with high efficiency (~95%) a fuel cell gas feed stream composed of 70 mole % H_2, 18 mole % N_2, 12 mole % CO_2 (after separation of the excess H_2O). The CO content of the stream was 0.3 mole % or less.

---

*UMDH: unsymmetrical dimethylhydrazine

In addition, a Pd membrane purification unit that supplies ultrapure H_2 from the reformer stream at 90% efficiency has been demonstrated.

The objective of the second task was to decompose N_2O_4 to an oxygen-rich feed stream for a fuel cell in a simple catalytic flow reactor. An extensive catalyst screening program failed to produce any catalysts that decomposed N_2O_4 at substantial rates below 800°C.

Four promising catalysts were tested for 13 days at 800-850°C, and only 2% Pt-on-alumina performed satisfactorily. Utilizing this catalyst, an N_2O_4 decomposer was developed that will convert 80-85% of input N_2O_4 to a gas stream consisting of a 2:1 mole ratio of oxygen to nitrogen for over 1000 hours. The output was contaiminated with unreacted N_2O_4, and the kinetic data indicated a prohibitive catalyst weight (residence time) would be required to produce 97% conversion (at which percentage simple KOH scrubbing was feasible). Thus, a means for removing the unreacted N_2O_4 is indicated.

The objectives of the third task were to develop electrode structures and techniques that would allow the direct utilization of gaseous N_2O_4 and Aerozine-50 as direct reactants in a fuel cell. A further requirement was that these reactants be used efficiently in a single pass through the electrode chamber of the fuel cell. Finally, the operation of fuel cells on the reformer product streams was to be investigated.

Optimization of the carbon-polytetrafluoroethylene (PTFE) cathode that had been demonstrated previously was investigated by careful design of reactant flow plates, investigation of permeation of N_2O_4 through the matrix, and a catalyst study.

A greatly improved N_2O_4 cathode coulombic efficiency (27%) was obtained primarily as a result of the design of an efficient reactant flow plate. The efficiencies reported here are nearly an order of magnitude better than those reported on our previous contract. The cathode was demonstrated in a 1/3 ft^2 size at practical current densities (100 amp/ft^2).

The same degree of success was not realized with the Aerozine-50 anode despite testing of a variety of catalysts and electrode structures for this service. Those electrodes with satisfactory electrical characteristics invariably also caused excessive self-decomposition of the fuel and/or precipitation of hydrazine phosphates due to mixing of fuel and electrolyte.

A rhodium-catalyzed electrode with a carbon-PTFE permeation barrier operating from pure anhydrous N_2H_4 was successfully demonstrated and could be developed for fuel cell service with an N_2O_4 cathode. A more promising system, however, might be an H_2/N_2O_4 cell with the H_2 supplied by the Aerozine-50 steam reformer. Both anodes operate at about 0.10 to 0.15 V vs SHE at 45°C, 100 mA/cm^2.

Half cells of 1/3 ft^2 size were operated on hydrogen and oxygen. The hydrogen half cell polarized less than 0.10 volt at 90 amp/ft^2 and operated at a coulombic efficiency above 95% on the stream from the Pd membrane diffuser. The oxygen electrode appeared to operate at nearly the same coulombic efficiency. However, it polarized more under load. Operation of the unscrubbed N_2O_4 decomposer stream was attempted, but unstable electrode potentials were found. It is recommended that scrubbing of residual N_2O_4 from this stream be included in system considerations.

The system that was investigated for scrubbing residual N_2O_4 from the decomposer stream consisted of a regenerable, two-column adsorption unit in which one column would desorb to space vacuum while the other was removing N_2O_4 from the stream.

Molecular sieve (13X) was found to be the best adsorbent for this application, with a total adsorption capacity of about 0.26 g N_2O_4/g sieve at 25°C. However, a prototype unit that was constructed using this system could not be operated because of excessively high bed temperatures. In addition, it was found that the as received N_2O_4 contained substantial quantities of H_2O. A purification train was constructed that successfully reduced the H_2O content (from 0.1 to 0.003 H_2O equivalents).

A much more detailed investigation of the sorption characteristics was undertaken utilizing a quartz mass adsorption balance. The results generally confirmed earlier work: the total adsorption capacities were within 30% of those measured under similar conditions in the early work (0.07 to 0.10 g N_2O_4/g sieve for a 200°C desorption) and desorption was found to be the major rate-limiting process. The isotherms were qualitatively similar to the type of adsorption behavior observed with other gases and vapors on molecular sieve.

A calorimetric study indicated that heat effects were quite strong for N_2O_4 adsorption (about 1.1 kcal/g adsorbed N_2O_4).

II. INTRODUCTION

A. BACKGROUND

The work reported here comprises the third stage of an investigation whose objective was to develop a capability for a fuel cell operable storable rocket propellant as primary or secondary reactants.

The initial contract (NAS8-2791) established the feasibility of utilizing storable rocket propellants as fuel cell reactants. Pertinent properties of the propellants were compiled and initial electrochemical testing demonstrated (Ref. 1).

Work on the next contract (NAS3-4175) largely concerned the investigation of a number of possible systems and cell configurations and culminated in the construction and long-term testing of two cell types. One configuration used hydrazine dissolved in potassium hydroxide electrolyte as the fuel and gaseous oxygen as the oxidizer. The other system used hydrazine dissolved in phosphoric acid electrolyte as the fuel and gaseous nitrogen tetroxide as the oxidizer. Both systems were developed to the point where system designs were submitted to NASA specifications (Ref. 2).

The work reported here involved the investigation and development of cells to operate on gaseous nitrogen tetroxide and Aerozine-50 (50 wt-% hydrazine - 50 wt-% unsymmetrical dimethylhydrazine) (UDMH) as direct reactants, and of a reforming capability to use these reactants to produce oxygen- and hydrogen-rich feed streams for fuel cells. The construction and operation of working laboratory reformers and cells were the objectives of this work.

The advantages of operating space fuel cells on storable propellants include the availability of reactants during space missions from propellant tank residuals and the resulting system weight and volume reductions that can be realized because separate tankage is not required. The excellent storage properties of propellants such as nitrogen tetroxide and Aerozine-50 allow an optimum design of equipment for very long mission times that would not be possible with reactants that require cryogenic storage. Because of their relatively high boiling points and low vapor pressure at normal temperatures, these propellants are capable of storage in thin-walled containers with minimal pressurization and insulation for years with virtually no venting losses. In addition, the high energy content and favorable heat effects due to the endothermic nature of some of the reactions involved with these reactants tend to have favorable effects in system designs.

B. SCOPE OF WORK

This report covers work on four major tasks performed during the course of this contract. These are:

(1) Production and purification of a hydrogen feed stream from Aerozine-50

(2) Decomposition of nitrogen tetroxide to produce an oxygen-rich feed stream

(3) Construction and operation of full cells utilizing both direct reactants and reformer product streams

(4) Removal of unreacted nitrogen tetroxide from the nitrogen tetroxide decomposer stream.

The work on Tasks 1 through 3 has been reported in detail in five quarterly reports (Ref. 3). The principal relevant results are presented in this report along with summaries of the experimental programs. The work involved in Task 4 has not been previously reported and is presented here in detail.

III. PRODUCTION AND PURIFICATION OF HYDROGEN FEED STREAM FROM AEROZINE-50

A. BACKGROUND

1. Objectives and Scope of Work

The objective of this task was to produce, in a simple catalytic flow reactor, a hydrogen-rich fuel cell feed stream from a 50 wt-% N_2H_4, 50 wt-% UDMH (Aerozine-50) feed stream at a maximum efficiency and at reasonably low temperatures.

Five systems have been investigated that allow tradeoffs between H_2 efficiency, temperature, simplicity, and the composition of the output stream. These are: (1) low-temperature, liquid-phase catalytic decomposition; (2) intermediate-temperature (450°C) steam reforming; (3) intermediate-temperature steam reforming followed by an NH_3 decomposer; (4) high-temperature (600-800°C) steam reforming; and (5) high-temperature steam reforming with a CO shift reactor. Each system was developed to the point where a determination of its feasibility was possible. Based on these tests three systems were chosen for long-term testing: (1) the low-temperature decomposer, (2) intermediate-temperature steam reforming, and (3) high-temperature steam reforming with CO shift.

In addition, a Pd membrane purification unit was investigated and demonstrated. The unit was designed to supply ultrapure H_2 to a fuel cell from the impure reactor streams.

2. Reactions and Possible System Tradeoffs

On the basis of the available literature, an examination of relative bond strengths, and the chemistry of analogous reactions, the following decomposition routes seemed the most likely:

(a) For N_2H_4:

$$N_2H_4 \longrightarrow N_2 + 2H_2 \qquad (1)$$

$$3N_2H_4 \longrightarrow 4NH_3 + N_2 \qquad (2)$$

Unless further NH_3 decomposition occurs (i.e., at higher temperatures), the competing NH_3 formation reaction can substantially reduce H_2 yields.

(b) For UDMH

$$(CH_3)_2NNH_2 \longrightarrow 2CH_4 + N_2 \quad (3)$$

$$(CH_3)_2NNH_2 \longrightarrow 2C + 2NH_3 + H_2 \quad (4)$$

$$(CH_3)_2NNH_2 \longrightarrow (CH_3)_2NH + 1/3N_2 + 1/3NH_3 \quad (5)$$

$$(CH_3)_2NNH_2 \longrightarrow C_2H_6 + 2/3N_2 + 2/3NH_3 \quad (6)$$

$$(CH_3)_2NNH_2 + 2H_2O \longrightarrow 2CO + 2NH_3 + 3H_2 \quad (7)$$

$$(CH_3)_2NNH_2 + 4H_2O \longrightarrow 2CO_2 + 2NH_3 + 5H_2 \quad (8)$$

$$(CH_3)_2NNH_2 + 4H_2O \longrightarrow 2CO_2 + N_2 + 8H_2 \quad (9)$$

Other reactions of possible significance here are:

$$CO + H_2O \rightleftharpoons CO_2 + H_2 \quad \text{(CO shift)} \quad (10)$$

$$2NH_3 \rightleftharpoons N_2 + 3H_2 \quad (NH_3 \text{ decomposition}) \quad (11)$$

$$CO + 3H_2 \rightleftharpoons CH_4 + H_2O \quad \text{(CO reduction)} \quad (12)$$

$$CO + H_2 \rightleftharpoons C + H_2O \quad \text{(carbon deposition)} \quad (13)$$

$$CO_2 + H_2 \rightleftharpoons CH_4 + 2H_2O \quad \text{(methanation)} \quad (14)$$

Thus a wide variety of reaction paths, products, and H_2 yields are possible depending on catalyst and reactor conditions, feed stock and, most particularly, temperature.

If, however, thermodynamic equilibrium prevails, the equilibrium steam reforming compositions can be calculated utilizing known thermodynamic data. The use of this technique to determine optimum conditions for highest H_2 efficiency is illustrated in Figure 1. Here temperature and amount of H_2O excess (over stoichiometric requirements) in the feed stock were considered to be the most important variables. Details of this analysis are presented in Ref. 3C.

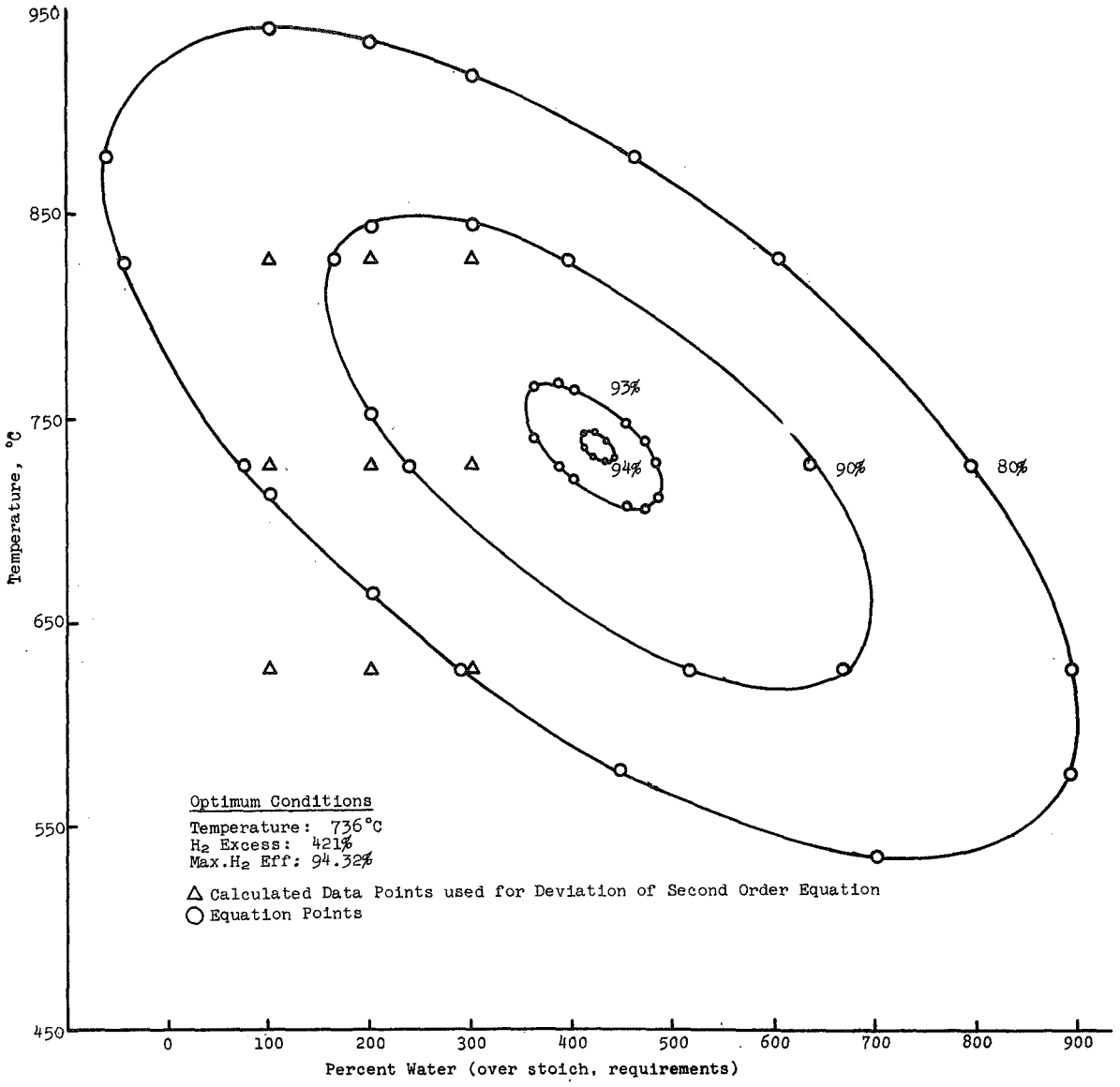

Figure 1. Hydrogen Efficiency Contour Map

B. LOW TEMPERATURE DECOMPOSITION

1. Initial Investigation - Batch Catalyst Screening

Decomposition at atmospheric pressure is potentially the simplest and most straight forward method of producing H_2 from liquid Aerozine-50 in the temperature range 30-50°C. Only the N_2H_4 component of the fuel can make significantly large contributions to H_2 production, and this limits the efficiency to a maximum of 32%.*

Initial catalyst screening for this system was conducted in a batch reactor. Figure 2 shows a schematic diagram of the experimental setup used for most of the tests. A thermostatted water bath was heated by a copper coil heater controlled by Thermistemp temperature regulator (±0.1°C). The reactor flask was a 50-ml round bottomed flask, with a magnetic stirring bar enclosed. An addition funnel was used to add the fuel instantly or in small increments. From the flask a gas exit line vented to a manometer used to check for pressure leaks and to a sulfuric acid scrubber for NH_3 removal. From the scrubber the gas passed through a gas sample calibration tube and then into a wet test meter for volume measurements.

The tests were conducted by adding a known weight and volume of catalyst to the reaction flask. The addition funnel was filled with the fuel to be tested, and the system was purged with N_2 to remove any air. The fuel was added dropwise to ensure safe decomposition rates. When it was obvious that no explosive decompositions would occur, the remainder of the fuel was added and the gas evolution rate measurements were started. The gas sample was analyzed by VPC.

All data on catalysts tested are included in Table I. Two catalysts showed sufficient promise to warrant consideration: (1) a promoted Raney Ni-water slurry, and (2) Rh on various supports. Although the Ni catalyst gave the highest conversion to H_2 (88% compared to 55% for a typical Rh catalyst) the slurry form would be nearly impossible to use in a flow reactor system. The best choice, then, is the Rh catalyst supported on alumina, with which the H_2 efficiency obtained was 17.6% based on the total H_2 content of Aerozine-50, or 55% based on the decomposition of the N_2H_4 component alone.

* All efficiencies reported as percent of maximum possible by reaction (9).

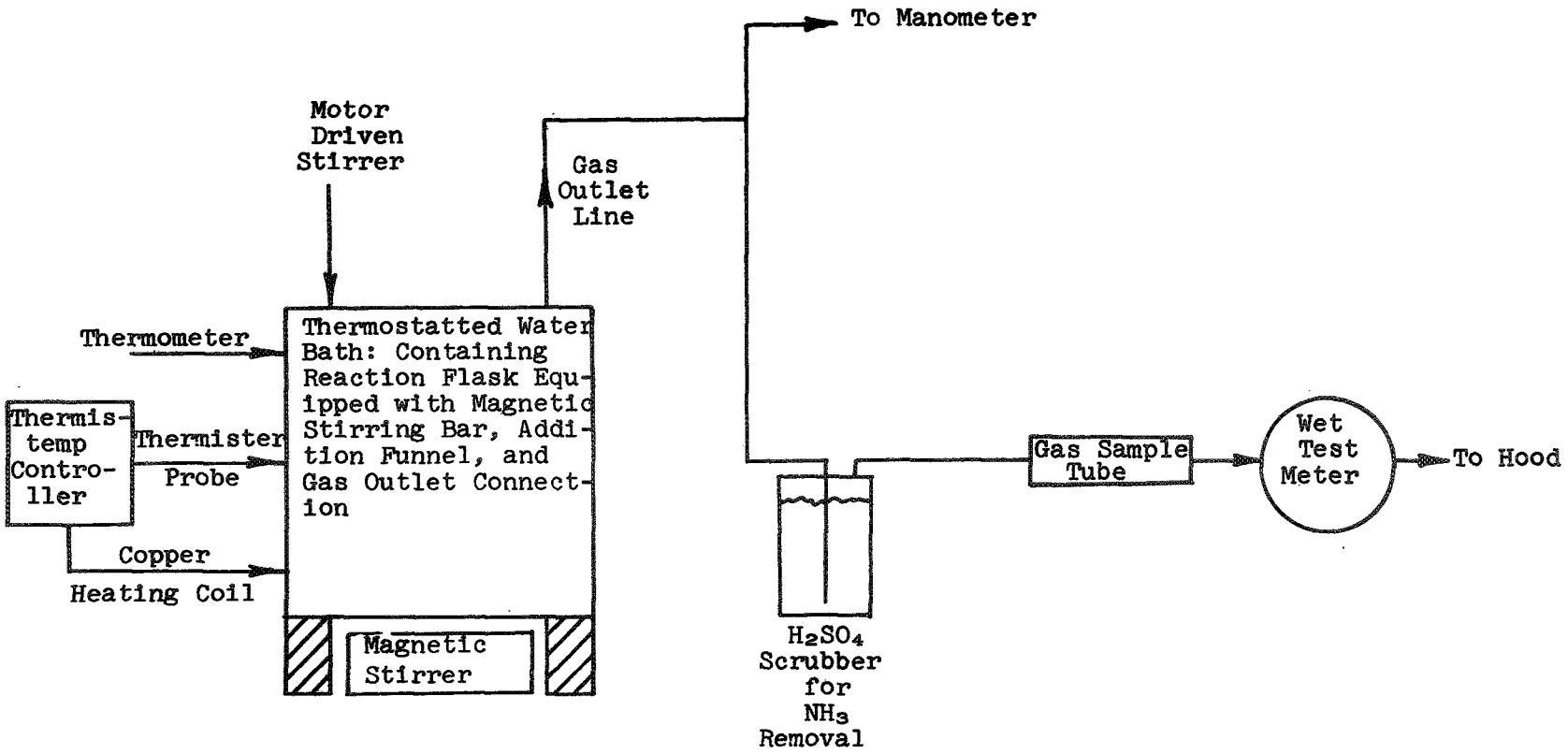

Figure 2. Low Temperature Decomposition Test Apparatus Schematic

Table I

LOW TEMPERATURE DECOMPOSITION OF UDMH, N_2H_4, AND AEROZINE-50

Catalyst Type	Weight, g	Fuel	Temp, °C	Gas Rate, ml/min	Specific Gas Rate, ml/min g *	Off Gas H_2/N_2 Ratio	% N_2H_4 Converted to H_2	% N_2H_4 Decomposed	Notes
Raney Nickel water slurry No. 28, Raney Nickel Corp.	-	UDMH	30	1.0	-	-	-	-	1 ml of slurry used
	-	UDMH	61	0.2	-	-	-	-	1 ml of slurry used
	-	N_2H_4	24	21.4	-	-	-	all	1 ml of slurry used
	-	N_2H_4	26	28.3	-	-	-	all	1 ml of slurry used
Raney Nickel water slurry with 0.3 g H_2PtCl_6	-	UDMH	61	0.2	-	-	-	-	1 ml of slurry used
	-	50/50	61	294	-	-	-	all	1 ml of slurry used
	-	UDMH	61	0.5	-	-	-	-	1 ml of slurry used
	-	25% N_2H_4			-				1 ml of slurry used
	-	75% UDMH	59	225	-	-	-	all	1 ml of slurry used
	-	N_2H_4	34	560	-	1.90	88	all	1 ml of slurry used
Girdler T-242 Ni + Cu Oxides	2.25	UDMH	30	0.9	0.4		-	-	1/8 in. tablets
	2.25	50/50	30	negligible	-	-	-	-	1/8 in. tablets
Baker 0.5% Pt on Alumina, 1/8 in. Tablets	1.80	UDMH	30	1.4	0.8	-	-	-	Rate decreasing with time
	1.80	50/50	30	0.6	0.3	-	-	-	Rate decreasing with time
Girdler T-308 0.05% Pd on Alumina	2.2	UDMH	30	0	-	-	-	-	1/8 in. tablets
	2.2	50/50	30	negligible	-	-	-	-	1/8 in. tablets
Girdler G-60 Promoted Nickel	2.8	UDMH	30	1.1	0.4	-	-	-	1/8 in. tablets
	2.8	50/50	30	negligible	-	-	-	-	1/8 in. tablets
Girdler T-325 reduced stabilized Nickel 1/8 in. tablets	2.3	N_2H_4	30	7.7	3.3	-	-	-	
	2.3	50/50	30	8.2	3.6	-	-	-	
	2.3	UDMH	30	0.6	0.3	-	-	-	
	2.3	50/50	30	6.7	2.9	-	-	-	Rate increasing

* Per gram of catalyst.

Table I (Continued)

Catalyst Type	Weight, g	Fuel	Temp, °C	Gas Rate, ml/min	Specific Gas Rate, ml/min g*	Off Gas H_2/N_2 Ratio	% N_2H_4 Converted to H_2	% N_2H_4 Decomposed	Noted
Girdler T-323 reduced stabilized cobalt 1/8 in. tablets	3.1	N_2H_4	30	explosive	-	-	-	-	Explosive decomposition
	1.0	UDMH	30	2.2	2.2	-	-	-	Stopped after 20 minutes
	1.0	50/50	30	49.7	49.7	0.05	0.9	all	Trace CH_4 in gas sample
Girdler G-52 reduced stabilized nickel on alumina	2.8	UDMH	30	1.1	0.4	-	-	-	Rate decreasing with time
	2.8	50/50	30	negligible	-	-	-	-	
Engelhard 5% Rh on Carbon Powder	0.7	N_2H_4	29.9	18.6	26.6	1.56	55	all	Rate decreasing with time
	0.7	UDMH	29.9	0.8	1.1	-	-		
	0.7	50/50	29.9	5.2	7.4	-	-	all	
	0.7	50/50	34.6	8.8	12.6	-	-	all	
	0.7	50/50	39.4	12.8	19.7	1.33	40	all	
Baker 0.5% Rh on Alumina	2.2	N_2H_4	29.9	2.8	1.3	1.56	55	all	1/8 in. tablets
Engelhard Rhodium Black	0.1	N_2H_4	49.7	24.3	243	1.6	57	all	
	0.2	50/50	50.0	27.2	136	1.65	61	all	
T-325 Reduced Nickel Catalyst	2.3	N_2H_4	49.5	-	-	0.96	24	all	Gas rate too fast to measure
	2.3	50/50	49.5	87.8	38.2	1.16	32	all	3 ml of catalyst was used
MRC Proprietary Catalyst 77604-4	0.1	UDMH	49.5	0	0	-	-	-	UDMH did not decompose
	0.1	50/50	49.5	12.3	123	1.37	42	all	
MRC Proprietary Catalyst 77604-5	0.1	UDMH	49.5	0	0	-	-	-	UDMH did not decompose
	0.1	50/50	49.5	76.8	768	0.70	15	all	
MRC Proprietary Catalyst 77604-1	0.1	UDMH	49.5	0	0	-	-	-	UDMH did not decompose
	0.1	50/50	49.8	36.8	368	0.89	21	all	

* Per gram of catalyst.

Table I (Continued)

Catalyst Type	Weight, g	Fuel	Temp, °C	Gas Rate, ml/min	Specific Gas Rate, ml/min g*	Off Gas H_2/N_2 Ratio	% N_2H_4 Converted to H_2	% N_2H_4 Decomposed	Notes
MRC Proprietary Catalyst 77604-2	0.1	UDMH	50.0	0	0	-	-	-	UDMH did not decompose
	0.1	50/50	50.0	16.1	161	0.82	19	all	
Thorium	0.1	UDMH	50.0	0	0	-	-	-	Heat treated in Ar 2 hr. No decomp. on UDMH or 50/50
	0.1	50/50	50.0	0	0	-	0	0	
Titanium	0.1	UDMH	50.0	0	0	-	-	-	Heat treated in air 1 min. No decomp on UDMH or 50/50
	0.1	50/50	50.0	0	0	-	0	0	
MRC Proprietary Catalyst 73578-A	0.5	UDMH	50.0	0	0	-	-	-	UDMH did not decompose
	0.5	50/50	50.0	204	408	0.69	15	all	
MRC Proprietary Catalyst 73578-B	0.5	UDMH	50.0	0	0	-	-	-	UDMH did not decompose
	0.5	50/50	50.0	-	-	0.87	20	all	Decomp rate was very fast to explosive

* Per gram of catalyst.

Table II

CATALYST SCREENING RESULTS FOR DECOMPOSITION OF AEROZINE-50

Temperature: 30°C

Catalyst and Support	Mole % H_2	Mole % N_2	Activity	Comments
Pt on carbon substrate	58.3	40.2	low activity	some NH_3
Rh on carbon substrate	69.4	30.6	active	little NH_3
Rh black powder	69.5	30.5	active	" "
Harshaw Ni-W sulfide (pellets)	-	-	inactive	
5 component precious metal alloy catalyst on carbon substrate	61.3	38.7	very active	slight amount NH_3
NiB catalyst	-	-	inactive	
Ir on carbon substrate	1.1	98.9	very active	mostly to NH_3
Ru on carbon substrate	9.7	89.9	active	mostly to NH_3
Cu chelate of ethylene Bisdithiocarbamate	-	-	no activity	
Co chelate of ethylene Bisdithiocarbamate	-	-	no activity	
Ni chelate of p,p'-diphenylene Bisdithiocarbamate	-	-	no activity	
Cu chelate of hexamethylene Bisdithiocarbamate	-	-	no activity	

Data from further tests that were run with the batch apparatus are presented in Table II.

The chelate catalysts were tried because of published reports of highly specific catalytic effects with N_2H_4 (Ref. 4). They were carefully prepared by published techniques (Refs. 5,6), washed with pyridine to remove soluble portions, and vacuum dried before testing. The single-component precious metal catalysts were made from standard commercial blacks incorporated in our MRD-carbon/catalyst electrodes which were subsequently cut up into small squares for testing. The NiB and the multiple component alloy were made in our laboratory. The Harshaw Ni catalyst was a commercial product.

The only new catalyst showing any promise in these tests was the 5-component precious metal alloy. Even this catalyst did not demonstrate any advantage over the previously tested Rh catalyst in this short-term testing.

2. Continuous Flow Reactor Tests

Following the initial work, a tubular, continuous-flow, liquid-phase reactor was constructed and operated. A schematic of this equipment is shown in Figure 3. The reactor consists of a 2-ft length of 1/2-in. diameter stainless steel tubing which contains the catalyst bed. The reactor tube was enclosed in a water jacket which was fed from a thermostatically controlled water bath. The feed stock was delivered to the reactor by a calibrated, positive displacement metering pump.

Initial tests of 4 to 6 hours duration were performed on the best catalysts found in the batch screening program; the results of these tests are summarized in Table III. The H_2 efficiencies found in the tubular reactor were greater than those found in batch testing. It is believed that some portion of the UDMH was decomposing in tubular reactor tests, probably by the following reaction:

$$(CH_3)_2NNH_2 \longrightarrow (CH_3)_2NH + 1/2\ N_2 + 1/2\ H_2 \qquad (15)$$

It is probable that this reaction was proceeding in the batch testing as well (since conditions and catalysts were nearly identical); however, no complete material balances were made in those initial tests and the reaction was never detected. Its only effect was to lower the H_2/N_2 ratio in the off-gases.

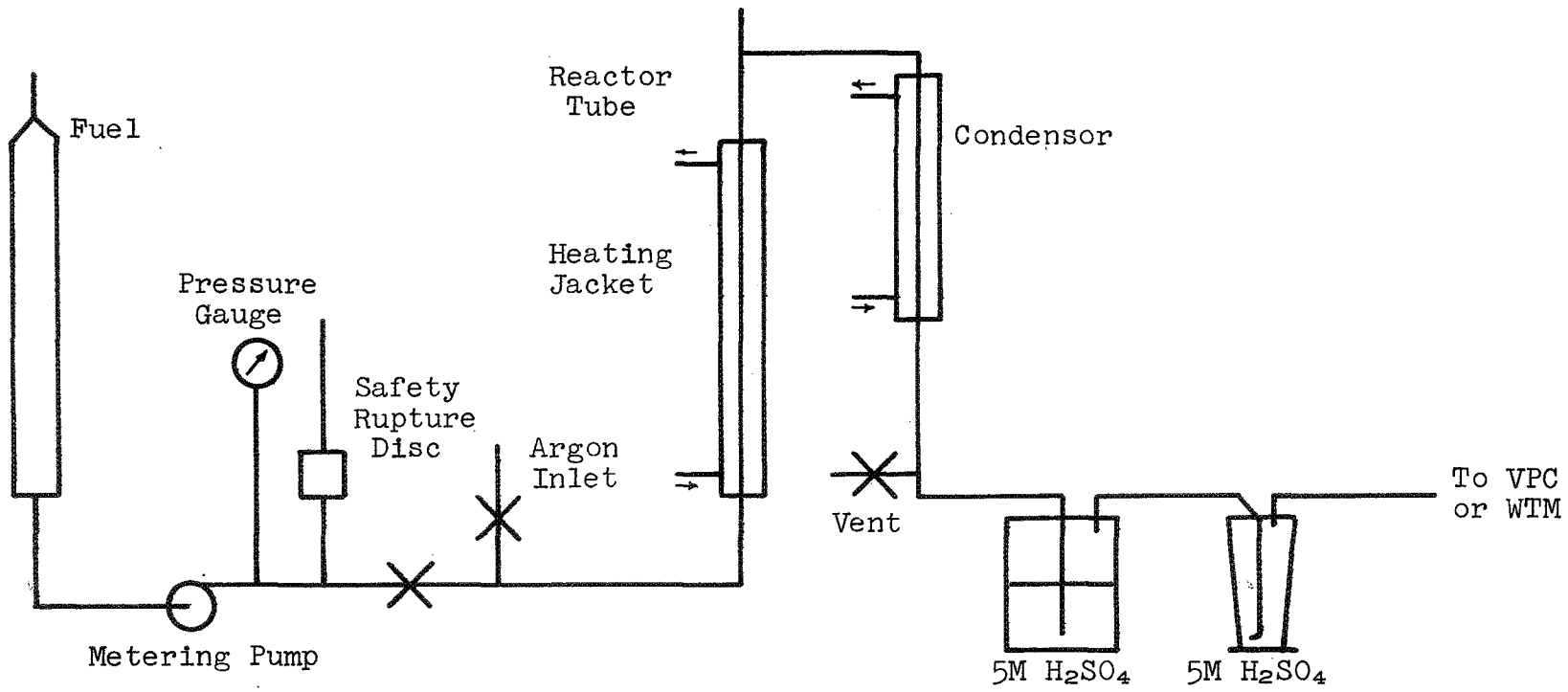

Figure 3. Aerozine-50 Liquid Phase Reactor Schematic

Table III

COMPARISON OF H_2 EFFICIENCIES --
CONTINUOUS VS BATCH LIQUID PHASE REACTORS

Fuel: Aerozine-50

	Continuous			Batch		
Catalyst	Temp, °C	Hydrogen Efficiency	H_2/N_2 Ratio	Temp, °C	Hydrogen Efficiency	H_2/N_2 Ratio
0.5% Rh on Alumina	50	24.8	1.5	30	17.6	1.6
T325 Reduced Stabilized Nickel	30	17.4	1.1	50	10.2	1.2

Table IV summarizes this liquid-phase testing. Several conclusions can be drawn from these data:

(1) All catalysts tested showed a drop in H_2 efficiency as the temperature was raised. The deterioration was caused by a shift to NH_3 formation.

(2) Most catalysts showed a deterioration of H_2 efficiency with time, even at lower temperatures. An exception was the T-325 reduced stabilized Ni which maintained a constant rate over a 20-hour period.

(3) The addition of water to the Aerozine-50 feed had no effect on the reaction.

(4) When N_2H_4 alone (no UDMH) was used as the feed stock, performance remained constant and no deterioration was found.

Based on these facts it appears likely that the UDMH portion of the fuel is partially reacting to form products which poison the catalyst in such a manner that the reaction shifts to NH_3 formation. At lower temperatures the UDMH reaction proceeds at a slow rate, and it takes some time for the poisoning effect to become dominant. As the temperature is increased, the UDMH reaction speeds up and the deterioration takes less time.

Longer-term tests were run with the Girdler T-325 Ni-based catalyst. A test of 125 hours duration (see Table V) with an Aerozine-50/H_2O solution (62.5% Aerozine-50 by weight) was made. The highest efficiency was 66.0% based on N_2H_4. After 86 hours the efficiency was still 64%. However, after this period, slow deterioration started, resulting in 50% efficiency after 124 hours.

The deterioration was due to lower rates of N_2H_4 decomposition, rather than to NH_3 formation, as has previously been noted in this work. This was shown by the constant H_2/N_2 ratio in the product gas, and also by qualitative information on the amount of $(N_2H_4)_2H_2SO_4$ precipitate formed.

Based on these results, the Girdler T-325 catalyst was chosen for the 1000-hour test on this system. Aerozine-50 (without H_2O) was fed to the reactor at a rate 50% higher than in the previous test. It was found necessary to purge the reactor with H_2O at the start of the test to avoid poisoning the catalyst by the highly exothermic reaction caused by the sudden ingress of the fuel. Over a period of one day the H_2O was displaced by the Aerozine-50, and the reactor reached a steady state.

Table IV

LIQUID PHASE AEROZINE-50 REFORMING DATA

Test No.	Catalyst Type	Catalyst Vol, ml	Fuel Composition, wt-%	Cumulative Time, hours	Input Fuel Rate, g/hr Aerozine-50	Temperature, °C Water Jacket	Temperature, °C Center of Reactor	Gas Evolution Rate, ℓ/hr	Output Gas Composition, mole-% H_2	Output Gas Composition, mole-% N_2	Hydrogen Efficiency Normal Basis	Hydrogen Efficiency Hydrazine Basis	Notes
1A	Girdler T-325 Reduced Stabilized Nickel 1/8-in. Tablets	50	100 Aerozine-50	2.0	9.5	30.7	28.0	7.8					
				3.0	9.5	30.7	28.0	7.6	61.0	39.0	20.0	64.0	
				4.0	9.5	30.7	28.0	7.0	52.8	47.2	15.8	50.6	All N_2H_4 decomposed (H_2/N_2 = 1.12)
				6.0	9.5	30.7	28.0	7.4	53.7	46.3	17.4	55.7	
1B	Same as above	50	100 Aerozine-50	1.0	10.7	30.5	28.0	8.9					Continued test over night.
				18.0	9.7	30.5	28.0	6.9	64.1	35.9	18.3	58.6	Not all N_2H_4 decomposed.
				19.5	10.3	38.0	30.5	7.4					Temperature raised.
				20.0	10.3	38.0	30.5	6.3					All N_2H_4 decomposed.
				21.0	10.3	38.0	30.5						Rate decreasing, mostly N_2.
2A	Engelhard 0.5% Rhodium on Alumina 1/8-in. Tablets	50	100 Aerozine-50	1.5	9.6	29.7	27.5	2.1					Not all N_2H_4 decomposed.
				3.5	9.1	40.2	32.0	4.9					Not all N_2H_4 decomposed.
				5.0	9.6	40.2	32.0	4.3					Not all N_2H_4 decomposed.
				6.5	8.9	50.0	35.0	9.9	59.8	40.2	24.8	77.6	Some N_2H_4 undecomposed.
				8.0	10.7	49.7	34.0	4.8					Argon atmosphere over night.
				11.5	10.7	49.7	34.0	4.9					Not all N_2H_4 decomposed.
				13.0	10.7	56.0	36.0	8.8					
				14.0	10.9	59.0	36.0	7.1					Argon atmosphere over night.
				14.75	10.9	59.0	36.0	1.4					N_2H_4 decomposed, gas rate decreasing.
				16.0	10.1	44.8	32.0	0.1					
				18.0	9.4	44.8	32.0	0.1					
2B	Same as above	70	100 Aerozine-50	1.0	10.0	30.5	28.0	7.1	59.2	40.8	17.2	53.6	Not all N_2H_4 decomposed.
				2.5	9.7	30.5	28.0	4.7					Not all N_2H_4 decomposed.
				4.0	9.5	36.0	30.5	7.3					
				5.0	10.0	38.0	31.0	6.4	55.3	44.7	15.4	48.2	Gas rate dropped to low value.

Table IV (Continued)

Test No.	Catalyst Type	Catalyst Vol, ml	Fuel Composition, wt-%	Cumulative Time, hours	Input Fuel Rate, g/hr Aerozine-50	Temperature, °C Water Jacket	Temperature, °C Center of Reactor	Gas Evolution Rate, ℓ/hr	Output Gas Composition, mole-% H_2	Output Gas Composition, mole-% N_2	Hydrogen Efficiency Normal Basis	Hydrogen Efficiency Hydrazine Basis	Notes
2C	Same as above	70	62.5 Aerozine-50	1.5	8.1	35.7	29.5	4.7					
				2.5	8.3	40.8	30.0	3.0					Not all N_2H_4 decomposed.
				4.5	8.3	40.8	30.0	4.6					
			37.5 H_2O	5.0	8.3	40.8	30.0	4.7	60.6	39.4	14.2	44.3	All N_2H_4 decomposed.
				7.5	8.3	40.8	30.0	4.7					
				23.5	6.1	30.0	27.0	1.0					Ran over night, all N_2H_4 decomposed
3	Raney nickel irregular lumps; leached 20% of Aluminum	50	100 Aerozine-50	1.0	10.0	26.0	25.0	3.0	63.6	36.4	8.2	25.7	Much undecomposed N_2H_4.
				3.0	10.0	32.8	28.0	4.8	62.6	37.4	12.3	38.3	Much undecomposed N_2H_4.
				5.5	10.0	42.1	32.0	8.0	62.3	37.7	21.0	65.7	Some undecomposed N_2H_4.
				21.5	9.2	42.4	32.0	3.8					After over night run.
4A	MRD Rhodium-Carbon-Teflon catalyst cut into 1/4-in. strips and then rolled into 1/4-in. porous spheres	50	100 Aerozine-50	1.0	10.1	30.0	27.5	11.3					
				2.3	10.1	30.0	27.5	7.9	59.4	40.6			Rate kept decreasing rapidly, all N_2H_4 decomposed.
		50	62.5 Aerozine-50 37.5 H_2O	1.0	6.8	30.0	27.5	9.5					
				2.5	6.8	30.0	27.5	5.2					Rate kept decreasing rapidly, all N_2H_4 decomposed.
		30	47.5 N_2H_4 52.5 H_2O	1.0	(N_2H_4) 5.6	30.3	27.0	9.3					
				2.5	(N_2H_4) 5.6	30.3	27.0	8.4	63.4	36.6		63.5	82% of the N_2H_4 decomposed, (some NH_3 found)
				5.0	(N_2H_4) 5.6	30.3	27.0	8.4					
		50	47.5 N_2H_4 52.5 H_2O	2.0	(N_2H_4) 5.6	31.6	28.0	5.7					Not all N_2H_4 decomposed.
				6.8		31.6	28.0	5.5					Not all N_2H_4 decomposed.
				23.8		31.6	28.0	5.9	65.7	34.3		50.2	Not all N_2H_4 decomposed.
				25.8		40.2	30.5	10.0					
				28.8		40.2	30.5	7.4	63.3	36.7		61.7	Little N_2H_4 undecomposed.
				47.5		41.2	30.0	8.2					All N_2H_4 decomposed.
				50.0		40.0	29.5	7.7	61.1	38.9		58.7	(H_2/N_2 = 1.57)

Table V

LOW TEMPERATURE, LIQUID PHASE REACTOR LONG-TERM TESTS WITH GIRDLER T-325 CATALYST

Bed Volume 2.21in^3

Running Time, hr	Temperature, °C: Water Jacket	Temperature, °C: Reactor Center	Composition, wt-%: A-50	Composition, wt-%: H_2O	Aerozine-50 Input Rate, g/hr	Output Gas Rate at 25°C, l/hr	VPC Analysis, mole-%: H_2	VPC Analysis, mole-%: N_2	H_2 Efficiency, Total Basis	H_2 Efficiency, N_2H_4 Basis	Notes
2.0	30.5	27.5	62.5	37.5	6.75	6.6					
4.0	30.5	27.5	62.5	37.5	7.12	6.0	59.1	40.9	20.7	65.0	
6.0	30.5	27.5	62.5	37.5	6.99	5.8					
26.0	30.5	27.5	62.5	37.5	6.75	5.7	59.6	40.4	20.9	65.4	Ran overnight.
56.0	30.5	27.5	62.5	37.5	6.63	5.6					Ran overnight.
62.0	30.5	27.5	62.5	37.5	6.50	5.4	61.4	38.6	21.1	66.3	Shut down over 5-day period and restarted.
86.0	30.5	27.5	62.5	37.5	6.75	5.4	61.2	38.8	20.3	63.6	
100.0	30.5	27.5	62.5	37.5	6.99	4.7	62.0	38.0	17.3	54.2	
124.0	30.5	27.5	62.5	37.5	6.99	4.3	62.2	37.8	15.9	49.7	Deterioration due to less N_2H_4 decomposed, not NH_3 formation.

This test was run continuously for 700 hours until the reactor tube ruptured because of an unrelieved over-pressure due to plugging of the tube by catalyst particles that had broken loose. Table VI gives a complete history of the 700-hour test. The maximum H_2 efficiency (based on N_2H_4) of 56.5% was reached at 30.6°C, after 49 hours. From then on a slow deterioration occurred until the efficiency reached 32.3% at 316 hours. At that time the low efficiency was primarily caused by incomplete N_2H_4 decomposition rather than NH_3 formation. The temperature was subsequently raised in small steps in an attempt to increase efficiencies. It was found that the reaction rate would increase for a time after each increase in temperature, but would then decline again. Finally at 700 hours, a rate equal to 37.0% was found at 45.6°C. However, nearly all the N_2H_4 was decomposed, indicating that a shift toward NH_3 formation had also occurred at the high temperature. This was confirmed by the lower H_2/N_2 VPC ratio occurring at 45.6°C.

It is evident from the data generated during this test that the Ni-based catalyst used was not satisfactory for this application both because of its physical disintegration and, more importantly, because of its loss in activity in long-term testing. Accordingly, a short screening program was initiated in an attempt to find a more active catalyst. The following catalysts were tested for short periods (1 to 2 days) in the reactor:

Harshaw ZN0701 (24% ZnO on activated alumina)

Girdler G-47 (Fe_2O_3; support unknown)

" G-49A (reduced, stabilized Ni on kieselguhr)

" G-49B (reduced, stabilized Ni on kieselguhr)

None of these catalysts showed any advantage over the T-325 catalyst.

Subsequent to this work, long-term, continuous-flow reactor tests were attempted with anhydrous N_2H_4 alone (no UDMH) utilizing a high-surface-area Rh catalyst. After several equipment problems were solved, the unit was started up. It was found that the spontaneous decomposition reaction was extremely difficult to control with pure N_2H_4. Moderation with water helped considerably, but conversion efficiencies were substantially below 50% even at low-flow rates. Long-term tests were not attempted. The results of this work, previously unreported, are given in detail in Appendix A.

Table VI

LIQUID PHASE REACTOR 1000 HOUR TEST

Bed Volume = 2.21 in^3 Catalyst = Reduced Stabilized Ni on Keisselguhr, 3/16 in. tablets

Running Time, hrs	Temp. °C	Aerozine -50 input rate, g/hr	Output Gas Rate at 25°C, l/hr	V.P.C. Analysis, Mole % H_2	N_2	Other	H_2 Efficiency Total Basis	N_2H_4 Basis	Notes
6	26.8	9.74	4.70	61.6	38.4	-	12.3	38.6	Started with 20 ml H_2O
25	26.6	9.97	3.66	61.6	38.4	-	9.9	31.0	in reactor, at normal
28	30.0	9.97	6.05	61.6	38.4	-	15.5	48.6	pumping rate of 11 ml/hr.
31	30.3	9.97	6.46	61.6	38.4	-	16.6	51.9	Takes one day to reach equilibrium
49	30.6	9.69	6.83	61.6	38.4	-	18.0	56.5	Some undecomposed N_2H_4 in
55	30.6	9.69	6.75	59.9	40.1	-	17.3	54.3	output
124	30.3	9.69	5.47	62.1	37.9	-	14.5	45.6	On over weekend
148	30.3	9.88	5.45	61.2	38.8	-	14.0	43.9	eff. drop due to less
172	30.7	10.09	5.23	61.2	38.8	-	13.1	41.2	N_2H_4 decomposed, not NH_3
196	30.6	9.74	4.99	61.2	38.8	-	13.0	40.8	formation
220	30.3	9.63	4.71	61.2	38.8	-	12.4	38.9	
292	31.0	9.92	4.55	62.1	37.9	-	11.8	37.1	On over weekend
316	31.0	9.62	3.81	62.7	37.3	-	10.3	32.3	
364	31.5	9.60	3.28	57.4	42.6	-	8.1	25.5	Eff. drop mostly due to less N_2H_4 decomposition
460	32.0	9.79	2.70	61.2	38.8	-	7.0	22.0	On over weekend
484	33.5	9.13	3.05	60.9	39.1	-	8.5	26.5	Raising temp to attempt
508	35.0	8.93	3.39	60.8	39.2	-	9.6	30.0	to increase eff.
628	37.0	8.95	3.18	60.8	39.2	-	9.0	28.1	On over weekend
652	40.8	9.31	3.90	57.7	40.8	1.5	10.0	31.4	CO_2 noticed on VPC, not
672	40.5	9.41	3.57	57.7	41.9	0.4	9.1	28.5	sure whether true or
676	42.2	9.41	4.21	58.2	41.1	0.7	10.8	33.9	contaminant.
696	42.4	8.98	3.64	58.2	41.1	0.7	9.8	30.7	
700	45.6	9.81	5.04	55.3	44.7	-	11.8	37.0	Most of N_2H_4 decomposed, more NH_3 being formed. Overnight reactor burst.

C. INTERMEDIATE TEMPERATURE SYSTEMS

1. Equipment

Figure 4 shows schematically the complete intermediate temperature reforming system. A calibrated one-liter graduate contained the water-fuel mixture, feeding into Milton Roy "mini-pump" (maximum pressure 200 psig), through a 5-micron stainless steel filter. Immediately following the pump outlet was a pressure gauge and rupture disc assembly that would release at 200 psig. The pressure gauge permitted the use of the pump calibration with pressure for accurate pumping rates. Following the rupture disc was a valve system to purge and clean the pump. A valved gas input line was used (argon or helium) to purge the system of air before testing and to purge the liquid and gases remaining after the test period. The reactor system, consisting of a 1-in. 304 stainless steel pipe with 3/4-in. I.D. was heated by a 3400-watt electric oven, with individual on-off switches on four heating elements. Thermocouples were attached to the reaction tube and connected to a West temperature controller and a Brown temperature recorder. The output of the reactor passed through a water condenser to a manostat consisting of a pressure gauge and a pressure switch that activated an on-off solenoid valve, maintaining pressure within 5 psig. Following the solenoid valve was the liquid-gas separator flask, cooled in an ice bath to lower the vapor pressure of the exit liquids. The flask was partially filled with 5N H_2SO_4 (100 ml) to trap the unreacted Aerozine-50 along with NH_3, while passing CO_2. The gases then entered an H_2SO_4 scrubber to remove any trace of NH_3, flowed through another condenser to a KOH trap to remove CO_2, and then flowed to the wet-test meter. Between the H_2SO_4 scrubber and the KOH scrubber was a valve to allow the gas to pass through the sample loop of a vapor phase chromatograph for analysis, and then back to the KOH scrubber. This permitted gas analysis at any time during the test. After the wet test meter, the out-gas was vented to a hood.

The reactor tube was 22 in. long and was packed with 10 in. of porcelain chips for preheating, then six inches of catalyst bed (43 ml volume), and then 4 more inches of porcelain chips.

2. Intermediate Temperature Decomposition

The objective of this work was to improve the N_2H_4 decomposition rate and efficiency by operating at higher temperatures where the reactants were in the vapor phase. The tubular flow reactor described above was used to evaluate Pt, Pd, Rh, and Ni catalysts at 10 psig from 100°C to 250°C on pure Aerozine-50 feed. The

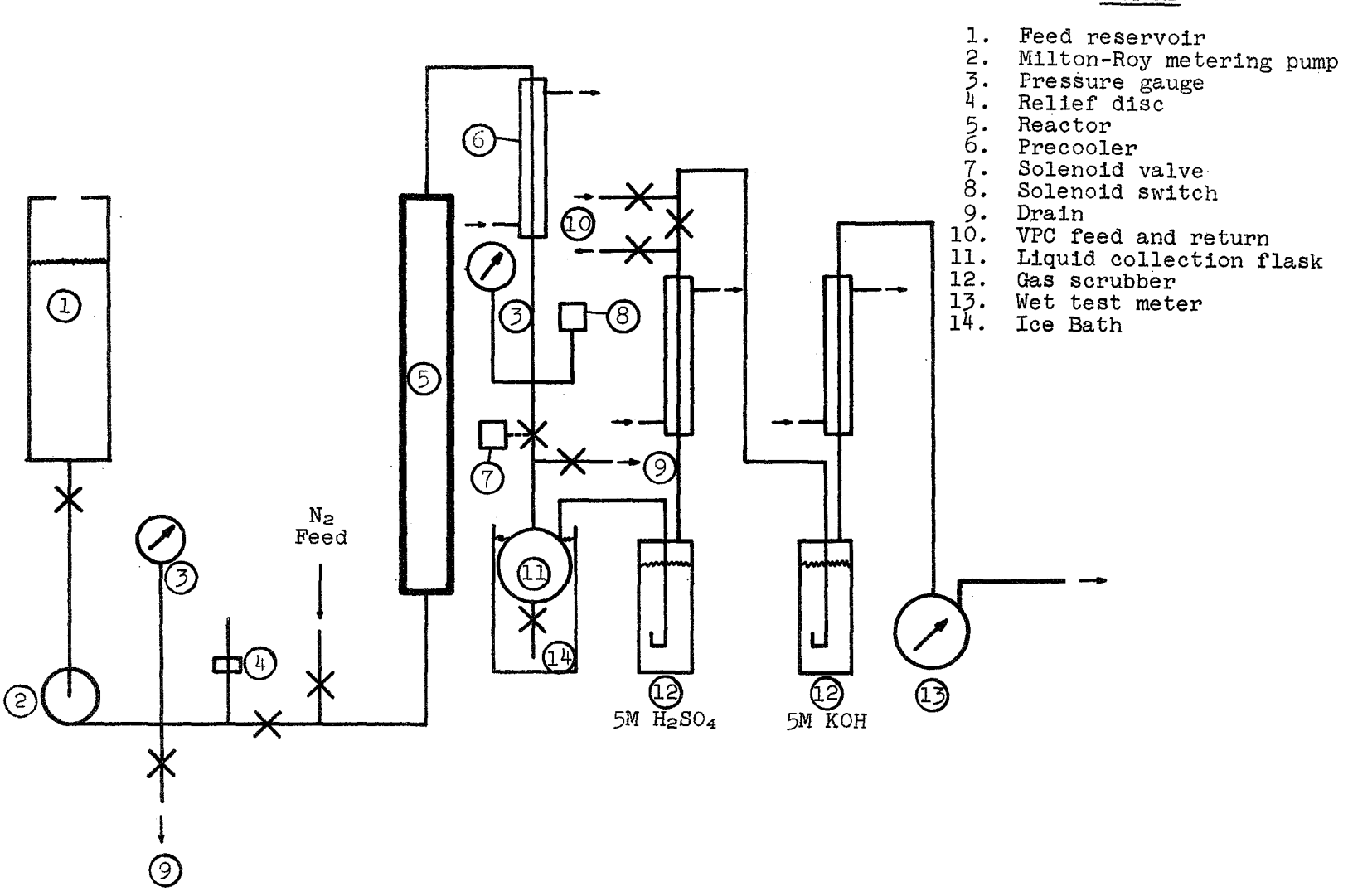

Figure 4. Intermediate-Temperature Reforming System Schematic

results are presented in Table VII. No significant H_2 formation was found with any catalyst above 140°C where only the vapor phase exists in the reactor. At 100°C, where Aerozine-50 is only partially vaporized, some H_2 production was realized with a Pd catalyst. These results seemed to indicate that the vapor phase reaction proceeded mainly to NH_3 on the catalysts tested. The H_2 conversion efficiency with the Pd catalyst was only 1.4%. Great improvement would be necessary for this system to be useful.

3. Intermediate-Temperature, Single-Reactor Steam Reforming-UDMH Only

The steam reforming reaction was investigated in the temperature range 300 to 500°C, 50 psig pressure, with a single catalyst in a single reactor. This system was attractive because of the relatively low temperature involved and its potential simplicity.

In order to characterize the reactor kinetics free from other possible reactions, only UDMH-H_2O mixtures were used as feed stocks for the initial catalyst evaluation. Efficiencies in this section are reported as percent of maximum H_2 available, i.e., from:

$$(CH_3)_2NNH_2 + 4H_2O \longrightarrow 2CO_2 + N_2 + 8H_2 \qquad (16)$$

yielding 13.33 moles H_2 per 100 g UDMH.

The tubular flow reactor used was described in Section C.1. Details on operating parameters, catalysts, analytical methods, and results are included in the original reports (Ref. 3).

Table VIII lists the total H_2 efficiency for each test performed. Three values are shown corresponding to

(1) Actual experimental values of H_2 efficiency,

(2) H_2 efficiency if CO is shifted to CO_2, and

(3) H_2 efficiency if CO is shifted to CO_2 and if NH_3 is decomposed.

The best actual efficiencies (26 to 30%) were obtained at 500°C, 50 psig, with a Ni-based catalyst (Girdler G56B), a Ni oxide catalyst (Girdler T-1144), and a ZnO on alumina catalyst (Harshaw Zn0701). The best extrapolated efficiencies (45-55%) for the system combining steam reforming with NH_3 decomposition and CO conversion occurred at 400°C with the following catalysts:

(1) Girdler T-310, 10% nickel oxide on activated alumina

(2) Girdler Ni-base reforming catalyst

(3) Girdler T-312 Ni and Cu oxides on alumina

(4) Girdler T-1144, 50% nickel oxide

Table VII

MEDIUM TEMPERATURE AEROZINE-50 DECOMPOSITION TESTS

Pressure: 10 psig

Catalyst	Temp, °C	Output Gas Composition H_2	N_2	CH_4	CO	Ethane	Input Aerozine g/hr	Moles N_2H_4 per hr	Moles H_2 per 100 g Aerozine	% of Maximum H_2 From N_2H_4	State of Aerozine In Reaction
Engelhard 0.5% Pt on Alumina	175	0	94.1	5.9	0	0	9.52	0.149	0	0	gas
	250	0.6	89.7	9.6	0	0.1	9.52	0.149	0.004	0.13	gas
Engelhard 0.5% Rh on Alumina	105	5.5	82.2	9.6	2.8	0	8.65	0.135	0.036	1.14	liquid
	170	0.2	90.1	9.7	0	0	9.09	0.142	0	0	gas
	250	2.3	76.8	20.0	0.6	0.2	9.09	0.142	0.018	0.6	gas
Engelhard 0.5% Pd on Alumina	100	52.1	47.9	0	0	0	9.01	0.141	0.07	2.3	liquid
	116	44.5	55.5	0	0	0	9.01	0.141	0.13	4.3	liquid
	134	5.6	84.8	9.6	0	0	9.01	0.141	0.04	1.1	
	178	0.5	81.6	17.3	0.6	0	9.01	0.141	0.005	0.1	gas
Girdler G-49A Nickel, reduced stabilized	105	7.1	83.5	8.7	0.7	0.1	9.46	0.148	0.05	1.5	liquid
	178	0	90.0	10.0	0	0	9.01	0.141	0	0	gas

NOTES

In all tests liquid outputs could not be obtained under equilibrium conditions. Therefore, the % decomposition of N_2H_4 and UDMH is not known. However, in general only a small amount of N_2H_4 was decomposed at 100 and 175°C. Most was decomposed at 250°C.

Table VIII

EXTRAPOLATION OF HYDROGEN EFFICIENCIES FOR INTERMEDIATE TEMPERATURE STEAM REFORMING OF UDMH

(Total input of 19.0 to 21.0 g per hour)

Catalyst Data	Temp, °C	Pressure, psig	Hydrogen Efficiency Actual, %	Hydrogen Efficiency if CO Shifted to CO_2, %	Hydrogen Efficiency if CO Shifted and All NH_3 Decomposed, %	% Carbon Deposition
Girdler T-310 10% Nickel Oxide on Activated Alumina	300	50	2.4	2.5	16.8	5
	300	150	3.9	4.7	26.9	24
	400	50	20.9	21.2	36.8	none
	400	150	20.8	21.3	53.9	none
	500	50	18.7	19.1	32.3	none
	500	150	23.3	23.8	36.6	none
Girdler G-56B Nickel Base Reforming Catalyst	300	50	0.4	0.4	3.4	none
	300	150	8.8	10.1	36.1	25
	400	50	19.3	19.4	51.6	17
	400	150	19.1	19.1	50.9	none
	500	25	20.4	20.6	41.9	42
	500	50	31.9	32.4	42.4	6
6-hour test	500	50	29.1	29.7	39.9	none
	500	150	25.4	25.4	37.2	none
Girdler G-43 0.5% Platinum on Alumina	300	50	0.9	1.3	21.5	34
	300	150	-	-	-	
	400	50	3.0	4.2	27.6	20
	400	150	6.9	8.5	28.2	none
	500	50	11.0	13.1	29.8	6
	500	150	16.2	17.4	28.1	none
Harshaw Cu 2501 all CuO in Chip Form	300	50		no reaction		
	400	50	0.5	0.6	5.0	none
	500	50	2.9	3.5	9.3	9
Girdler T-309 Pt Oxide on Activated Alumina	400	50	2.8	6.6	30.7	23
	400	150	1.9	6.1	28.1	8
	500	50	10.5	13.6	43.1	59
	500	150	15.6	20.7	37.0	none

Table VIII (continued)

Catalyst Data	Temp, °C	Pressure, psig	Hydrogen Efficiency Actual, %	Hydrogen Efficiency if CO Shifted to CO_2, %	Hydrogen Efficiency if CO Shifted and All NH_3 Decomposed, %	% Carbon Deposition
Girdler G-47 Promoted Iron Oxide	300	50	0.2	0.2	9.0	11
	300	150	-	-	-	
	400	50	1.9	2.1	13.5	11
	400	150	1.1	1.4	7.8	3
	500	50	13.0	13.6	22.7	none
	500	150	10.9	11.5	22.6	7
T-312 Girdler Nickel and Copper Oxides on Alumina	300	50	4.9	5.6	24.2	none
	300	150	1.1	1.2	14.1	none
	400	50	18.9	21.2	45.8	none
	400	150	18.9	21.0	45.4	none
	500	50	21.1	22.2	38.6	none
	500	150	15.1	15.4	28.3	none
Harshaw ZnO 308 Zinc Chromate	300	50	8.6	8.6	25.7	5
Girdler T-1144 50% Nickel as Oxide on Oxide Base	300	50	1.6	1.6	15.4	16
	400	50	22.6	23.8	52.9	14
	500	50	28.3	28.6	33.6	none
Girdler T-317 10% Cu Oxide on Alumina	300	50	15.1	15.2	40.2	43.5
	400	50		test invalid		
	500	50	17.8	22.7	38.0	none
Zn 0701 10% ZnO on Alumina	300	50	0	0	0	none
	400	50	16.7	16.9	43.2	13
	500	50	26.0	26.7	40.9	none
Norton Zeolite Cation Acidic	300	50	-	-	-	-
	400	50	0.2	2.4	15.7	1
	500	50	3.0	4.7	11.5	2

Analysis of product streams from these produced the following general conclusions (Ref. 3b):

(1) All catalysts cause NH_3 formation at 300 and 400°C. The amount produced decreases as the temperature increases; in some cases none is formed at 500°C with the pressures used in this study.

(2) Methane production increases with temperature and pressure for most of the catalysts. The maximum found was 60 to 70% of the UDMH reacting by this path.

(3) Carbon deposition occurs with many of the catalysts at 300 and 400°C. This reaction produces H_2, but is undesirable because of eventual catalyst fouling.

(4) In some cases the direct formation of NH_3 from the elements appears to have occurred to some extent.

4. Intermediate-Temperature, Single-Reactor Steam Reforming-Aerozine-50

The initial tests with Aerozine-50, in which parallel decomposition of N_2H_4 was expected, were conducted on the two best UDMH steam reforming datalysts found in the previous tests. The results are presented in Table IX.

Comparison of these results with the data acquired with UDMH alone indicates that the fraction of UDMH undergoing steam reforming was reduced at 500°C, and the amount of CH_4 formed and carbon deposited at 400°C also increased slightly. The net effect was a slightly reduced H_2 efficiency from the steam-reforming reaction. However, a significant increase in NH_3 decomposition was found (24% for Girdler G56B and 56% for T-1144), which tended to increase H_2 yield. The overall H_2 efficiency (including the N_2H_4 component of the fuel) was 27.0% for T-1144 at 500°C, 50 psig.

Further testing conducted with several new catalysts is summarized in Table X.

Table IX

STEAM REFORMING OF AEROZINE-50

Input Composition, wt-%: 23.1 UDMH
23.1 N_2H_4
53.8 H_2O

Catalyst	Temp, °C	Pressure, psig	% NH_3 Dissociation	Actual H_2 Efficiency	H_2 Efficiency Assuming 90% Dissociation of NH_3 and CO Shift	% UDMH to Deposition of Carbon	% UDMH to CH_4 and N_2	% UDMH To Steam Reforming
G56B	300	25	0	3.2	43.5	24	3	8
	300	50	0	0.3	47.3	57	5	0.1
	400	25	0	14.2	60.3	29	27	36
	400	50	0	15.2	64.9	32	19	41
	500	50	24	22.8	50.4	0	68	33
T-1144	400	50	0.6	16.2	57.6	15	10	35
	500	50	56	27.1	41	1	67	15

Table X

STEAM REFORMING OF AEROZINE-50

Input Composition: 23.1 wt-% UDMH
23.1 wt-% N_2H_4
53.8 wt-% H_2O
% of N_2H_4 Unreacted: none

Catalyst	Temp °C	Pressure, psig	Input Rate of Aerozine-50, g/hr	% Actual Hydrogen Efficiency	Hydrogen Efficiency With 90% NH_3 Decomposition and CO Shift	Carbon Deposition of UDMH, %	UDMH Unreacted, %	UDMH to CH_4 and N_2, %	UDMH to Steam Reforming, %	Notes
Girdler G-72	300	50	9.98	6.5	43.7	none	59.2	2.0	24.3	
100% zinc oxide	400	50	9.73	13.3	48.0	none	2.4	16.8	27.9	
1/8-in. pellets	500	50	9.73	26.9	63.5	none	none	43.3	56.6	
Linde SK-200	300	50	9.68	6.5	49.5	10.2	2.0	2.0	4.6	
0.5% Pt on	400	50	9.78	17.5	56.4	none	none	7.3	42.5	
molecular sieve	500	50	9.96	22.2	57.6	none	none	53.1	44.5	
1/8-in. pellets										
Zn-Cu on alumina	300	50	9.53	1.1	37.4	3.7	none	12.5	7.4	
(MRC prepared)	400	50	9.76	3.3	34.5	none	none	29.3	6.3	
chips	500	50	9.58	22.7	62.8	none	none	32.4	56.1	
Harshaw Zn-0701	450	50	8.85	28.8	74.8	6.3	1.4	21.4	65.9	8 hr operation
10% ZnO on alumina	450	50	9.53	29.1	71.8	1.3	0.5	24.8	63.8	11 hr operation
1/8-in. pellets	500	50	9.53	20.1	55.2	none	none	50.9	38.3	
Girdler T-310	450	50	9.48	21.4	66.4	8.9	none	25.3	51.9	much CO
12% NiO on alumina	500	50	10.16	23.2	62.4	none	none	44.2	47.0	
1/8-in. pellets										
Composite catalyst										
3 inches G56B	440	50	10.44	31.3	47.3	19.7	none	63.9	16.5	Less NH_3 formation
3 inches T-1144	500									than normal
Composite catalyst										
3 inches G56B	385	50	9.68	25.5	49.0	29.5	none	48.0	13.5	Less NH_3 formation
3 inches T-1144	500									than normal
Composite catalyst										
3 inches Zn-0701	440	50	9.07	24.0	44.6	none	none	63.1	21.9	Less NH_3 formation
3 inches T-1144	500									than normal
Harshaw ZnO401	400	50	9.72	25.1	60.1	none	19.2	19.5	52.8	
100% ZnO	450	50	9.49	38.4	73.9	none	0.6	29.9	76.9	
Harshaw Ni 1404	300	50	9.48	2.5	49.1	13.3	0	42.2	24.9	
70% Ni on Prop.	400	50	9.68	6.4	47.6	3.8	0	36.6	25.8	Carbon deposition
Base										fouled the reactor

Three ZnO-containing catalysts gave the best single catalyst results in these tests, with an H_2 efficiency of 38% for Harshaw Zn0401. Two of these catalysts were selected for secondary testing. These tests were made in conjunction with second in-line reactors for NH_3 decomposition and high-temperature steam reforming of the product stream. The product stream from the reactor containing the catalysts in question was analyzed separately. The data on G-72 ZnO catalyst over 48 hours of intermittent operation are presented in Table XI. The H_2 efficiency was constant over the first 24 hours at 32-35%, but it then dropped to 28%. The deterioration was undoubtedly caused by carbon deposition on the catalyst bed; carbon was definitely visible when the catalyst was removed from the reactor. Similar results were obtained with the Zn0401 catalyst (Table XII). It is possible that the carbon deposition occurred because of temperature cycling during the test period. The reactors were not run overnight in these tests. In any event, it is known that increasing the water excess in the input stream reduces the amount of carbon deposition.

The effect of small changes in residence time was investigated with G-72 catalyst (Table XII). Input rates of 20 and 26 g/hr produced essentially the same H_2 output, indicating little effect in this range.

5. Intermediate Temperature Steam Reforming Followed by NH_3 Decomposition

Calculations showed that the H_2 efficiency of the ZnO steam reforming catalysts could be greatly increased if significant NH_3 decomposition could be effected. For example, if 90% of the NH_3 in the product stream from the Zn0401 catalyst bed were decomposed, the overall H_2 efficiency would be 75%.

A second in-line reactor was necessary in this sytem because NH_3 decomposition is thermodynamically favored at lower pressures than were used in the steam reforming reactor. The catalyst choice for the second reactor was difficult: the standard NH_3 dissociation catalysts (promoted iron oxides) will not work in the presence of H_2O, CO, or CO_2. Furthermore, the test results on single-bed composite catalysts (Table X) showed that Ni catalysts reduced the hydrogen efficiency by promoting the methanation reaction:

$$CO + 3H_2 \longrightarrow CH_4 + H_2O \qquad (17)$$

Table XI

LONG-TERM TESTING OF GIRDLER G-72 CATALYST FOR AEROZINE-50 STEAM REFORMING

Temperature: 450°C ± 5°C
Pressure: 50 psig ± 3 psig
Input Composition: 23.1% N_2H_4
(weight-%) 23.1% UDMH
53.8% H_2O
Total Input Rate: 20 grams/hour

Total Time*, hours	Running Time, hours	UDMH** Reacted, %	Hydrogen Efficiency, %	Carbon Deposition of UDMH, %	Output Composition, mole-%									
					UDMH	H_2O	NH_3	H_2	N_2	CH_4	CO	CO_2	Ethane	DMA
4.0	4.0	100	34.0	none	0	31.7	24.3	24.8	6.4	3.3	0.4	9.1	<0.1	0
28.0	11.0	100	35.0	none	0	32.6	21.4	26.2	7.5	3.3	0.5	8.2	<0.1	0.3
42.0	18.0	100	35.7	none	0	31.2	21.8	26.5	7.3	4.0	0.4	8.8	0.1	0
162.0	25.0	98.4	32.7	9.6	0.1	35.0	21.5	24.6	7.6	3.7	0.3	7.2	0.1	0
210.0	32.0	(Not tested on first reactor.)												
234.0	39.0	(Not tested on first reactor.)												
258.0	44.0	99.0	27.8	none	0.1	35.9	22.9	21.8	7.2	3.1	0.2	7.8	0.1	0.9
262.0	48.0	100	27.9	none	0	36.0	23.1	21.7	7.0	3.1	0.3	7.6	0.1	1.1

* Includes downtime under argon at room temperature.

** N_2H_4 always completely reacted.

NOTE: Catalyst was thinly coated with carbon upon removal from the reactor.

Table XII

DOUBLE REACTOR DATA FOR DECOMPOSITION OF NH_3

Conditions	First Reactor	Second Reactor
Temperature	450°C	450°C
Pressure	50 psig	5 psig (average)
Catalyst Bed Volume	43 ml	86 ml

Input Composition (weight-%): 46.2% Aerozine-50, 53.8% H_2O
Total Input Rate: 20 grams/hour

Reactor	Catalyst	Hydrogen Efficiency, %	Carbon Deposition of UDMH, %	Output Composition, mole-%									
				UDMH	DMA	NH_3	H_2	N_2	CH_4	CO	CO_2	H_2O	Ethane
First	G-72	35.0	none	0	0.3	21.4	26.2	7.5	3.3	0.5	8.2	32.6	0.1
Second	0.5% Pt	33.1	none	0	0	21.2	25.0	7.2	5.1	0.2	8.5	32.8	0
First	Zn 0401	37.9	none	0.1	0.5	21.9	28.2	7.0	2.2	0.5	9.0	30.8	0
Second	Silica-Alumina	34.4	24.2	0	0	20.9	25.5	7.7	3.1	0.2	6.3	36.3	0
First	Zn 0401	29.0	none	0.2	1.2	22.5	22.5	7.0	2.8	0.2	7.6	36.1	0
Second	Silica-Alumina	22.3	18.6	0	0.6	24.4	18.0	7.3	3.0	0.1	6.9	39.8	0
First	Zn 0401	23.9	none	0.4	1.5	24.7	19.0	6.4	2.4	0.1	7.1	38.4	0
Second	Co-Mo-0402	32.1	none	0	0.5	22.5	24.3	7.0	3.2	0.8	7.8	33.8	0
First*	G-72	34.9	none	0.1	0	22.8	26.6	7.2	2.7	0.2	9.8	30.6	0
Second*	Co-Mo-0402	36.2	none	0	0	23.4	27.4	6.8	2.7	0.6	10.2	29.0	0

* Input rate was 26 grams/hour.

Three catalysts have been tested: Engelhard 0.5% Pt on alumina, Socony silica-alumina cracking catalyst, Harshaw Co-Mo-0402 (containing 6% Co as the oxide) on silica. These catalysts were incorporated in the second reactor, which was fed with the product stream from the steam reforming reactor (ZnO catalyst). The results are shown in Table XII. The platinum catalyst lowered the hydrogen efficiency by promoting the methanation reaction. The silica-alumina catalyst gave large carbon deposition and lower hydrogen efficiency, probably reacting as:

$$H_2 + CO \longrightarrow C + H_2O \qquad (18)$$

The Co-Mo catalyst did increase the hydrogen efficiency (from 24% to 32% in the best test) but analysis of the product stream indicated that the increase was due to greater steam reforming rather than to NH_3 decomposition. In fact, the evidence indicated that this catalyst would have had no appreciable effect if it had not been coupled with a steam reforming catalyst that had been partially "poisoned" by carbon deposition.

Thus no effective NH_3 decomposition was realized, and this system did not appear very promising.

D. HIGH-TEMPERATURE STEAM REFORMING

1. Background

There is a simple justification for investigating steam reforming in the temperature range 600-800°C: the highest possible H_2 outputs can be realized at these conditions since thermodynamic equilibrium will prevail. It is possible to calculate the equilibrium composition of the product stream from thermodynamic data. Table XIII lists equilibrium compositions for this reaction in the temperature range 627-827°C. The calculation details are given in Ref. 3c.

An examination of these data shows that the CO content of the product stream will be relatively high at most of the conditions considered. Since, in these concentrations, CO is known to be deleterious to H_2 fuel cell anodes, this product stream could not be used directly in a fuel cell. Two possible routes were available:

(a) A third in-line reactor that would operate at 150-300°C with a standard commercial CO shift catalyst to effectively eliminate CO from the stream. With this approach the steam reforming conditions that lead to the lowest CH_4 content are preferred. From Table XIII these conditions are 827°C, 50 psig, 200% H_2O excess, and an H_2 efficiency of 99.8% is possible.

Table XIII

EQUILIBRIUM COMPOSITION OF HIGH TEMPERATURE AEROZINE-50 STEAM REFORMING

Temp, °C	Pressure, psig	H_2O Excess, %	Output Composition, mole-% *							Hydrogen Efficiency	Hydrogen Efficiency With CO Shift	Steam Reforming of UDMH %
			H_2	N_2	H_2O	NH_3	CH_4	CO	CO_2			
627	50	300	34.3	10.4	48.1	<0.1	1.7	1.3	4.2	80.7	83.7	76.3
627	50	100	40.0	15.4	33.8	<0.1	5.3	1.8	3.6	63.5	66.4	51.0
627	150	300	29.0	10.7	52.7	<0.1	3.5	0.8	3.2	66.1	67.8	53.0
627	150	100	33.5	16.1	39.0	0.1	7.8	0.9	2.5	50.9	52.3	30.3
627	50	200	37.1	12.3	41.9	<0.1	3.0	1.6	4.1	73.4	76.5	65.7
727	50	100	48.2	14.3	27.5	<0.1	1.4	4.7	3.9	82.2	90.1	85.5
727	50	200	42.6	11.8	37.3	<0.1	0.5	3.4	4.3	88.4	95.4	93.4
727	50	300	37.9	10.1	45.1	<0.1	0.2	2.5	4.3	91.8	97.9	96.8
727	100	200	40.9	12.0	38.8	<0.1	1.3	3.0	4.1	83.5	89.6	84.8
727	150	100	42.6	15.0	31.9	<0.1	3.9	3.1	3.4	69.3	74.4	62.5
727	150	300	35.7	10.2	46.8	<0.1	1.0	2.1	4.0	85.5	90.7	86.5
827	50	100	50.1	14.0	26.1	<0.1	0.2	6.3	3.3	87.7	98.6	98.0
827	50	200	43.2	11.7	37.0	<0.1	<0.1	4.3	3.8	90.5	99.5	99.3
827	50	300	37.8	10.0	45.1	<0.1	<0.1	3.2	3.8	92.0	99.8	99.6
827	150	100	48.5	14.2	27.4	<0.1	0.9	5.7	3.2	83.6	93.5	90.7
827	150	200	42.5	11.7	37.6	<0.1	0.3	4.2	3.7	88.4	97.1	96.0
827	150	300	37.4	10.1	45.5	<0.1	0.2	3.1	3.7	91.0	98.6	98.0
800	5	100	51.3	14.1	24.8	<0.1	<0.1	6.1	3.6	88.9	98.6	99.2

* None of these conditions lead to carbon deposition at equilibrium.

(b) A Pd membrane H_2 purification unit that would supply practically pure H_2 to the fuel cell. In this case the highest possible H_2 efficiencies from the steam reforming reaction are desired, regardless of product composition. The maximum yield cannot be determined directly from Table XIII; however, by making several reasonable assumptions the effect of H_2O excess and temperature on H_2 efficiency can be calculated. These assumptions and the details of the calculations are included in Ref. 3c. The optimum conditions are: 736°C, 421% H_2O excess, 50 psig, where an H_2 efficiency of 94.3% is expected.

2. Initial Results

Initial testing of high-temperature reforming was tried at 800°C with a single catalyst. However, the results were unfavorable because of excessive carbon deposition on the preheater chips in the catalyst bed. The reactant stream passed through a large temperature gradient in the preheater zone, and thermal cracking of the UDMH occurred. Several different methods of feeding were tried without much success. The experimental scheme finally used was to feed the reactant stream to a 450°C pre-reactor containing a ZnO catalyst where the initial steam-reforming reaction produced low molecular weight gases. The product composition was identical with that previously described for the intermediate temperature steam reformer. Carbon deposition was minimized in this reactor. The product stream was then fed directly to a second reactor, operating at 800°C and containing a commercial steam reforming catalyst (Girdler G-56B). This catalyst is specific for low-molecular weight hydrocarbons and is recommended for temperatures up to 1000°C. In later tests a CO shift reactor was added to the system to reduce the CO content of the product stream. A schematic diagram of the complete system is shown in Figure 5.

The results of initial testing with the double reactor are presented in Table XIV. At 800°C the measured output composition was well within experimental error of that calculated for equilibrium conditions (see Table XIV). A second series of tests were run, corresponding to the optimum conditions calculated for use with a Pd H_2 purification unit (750°C, 400% excess H_2O). The H_2 efficiency measured in this test was 90.4%, indicating the equilibrium conditions were not quite reached. Because of the large amount of excess water the mass flow rate through the reactor was much higher than in the preceding test. Possibly this explains the discrepancy in the results. Table XV summarizes the results of these tests.

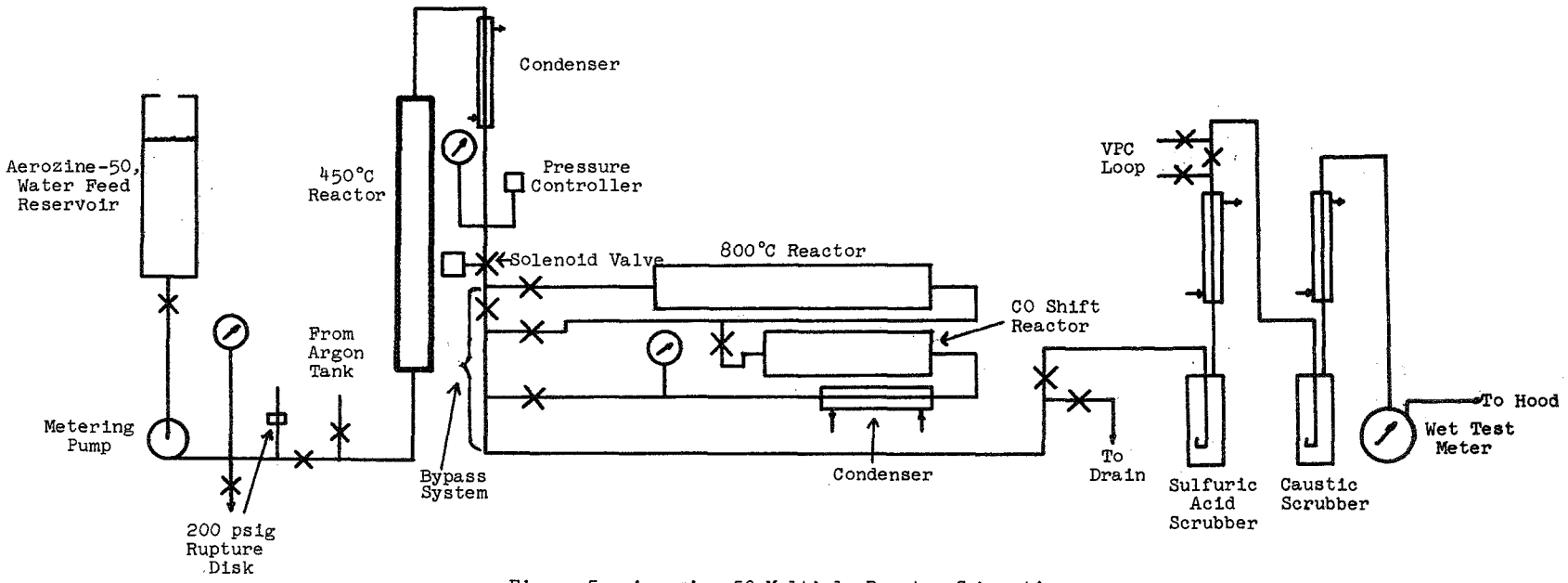

Figure 5. Aerozine-50 Multiple Reactor Schematic

Table XIV

HIGH TEMPERATURE STEAM REFORMING OF AEROZINE-50 WITH DOUBLE REACTOR SYSTEM

First Reactor: G-72, 100% ZnO at 450°C, 50 psig
Second Reactor: G-56B, Nickel base steam reforming catalyst at 800°C, 5 psig (average)
Total Input Rate: 20 grams/hour
Input Composition: (weight-%) 23.1% N_2H_4
23.1% UDMH
53.8% H_2O

Total Time*, hours	Running Time, hours	Output Composition, mole-%							Hydrogen Efficiency, %	H_2 Efficiency If CO Shifted to CO_2 in Third Reactor, %
		H_2	N_2	NH_3	CH_4	CO	CO_2	H_2O		
5.0	5.0	51.8	14.0	0.6	≈0	6.4	4.1	23.2	90.0	101.2
127.0	8.0	50.1	13.9	0.5	≈0	6.5	3.7	25.4	83.9*	94.8
175.0	11.0	51.9	14.0	0.1	≈0	5.8	4.6	23.7	88.8	101.2
178.0	14.0	51.9	14.8	0.2	≈0	5.2	4.2	23.7	92.0	101.2
202.0	18.0	51.3	14.7	0.2	≈0	5.7	4.9	23.2	87.3	97.2
226.0	24.0	51.9	14.0	0.2	≈0	5.6	4.4	23.6	90.4	100.1

* Carbon deposition took place in first reactor for a short time period.

Table XV

OUTPUT COMPOSITION OF HIGH TEMPERATURE STEAM REFORMING

Temperature: 750°C
H_2O Excess: 400%
Input Rates: 20.2 g/hr Aerozine-50
48.4 g/hr H_2O

Product Gas Composition, Mole-%					
H_2	N_2	NH_3	H_2O	CO	CO_2
37.3	9.8	0.5	45.8	2.5	4.1

Hydrogen Efficiency: 90.4%

The third series of tests, in which the CO shift reactor was added to the system, are summarized in Table XVI. The catalyst used to shift CO was a standard commercial catalyst with well proven characteristics (Girdler G-66B). The reaction was carried out at 200°C. The CO content of the stream was reduced from 2.5% to 0.5%, and the H_2 efficiency was increased to a maximum of 99.5%.

3. Long-Term Evaluation

Long-term testing on both the intermediate temperature and the high temperature steam reformers was done in a single experimental setup; the intermediate temperature reformer essentially served as a pre-reactor for the high-temperature reformer, which, in turn, fed the CO shift reactor.

The 1000-hour test was started 16 December 1965. The complete history of this test including operating parameters is reported in Table XVII, and the details on each analytical determination are included in Ref. 3d. The modest decrease in H_2 efficiency (from 98.7% to 95.6%) over the life of the test was caused by slight decreases in NH_3 decomposition and in steam reforming (CH_4 content higher). After 1000 hours the NH_3 in the output stream corresponded to only 3% of available nitrogen, and the CH_4 content to 2.4% of available carbon. The theoretical equilibrium composition listed at the bottom of Table XVII, was calculated by a computer program (Ref. 3d). The final output composition was very close to the theoretical values and indicates that near-equilibirum conditions were obtained even after 1000 hours of testing.

The H_2 efficiency of the first reactor (at 450°C) at the start of the test was 35%. The efficiency declined to 28% after 50 hours and subsequently to 11 $\pm$3% at 1000 hours. However, the ability of the high-temperature reactor to accept a large variation in composition of the feed stream is shown by the fact that the overall system efficiency declined very little. This is an indication of the reliability that could be obtained in such a multiple reactor system.

E. Pd MEMBRANE PURIFICATION OF STEAM REFORMER PRODUCT STREAM

1. Background

The objective of this task was to modify the impure H_2 stream from the steam reformer to supply ultrapure H_2 to the fuel cell. The gas composition from the reformer was 70% H_2, 17% N_2, 12.5% CO_2, with trace CO and CH_4. If the impurities could be eliminated, the stream could be used in any type of H_2 fuel cell without purge,

Table XVI

OUTPUT COMPOSITION FROM HIGH TEMPERATURE
STEAM REFORMING WITH CO SHIFT REACTOR

Three Reactor System

	Temp, °C	Pressure, psig	Catalyst	Bed Volume, ml
Reactor 1	450	50	G-72	43
Reactor 2	750	5	G-56B	86
Reactor 3	150-200	atm	G-66B	67

Input Composition, wt-%: 29.4 Aerozine-50, 70.6 H_2O

Test No.	Input Rate, g/hr	Output Composition, Mole-%							Hydrogen Efficiency, %
		H_2	N_2	NH_3	H_2O	CO	CO_2	CH_4	
74122	58.3	39.8	9.9	0.2	43.0	0.5	6.5	<0.1	96.2
74123	61.4	40.4	10.2	0.2	42.9	0.4	6.0	<0.1	99.5

Table XVII

1000 HOUR TEST OF HIGH TEMPERATURE STEAM REFORMER

Input Composition = 64.3% H_2O, 35.7% A-50 by weight; H_2O/C Mole Ratio = 6.0

Total Input Rate = 19.5 to 21.5 ml/hr; 7.25 to 7.65 gm/hr A-50

Reactor No.	Function	Press, Psig	Temp, °C	Catalyst
1	Prereactor	50	445-450	G-72, 100% ZnO, 1/8 in. extr.
2	Equil. Steam Reforming and NH_3 Decomp.	5	770-800	G-56B, Ni base, 1/8 in. tablets
3	CO Shift	5	255-275	G-66B, Promoted Fe_2O_3, 1/8 in. tablets

Reactor Tubes are 1 in. O.D. and 3/4 in. I.D.

Time, hrs	Hydrogen eff.	Amp - hr H_2 per Hr.	Total Mass Balance	Output Composition, Mole %							Composition to Fuel Cell after Stripping H_2O, NH_3 & CO_2 (Mole %)			
				H_2O	NH_3	CH_4	H_2	CO	CO_2	N_2	H_2	N_2	CH_4	CO
72	98.7	36.35	99.6	31.4	<.1	0	48.2	0.1	8.6	11.7	80.2	19.4	0	0.2
247	96.5	37.04	99.9	33.1	0.2	0	46.7	0.1	8.1	11.8	79.7	20.1	0	0.2
335	96.8	34.26	99.4	33.9	0.3	0	46.4	0.2	7.4	11.8	79.6	20.1	0	0.3
557	95.0	37.08	98.1	33.4	0.9	0	46.3	0.1	8.2	11.2	80.4	19.4	0	0.2
662	96.4	35.63	100.2	32.9	0.8	0.1	46.5	0.1	8.2	11.4	80.0	19.6	0.2	0.2
859	96.2	37.70	100.2	32.8	0.7	0.2	46.5	0.2	8.2	11.4	79.8	19.6	0.3	0.3
1000	95.6	33.55	101.7	33.5	0.7	0.2	46.1	0.2	7.8	11.5	79.5	19.9	0.3	0.3
		Theoretical Output Composition		32.7	<0.1	<0.1	47.5	0.2	7.9	11.7				

Note: for 24 watt fuel cell at 100% H_2 eff Amp/hr/hr needed = 26.63
at 80% H_2 eff Amp/hr/hr needed = 33.29

and the advantages might outweigh the disadvantages of increased complexity. We investigated Pd-Ag alloy membranes for this application.

Palladium membranes purify hydrogen-containing streams by selectively transporting hydrogen, presumably in atomic form, under an H_2 partial pressure gradient. The steps involved in this transport are:

a. Diffusion to the membrane surface from the gas phase;
b. Adsorption on the surface, and dissociation to atomic form;
c. Activated diffusion of atomic hydrogen through the membrane;
d. Recombination to molecular hydrogen at the surface; and
e. Desorption from the surface.

As long as the other gases are inert to the Pd membrane, the transfer rate depends on the temperature, the partial pressure of H_2 in the impure stream, and the pressure of the pure H_2 outlet.

Commercial Pd membrane units have been optimized and well characterized for the purification of H_2 streams. We selected a Model A-1-DH (J. Bishop and Co.), which consisted of a single Pd-Ag alloy tube, 1 ft long and 0.063 in. O.D. with a wall thickness of 0.003 in., closed at one end. The tube was mounted in a jacket that served as the impure stream purge manifold. Ultrapure H_2 exited through the open end of the Pd-Ag tube. The unit was rated at 1 SCFH of ultrapure H_2 at 370°C and 200 psig. The manufacturer supplied kinetic data for the unit in the form of transfer rate (cu ft/hr) of H_2 vs pressure of H_2 at various pure H_2 output pressures.

For 1 atm H_2 output pressure, the rate data can be represented by:

$$R_H \text{ (cu ft/hr)} = C_o P_{H_2} 0.85, \text{ where } P_{H_2} \text{ is psig.} \qquad (19)$$

With appropriate C_o, this represents the kinetic data within 1% over the range 0-100 psig H_2. To evaluate our experimental results, we calculated the maximum removal efficiencies for various pressures, input rates and compositions, including the possibility of connecting two units in series. The details of the computer program used in these calculations are given in Ref. 3e and some of the results of the calculations are shown in Figure 6. In general, removal efficiencies of 60% to 80% with a single unit are possible in the range of conditions used, and the efficiency can be increased to over 90% by using two units in series.

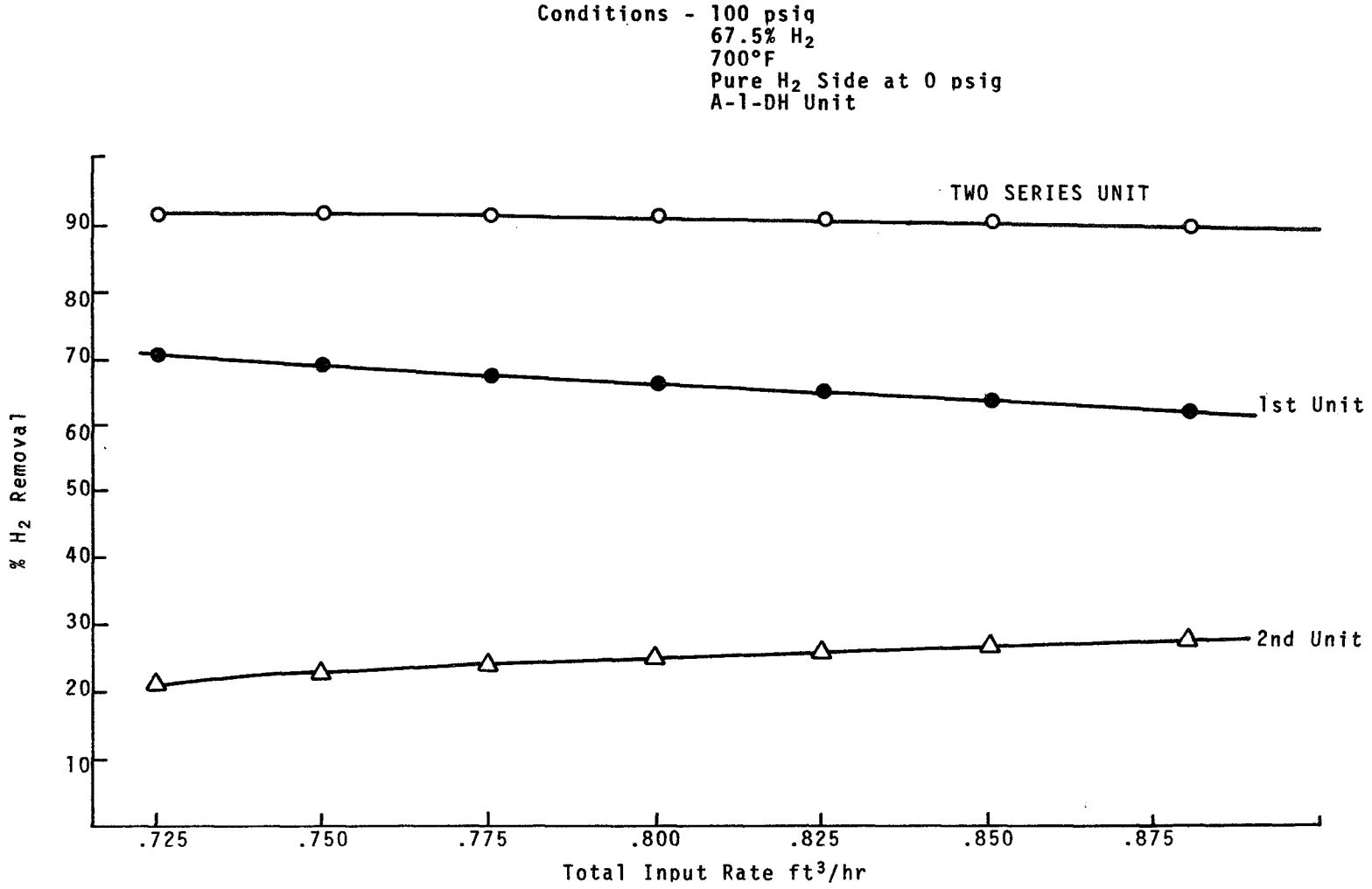

Figure 6. A-1-DH Pd. Diffuser Efficiency vs Total Input Rate

2. Results and Discussion

A schematic diagram of the equipment used in the experimental work is shown in Figure 7. A water trap condensed excess water from the stream reformer leaving the gas stream saturated with water vapor at 35-45°F. Provisions were made for analysis (by VPC) of the input stream, the exit stream from the diffuser jacket, and the ultrapure H_2 exit stream. Pressure in the jacket was maintained by a solenoid valve triggered by an adjustable pressure sensor. The volume output of each stream was measured with wet-test meters. Input rates were changed through a bleed valve in the input line.

Initial testing with tank H_2 indicated the unit was operating satisfactorily; the H_2 diffusion rates were within experimental error of the manufacturer's specifications. The unit was then operated on the reformer product stream in short-term testing.

The testing sequence was:

(1) Determine gas output rate (liters/hr) and composition from steam reformer over a 2-hr period.

(2) Switch stream to Pd diffuser and allow 30 min for equilibrium.

(3) Measure gas output rate (liters/hr) from ultrapure H_2 line and from bleed stream for 1 hr.

(4) Determine gas output composition from bleed stream, and check pure H_2 output for possible leaks.

Total gas rates to the diffuser were decreased by splitting the reformer stream ahead of the diffuser. Since the bleed stream was not constant, but rather was pulsed because of the type of pressure control used, residence times in the diffuser varied and the data at the lower input rates were less accurate than at the high rates. Adding to this inaccuracy was the fact that VPC analysis of this stream was more difficult because of the non-uniform residence times. Thus, the most accurate calculation of purification efficiency was from the volumes recovered from each gas stream. Data from these tests are compiled in Table XVIII.

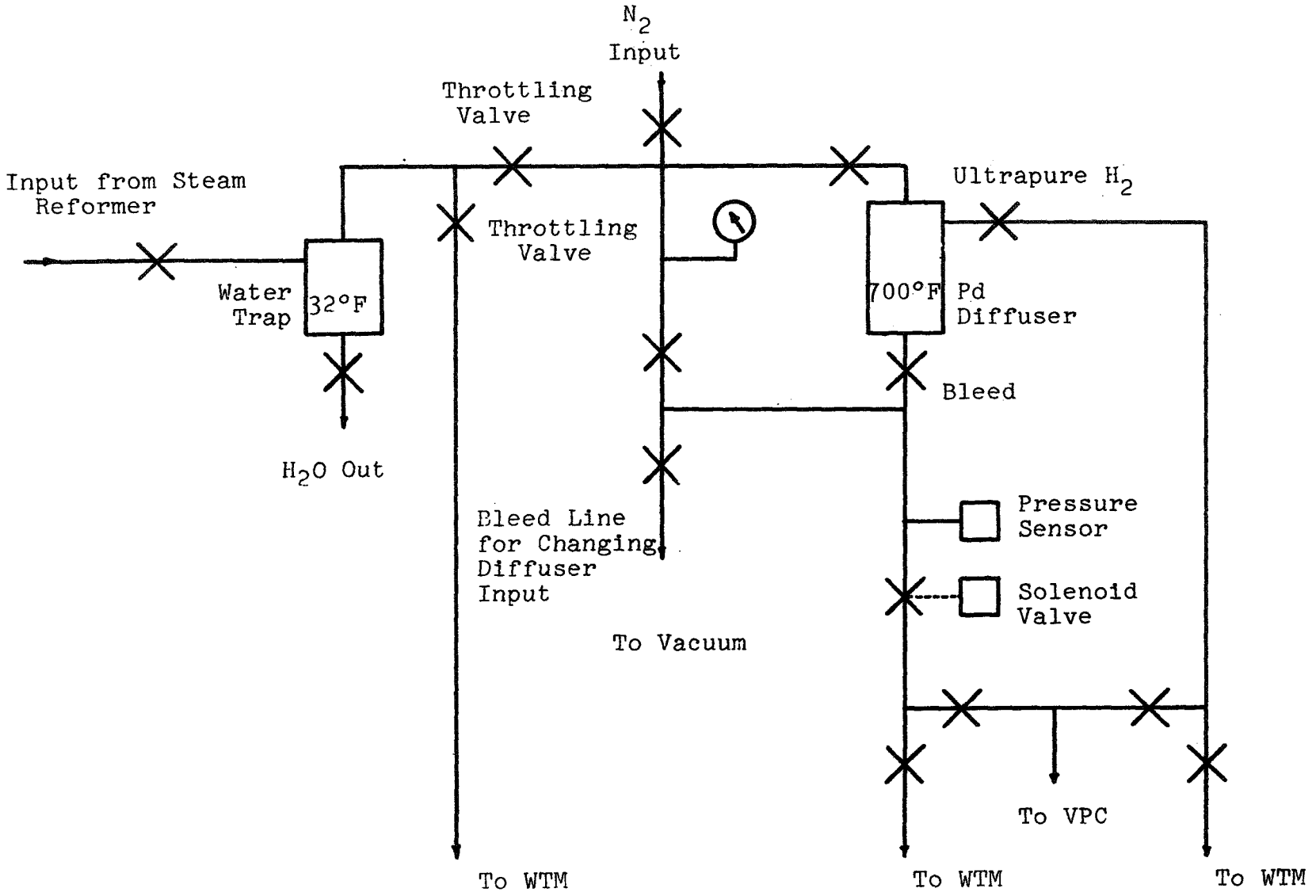

Figure 7. Schematic Diagram of Palladium Diffusion Hydrogen Purification Unit

Table XVIII

DATA FROM H_2 PURIFICATION OF STEAM REFORMING OUTPUT USING BISHOP MODEL A-1-DH PALLADIUM DIFFUSER

Diffuser Temp. 700°F ± 5°F; Ultrapure H_2 output pressure 1 atm.

Note: Tests are in chronological order, since improvement of the diffuser with time is suspected.

Input Pressure psig	Composition from Steam Reformer Mole % H_2	N_2	CH_4	CO	CO_2	Diffuser Input Rate ℓ/Hr*	Bleed Output ℓ/Hr*	UPH Output ℓ/Hr	Hydrogen Efficiency %	Bleed Output Comp. Mole % H_2	N_2	CH_4	CO	CO_2
50	69.8	17.2	0.3	0.1	12.6	25.9	21.0	4.9	27.1	62.4	20.8	0.4	0.6	15.9
100	68.3	17.6	0.9	0.1	13.1	25.5	16.4	9.1	52.4	53.7	25.7	1.6	0.5	18.6
100	"	"	"	"	"	8.94	4.72	4.22	68.2	-	-	-	-	-
100	69.2	18.0	1.0	0.2	11.6	12.37	6.79	5.58	65.2	-	-	-	-	-
100						11.66	5.78	5.88	72.9	39.1	34.1	1.9	2.2	22.5
100	"	"	"	"	"	7.22	3.22	4.00	80.0	-	-	-	-	-
100	"	"	"	"	"	"	"	"	"	-	-	-	-	-
100	"	"	"	"	"	10.58	4.58	6.00	81.9	-	-	-	-	-

* All rates corrected to 25°C, 1 atm.

Eighty percent H_2 recovery as ultrapure H_2 was obtained at the lowest input rate tested (7.22 liter/hr) at 100 psig input pressure. At 25 liters/hr input rate, 52% and 27% recovery was found at 100 psig and 50 psig, respectively. The following points are noteworthy:

(1) The diffuser system seemed to improve with time. Reasons for this might be removal of "poisons" caused by prior air contact, or changes in the membrane crystal structure in contact with the H_2 stream.

(2) The composition of the bleed stream was considerably higher in CO than can be accounted for by the change in volume due to loss of H_2 through the membrane. It seems probable that the reverse of the CO shift reactions was being catalyzed by the palladium surface through the reaction:

$$CO_2 + H_2 \longrightarrow CO + H_2O \qquad (20)$$

The excess water from the reformer was condensed out of the stream before it entered the diffuser and this would tend to favor the above reaction.

(3) The steam reforming equilibrium at 800°C yields 1.0% CH_4 at 100 psig compared to 0.3% CH_4 at 1 atm operating conditions used in the 1000-hr test. This higher pressure does not significantly decrease the reformer efficiency, but if still higher pressure were used to gain higher recovery of the H_2, its influence on the steam reforming efficiency would have to be taken into account fo optimum conditions.

Following these tests, the reformer-diffuser combination was run continuously for over 250 hours. During this period the effect of varying input rates and of throttling the output stream was also investigated. The results of these tests (Table XIX) are in chronological order over the 250-hour period. Examination of these data indicate the following:

(1) There was no degradation in performance of the unit over the 250-hour period, (compare tests 3 and 15) and the experimentally observed efficiencies were within experimental error of the calculated values.

Table XIX

250 - HOUR TEST OF DIFFUSER

Conditions: 700°F
Pure H_2 Outlet at 0 Psig.

Test No.	Total Input Rate ft^3/hr	Total H_2 in Input Stream mole %	Total H_2 in Input Stream ft^3/hr	Pressure Psig	Experimental Eff. %	Experimental Pure H_2 ft^3/hr	Calculated** Eff. %	Calculated** Pure H_2 ft^3/hr	Throttling*
1	0.819	67.5	0.553	100	38.9	0.215	65.5	0.362	O
2	0.814	67.5	0.549	100	49.6	0.273	65.7	0.361	M
3	0.789	67.5	0.533	106	68.3	0.364	69.8	0.369	H
4	0.799	67.5	0.539	105	65.2	0.352	68.3	0.368	H
5	0.792	67.5	0.535	108	67.5	0.361	70.0	0.375	H
6	0.805	67.5	0.543	103	64.5	0.351	66.7	0.362	H
7	0.811	67.5	0.547	107	66.9	0.366	67.9	0.371	H
8	0.800	67.5	0.540	98	38.0	0.205	65.0	0.351	O
9	0.703	67.5	0.475	109	73.4	0.349	76.5	0.363	H
10	0.720	67.5	0.486	109	73.7	0.358	75.5	0.367	H
11	1.181	66.3	0.783	108	51.7	0.405	51.4	0.402	H
12	1.205	66.3	0.799	100	49.2	0.393	47.5	0.380	O
13	1.190	66.3	0.789	103	51.0	0.402	49.2	0.388	M
14	1.173	66.3	0.778	104	53.5	0.416	50.2	0.390	H
15	0.779	67.5	0.526	100	66.2	0.348	67.1	0.353	H
16	0.523	67.5	0.353	108	86.1	0.304	86.9	0.307	H

*Throttling the output from the diffuser gave more uniform flow raising the efficiency to near calculated values. O-no throttling, M-medium throttling, H-high throttling.
**Calculated by computer from kinetic data; assumes steady state flow.

(2) Throttling the output stream had a decided effect on efficiency: higher throttling produced higher efficiencies (compare tests 1, 2, 3). Throttling tended to reduce the gas surge through the diffuser jacket when the solenoid valve opened and thus increased the average residence time in the diffuser.

(3) The effect of input rate on performance was within experimental error of calculated values. These results confirmed the calculations and showed the validity of the calculation method for extrapolating the performance to larger units.

In general, the testing results were quite promising, demonstrating that very reasonably sized purification units can be assembled that will operate at high efficiency and reliability for a minimum of 250 hours.

F. CONCLUSIONS AND SYSTEM COMPARISONS

1. System Comparisons

A full systems analysis has not been attempted. However, enough data are now available to allow a meaningful comparison of the advantages and disadvantages of each system with respect to a number of important parameters. To be relevant, such a comparison must be directed to the end use: the production of electric power in a fuel cell in a space environment. The reformer can be considered a "black box" whose sole function is to modify a fuel feed stream so that it can be more readily used in a fuel cell. In this kind of analysis the characteristics and requirements of the fuel cell itself are as important as the characteristics of the reformer, and the limitations of both components must be considered.

a. Weight of Fuel Required for a Given Electrical Output

The ampere-hours of H_2 produced from a given weight of fuel for each system are listed in Table XX, based on current experimental data. The data for the liquid phase reactor are straightforward since Aerozine-50 is the only feed. However, the steam reformer feed stock includes a large portion of H_2O which complicates the analysis. If it is assumed that all necessary H_2O is carried along separately on a space mission, then the relevant factor is the ampere-hours/g total feed.

Table XX

SYSTEM COMPARISONS

	System No.	Electrical Output Factors: Ampere-Hours H_2 per g Aerozine-50	Electrical Output Factors: Ampere-Hours H_2 per g Aerozine-50 and Stoichiometric H_2O	Electrical Output Factors: Ampere-Hours H_2 per g Total Input*	Product Stream Composition: % of H_2 In Off-Gas	Product Stream Composition: % of CO In Off-Gas	Product Stream Composition: Other Contaminants	Heat Balance kcal/mole Aerozine-50**
Liquid Phase Low Temperature	1	0.894	-	0.894	59.0	0	UDMH, N_2, DMA, NH_3	- 7.9
Single Catalyst 450°C	2	1.369	0.744	0.561	56.6	1.4	N_2, CH_4, and water soluble species	- 5.6
Medium Temperature with NH_3 Decomposition	3	No better than single catalyst.						
High Temperature 800°C Reforming	4(a)	3.171	1.723	1.299	67.9	7.8	N_2, CH_4, and water soluble species	+17.4
High Temperature 800°C Reforming with CO Shift	4(b)	3.502	1.903	1.435	70.2	0.8	N_2, CH_4, and water soluble species	+17.6

* Based on 100% excess water for steam reforming.

** - means exothermic, + means endothermic.

However, the fuel cell reaction produces water as a by-product, and it seems reasonable to recycle this water to reduce the total system weight. Calculations show that enough water is available from the fuel cell reaction to continuously supply the reformer with the stoichiometric requirements as well as a reasonable excess. The details are presented in Ref. 3c.

b. Product Stream Composition

The use of a Pd membrane H_2 purification unit would allow a pure H_2 fuel cell feed stream, regardless of the composition of the impure reformer stream. If such a unit is not used, the impurities in the reformer stream become important.

The presence of CO in the product stream from the reformers has been discussed previously. Fuel cell anodes have been reported that will accept up to 1% CO in the H_2 feed (Ref. 7). Thus, system 4 with a CO shift reactor may produce a directly usable stream.

The presence of N_2 in the product stream from all the systems is important because this dictates a purge on the fuel cell anode to maintain sufficient H_2 concentrations in the cell. Since some amount of H_2 will be lost through this process, the system efficiencies are correspondingly reduced.

All other possible contaminants can be accounted for as follows. In system 1, UDMH, NH_3, and possibly some amines (from UDMH decomposition) will also be present. The use of such a stream directly is somewhat questionable, and the effect of each would have to be determined in cell tests. All are basic compounds and it is reasonably certain that an acid electrolyte cell could not accept this stream without prior purification.

For the steam reforming systems, all contaminants not previously discussed are either water soluble (e.g., NH_3, CO_2, DMA, etc) or inert (CH_4, ethane). The water-soluble components will concentrate in the condensed excess water in the reformer output. A phase separation can be used to remove these components.

c. Heat Balance

Heat balances were calculated for each system and are included in Table XX. The calculation details are included in Ref. 3c. Systems 1 and 2 are moderately exothermic and cooling will be required to maintain the reactor temperature. With proper hardware design a balance might be possible through simple radiation losses. System 4 is definitely endothermic and heat will have to be supplied to maintain operating temperatures. The most likely method of supplying this heat is by hypergolically burning Aerozine-50 and N_2O_4. This means that some of the Aerozine-50 input to the reactor must be diverted. Calculations show that 0.07 mole of Aerozine-50 will be required for heating 1 mole of Aerozine-50 in the reformer. This limits the maximum efficiency to 93.3%.

d. Temperature

The problem of removing waste heat from spacecraft, the potential hazards involved in operating equipment at high temperature, materials problems, etc, all dictate operating at as low a temperature as possible. However, final system efficiencies and other considerations may modify the choice. Trade-off studies are required to characterize the possible choices.

e. Operating Life

The potential operating life of the multiple reactor steam reforming system is well established by the results of the 1000-hour test.

The results with the liquid phase reactor are not as promising because of the drop in efficiency experienced with the best catalysts tested. A feasible system for this application may depend upon a periodic regeneration of the catalyst (e.g., a periodic flush with H_2O), and the development of a physically stronger catalyst.

The best intermediate temperature reactor (the pre-reactor in the multiple system) also showed a marked decrease in performance that was due to a gradual buildup of carbon deposits on the catalyst. This situation could undoubtedly be improved by higher H_2O contents in the feed stream and larger amounts of catalyst.

2. Conclusions and Recommendations

The most promising system based on overall performance is undoubtedly the multiple reactor steam reformer. We have demonstrated a combined steam reforming-CO shift reactor system that produces with high efficiency a fuel cell gas feed stream composed of 70 mol-% H_2, 18 mol-% N_2, 12 mol-% CO_2 (after separation of the excess H_2O). The CO content of the stream is 0.3 mol-% or less. This stream could be fed directly to a fuel cell with a CO_2 rejecting electrolyte (either acid, carbonate or acid ion exchange membrane). If the CO_2 content of the stream were scrubbed out, the stream could be used with any fuel cell electrolyte. A CO-tolerant anode catalyst would be necessary. If a Pd membrane purification unit were used, the stream could be used with any H_2-utilizing fuel cell since a completely pure H_2 stream would result.

In further work with the multiple reactor steam reformer it is recommended that a much more careful parametric study be made of both the individual components and the overall system. In particular, the effect of residence time, H_2O excess, temperature, and pressure should be determined for each reactor to ensure proper design and operation of the components in the final module. The possibility of entirely eliminating the pre-reactor by proper design of a preheater should be explored. The response to transient changes in operating conditions should be determined in order to delineate the amount of measurement-control equipment necessary. Finally, the operation of the entire system at a single pressure in the range 25 to 100 psig should be determined in an effort to eliminate the compressor requirements for the Pd diffuser.

IV. DECOMPOSITION OF N_2O_4 TO PRODUCE AN OXYGEN-RICH FEED STREAM

A. BACKGROUND

The objective of this task was to decompose nitrogen tetroxide to N_2 and O_2 in a simple catalytic flow reator to provide an oxygen-rich stream for a fuel cell. The decomposition of N_2O_4 occurs in several steps, depending on the conditions used. It is generally accepted that the decomposition occurs as shown below.

$$N_2O_4 \rightleftharpoons 2NO_2 \qquad (21)$$

ΔH = +13.9 Kcal/g-mole
complete to NO_2 above 140°C

$$2NO_2 \rightleftharpoons 2NO + O_2 \qquad (22)$$

ΔH = +13.5 Kcal/g-mole
complete to NO above 600°C

$$2NO \longrightarrow N_2 + O_2 \qquad (23)$$

ΔH = -21.5 Kcal/g-mole
catalytic

Reactions 21 and 22 are homogeneous and reversible (Ref. 8). It is evident that any oxygen liberated by reaction (22) must be used or otherwise removed from the reaction site before the temperature is reduced. The oxygen liberated by reaction (23) is not recombined when the temperature is reduced. Thus, the decomposition of N_2O_4 really depends on the catalytic dissociation of NO.

Several investigators have found that NO can be decomposed on suitable catalysts when it is contained in high dilution in a stream of inert gas or in a stream containing carbon monoxide (Refs. 9,10). It is interesting to note that in the reported work there were indications that reaction products, particularly oxygen, interfere with the decomposition of nitric oxide.

Several studies (Refs. 11, 12) have been made at much higher temperatures (800-1400°C) where nitric oxide (NO) has been decomposed. It is not clear if these results were thermal or catalytic decomposition. In reviewing this work it also becomes apparent that there is some disagreement about the reaction products formed.

The greatest difference between the work done in our study and that done by previous workers is in the concentration of nitrogen oxides in the reactor stream. In the earlier work a maximum of 2000 ppm NO_2 or NO in the gas stream was used. In the work reported here pure N_2O_4 was fed to the reactor with no inert gas dilution.

B. INITIAL CATALYST SCREENING

1. Equipment and Procedure

Our approach to finding the best catalysts and operating conditions for decomposing N_2O_4 to nitrogen and oxygen is based on studies utilizing the reactor shown schematically in Figure 8. This reactor system was designed to permit operation from 50-800°C, using a wide range of flow rates. The residence time and space velocity of the reactants can also be varied easily. The analysis of the product stream is determined by cooling the gas stream from the reactor and passing it through a time delay tube of adequate residence time to assure that reaction (22) is complete to NO_2.

The calculation of the tube size was based on the work of Treacy and Daniels (Ref. 13). This calculation was checked using high flow rates of N_2O_4 thermally decomposing to NO + O_2 at 600°C and feeding the mixture to the delay tube. A cold trap following the tube collected the N_2O_4 formed. No gas was detected downstream from the trap, indicating all the NO + O_2 had recombined.

The NO_2 in the product stream was condensed and frozen out in the cold trap using a Dry Ice/Triclene mixture. The remaining products (NO, N_2, O_2) were passed to a wet-test meter for total volume or to either a VPC or oxygen analyzer for composition determination.

The reactor temperature was measured and controlled using iron-constantan thermocouples with a West controller and a Honeywell recorder. The feed flow rates were determined using calibrated flow meters manufactured by Brooks Instruments.

Each catalyst was packed in a 3/4-in. ID stainless steel tube to the depth of 12 inches. The remainder of the tube was then filled with porcelain chips to provide preheating of the gas stream and support for the catalyst bed. Initial tests consisted of heating the tube to four temperatures (200, 400, 600, and 800°C) while passing N_2O_4 through it.

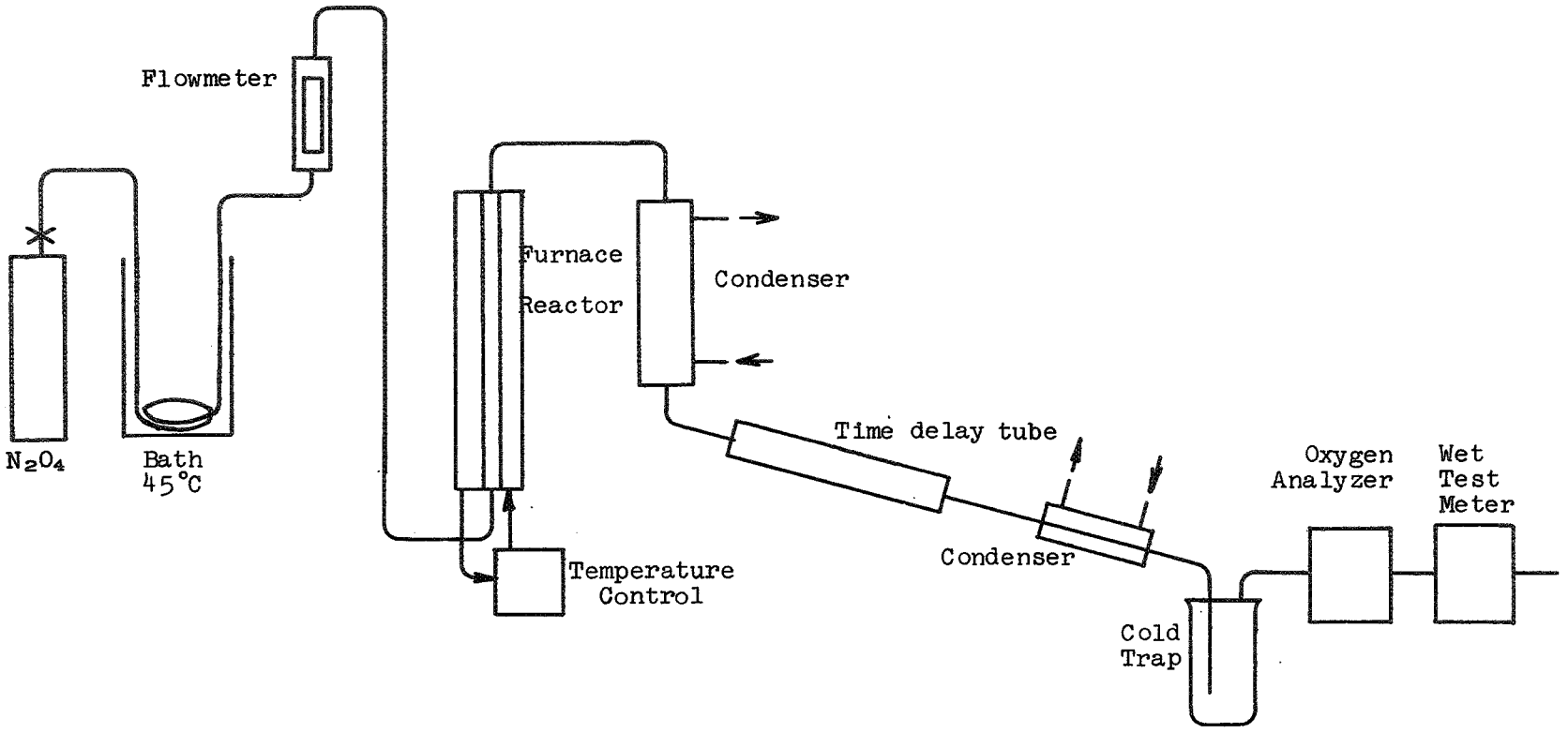

Figure 8. N_2O_4 Reactor Flow Diagram

2. Results and Discussion

Twenty-two catalysts were screened initially. Data in Table XXI show that none of them exhibited sufficient activity to be useful at temperatures below 750-800°C. Detailed data on all catalysts tested are included in Refs. 3a,b,c).

The screening tests were performed using 20 grams per hour of N_2O_4 feed. At this feed rate, 100% decomposition of the N_2O_4 would yield 0.511 cu ft/hr of gas of the composition 66.6 mol-% O_2, 33.3 mol-% N_2. The highest gas evolution rate obtained was 0.32 cu ft/hr of a gas that approximates the 2:1-O_2:N_2 mole ratio (see Test 77457-1, Table XXI) which represents a conversion efficiency of 62.6%. This was obtained using a 0.5% platinum catalyst at 800°C. With other catalysts having some activity at 800°C, the gas evolution rate was reduced by at least 50% when the temperature was lowered to 700°C.

The noble metals have shown activity for decomposing N_2O_4. The extent of this activity appears to be related to the support used or the method of application to the support. Tests 77433 and 77455 illustrate this behavior. In both tests, the active material was platinum and the support was alumina. The catalysts were prepared by different suppliers, and the performance difference at 800°C is obvious.

The palladium catalyst tested showed the same order of activity at 800°C as the best platinum catalyst. Test 77441 indicated the gas evolution rate change as the temperature was lowered. This catalyst was active in the 750-800°C range, and was only mildly active at 700°C. No activity was apparent at 650°C.

A test of the rhodium catalyst showed only mild activity at 800°C (see Test 77444).

Nickel, copper, iron, and silver metals were tested. Where the reduced metal was the active material on the support, the metal was oxidized at 200 and 400°C by the N_2O_4 (see Test 77429, 77437, and 77453). The gas evolved during this portion of the tests was mostly nitrogen. The composition shifted gradually to nitric oxide just before the flow stopped, indicating the oxidation of the catalyst was complete. Only trace amounts of oxygen were found. At higher temperatures these catalysts exhibited no activity for decomposing N_2O_4.

One of the catalysts, containing copper oxide on supported alumina, was active for N_2O_4 decomposition (see Test 77461). This catalyst, although not as active as platinum or palladium catalysts, does not appear to have the great absorption for oxygen that caused the delay in operation observed with the Pt and Pd catalysts. The catalyst did display the typical decrease of activity as the temperature was reduced from 800°C (see Tests 77462-2 and 77462-3).

Table XXI

N_2O_4 REFORMING DATA

N_2O_4 Feed Rate: 20 g/hour

Run No.	Catalyst	Reactor Temp, °C	Gas Evolved, ft^3/hr	Run Duration, hours	Notes
72102-1	Baker 0.5%Pd lot 3107	198	0	0.75	Wet test meter reversed as volume reduced during run.
72102-2	Baker 0.5%Pd lot 3107	399	0	2.0	
72102-3	Baker 0.5%Pd lot 3107	600	0	1.0	
72102-4	Baker 0.5%Pd lot 3107	800	7.5×10^{-2}	1.50	Gas sample: O_2/N_2 = 1.5 mole/mole 100% decomposition yield = 0.511 ft^3/hr; N_2O_4 decomposition 14.7%**
72103-1	Baker 0.5%Pd lot 3107	800	13.2×10^{-2}	7.0	Gas sample: O_2/N_2 = 1.95 mole/mole
72106-1	Pt-Rh gauze (90/10-80 mesh)	200	0.1×10^{-2}	1.0	Rate too low for VPC analysis
72106-2	Pt-Rh gauze (Engelhard)	400	0.2×10^{-2}	2.0	
72106-3	Pt-Rh gauze	600	0	1.0	
72107-1	Pt-Rh gauze	800	0.45×10^{-2}	1.50	Rate too low for VPC analysis
77426-1	Norton Zeolon®H-BPS	200	0.18×10^{-2}	1.0	Rate too low for VPC analysis
77426-2	Norton Zeolon H-BPS	400	0.02×10^{-2}	1.0	
77426-3	Norton Zeolon H-BPS	600	0.25×10^{-2}	1.0	
77426-4	Norton Zeolon H-BPS	800	0.8×10^{-2}	1.0*	
77426-4	Norton Zeolon H-BPS	800	0.4×10^{-2}	0.75*	
77429-1	G-49A (Girdler-reduced	202	31.2×10^{-2}	0.6	VPC analysis N_2 + NO
77429-2	G-49A Ni on Kieselguhr)	400	41.0×10^{-2}	0.9	VPC analysis N_2 + NO
77429-3	G-49A	600	1.2×10^{-2}	1.0	Thermocouple opened
77433-1	G-43 Pt (Girdler)	200	2.8×10^{-2}	1.0	
77433-2	G-43 Pt	400	0	1.0	
77433-3	G-43 Pt	600	0	1.0	
77433-4	G-43 Pt	800	9.4×10^{-2}	2.7	VPC analysis N_2 and trace O_2
77433-5	G-43 Pt	750	3.7×10^{-2}	1.25	
77433-6	G-43 Pt	700	1.4×10^{-2}	0.5	Rate too low for VPC analysis

* Gas was measured after the first hour and after the next 3/4 hour in run 77426-4.

** Not steady state conditions.

Table XXI(Continued)

Run No.	Catalyst	Reactor Temp, °C	Gas Evolved, ft^3/hr	Run Duration, hours	Notes
77462-2	Cu-0803	750	9.2×10^{-2}	1.0	18% N_2O_4 decomposed**
77462-3	Cu-0803	700	6.0×10^{-2}	0.25	11.8% N_2O_4 decomposed**
77450-1	MRC Pt-Hg (MRC Proprietary)	200	1.1×10^{-2}	0.75	Contained no O_2
77450-2 thru 77450-12	MRC Pt-Hg	400-600	0	4.75	Gradual temperature increase during run
77450-13	MRC Pt-Hg	800	4.3×10^{-2}	4.3	VPC - 1.9 to 1 mole ratio O_2:N_2 8.4% N_2O_4 decomposed**
77452-1	Ag-101E (Harshaw-Ag on Alumina)	200	3.4×10^{-2}	1.0	N_2 - flow stopped after 30 minutes
77452-2	Ag-101E	400	0	1.0	
77452-3	Ag-101E	600	2.1×10^{-2}	1.0	N_2 - flow stopped after 15 minutes
77452-4	Ag-101E	800	0	1.5	
77453-1	Cu-0402T (Harshaw-copper chromite on Alumina)	200	4.9×10^{-2}	1.0	N_2 - oxidizing catalyst
77453-2	Cu-0402T	400	2.4×10^{-2}	1.2	N_2 - oxidizing catalyst
77453-3	Cu-0402T	600	0.1×10^{-2}	0.8	Flow stopped
77453-4	Cu-0402T	800	0.3×10^{-2}	0.75	Too small for VPC
77454-1	Ni-4305E (Harshaw-Ni, Tungsten on Alumina)	200	3.9×10^{-2}	1.0	Flow stopped after 45 minutes
77454-2	Ni-4305E	400	0	1.0	Oxidizing catalyst
77454-3	Ni-4305E	600	0	1.0	
77454-4	Ni-4305E	800	0	1.0	
77455-1	II-077 (0.5% Pt) (Engelhard, on Alumina)	200	3.7×10^{-2}	1.1	Oxidizing catalyst
77455-2	II-077 (0.5% Pt)	400	0	1.3	Flow stopped at 1 hour
77455-3	II-077 (0.5% Pt)	600	0.2×10^{-2}	1.0	
77455-4	II-077 (0.5% Pt)	800	23.0×10^{-2}	0.75	45% N_2O_4 decomposed**
77455-5	II-077 (0.5% Pt)	200-800	5.0×10^{-2}	7.0	Linear program approximately 100°C/hour rate given is maximum for 700-800° portion of test

** Not steady state conditions.

Table XXI (Continued)

Run No.	Catalyst	Reactor Temp, °C	Gas Evolved, ft^3/hr	Run Duration, hours	Notes
77445-1	Ag-Hg (Proprietary)	200	5.9×10^{-2}	0.92	Catalyst oxidizing
77445-2 thru 77445-12	Ag-Hg	400-490	2.0×10^{-2}	*	Flow stopped and traps backed up as temperature was raised
77445-13	Ag-Hg	500	0	0.5	
77445-14	Ag-Hg	550-600	0	*	
77445-15	Ag-Hg	800	0.2×10^{-2}	1.0	
77447-1	Pd-Hg (Proprietary)	200	7.45×10^{-2}	1.0	Catalyst oxidizing
77447-2 thru 77447-9	Pd-Hg	400-500	0	*	
77447-10	Pd-Hg	600	0	0.25	
77447-11	Pd-Hg	800	0	0.57	
77457-1	II-077 (0.5% Pt) (Engelhard, on Alumina)	800	32.0×10^{-2}	0.75	Nearly steady gas evolution rate for 45 minutes; 62% N_2O_4 decomposed
77457-2	II-077 (0.5% Pt)	800	18.0×10^{-2}	0.5	Argon saturated with H_2O added at 4×10^{-2} ft/hr rate
77457-3	II-077 (0.5% Pt)	800	24.0×10^{-2}	1.1	Nearly steady gas evolution rate for 68 minutes; 47% N_2O_4 decomposed
77457-4	II-077 (0.5% Pt)	800	8.0×10^{-2}	1.0	Helium saturated with H_2O added at 10×10^{-2} ft^3/hr
77460-1	Cu-2501 (Harshaw-$CuCo_3$ on Silica)	200	3.6×10^{-2}	1.0	Flow stopped at 32 minutes
77460-2	Cu-2501	400	0	1.0	
77460-3	Cu-2501	600	0	1.0	
77460-4	Cu-2501	800	0	1.0	
77461-1	Cu-0803 (Harshaw-CuO on Alumina)	200	1.1×10^{-2}	1.0	Flow stopped at 30 minutes
77461-2	Cu-0803	400	)	1.0	
77461-3	Cu-0803	600	2.5×10^{-2}	0.9	
77461-4	Cu-0803	800	9.4×10^{-2}	1.0	
77461-5	Cu-0803	800	12.4×10^{-2}	1.0	VPC - 1.95 to 1 mole ratio $O_2:N_2$ 24% N_2O_4 decomposed**

* Temperature program approximately 10°C/hour.
**Not steady state conditions.

Table XXI (Continued)

Run No.	Catalyst	Reactor Temp, °C	Gas Evolved, ft^3/hr	Run Duration, hours	Notes
77436-1	T-309 (Girdler-	200	1.0×10^{-2}	1.0	
77436-2	T-309 Pt oxide on	400	0	1.0	
77436-3	T-309 Alumina)	600	0	1.0	
77436-4	T-309	800	1.2×10^{-2}	1.0	Rate too low for VPC analysis
77437-1	Ag-Alumina (Proprietary)	200	5.1×10^{-2}	1.0	Decreasing rate indicating oxidation of catalyst
77437-3	Ag-Alumina	300	0	1.0	
77437-4	Ag-Alumina	348	0.1×10^{-2}	1.0	
77437-5	Ag-Alumina	396	0	0.75	
77437-6	Ag-Alumina	600	0	1.0	
77438-1	Ag-Alumina	200-240	0	2.0	
77439-1	T-366 (Girdler-Cu 55%)	204			Reactor blocked
77440-1	G-47 (Girdler-Iron oxide)	200	2.7×10^{-2}	1.0	Flow stopped at 33 minutes
77440-2	G-47	400	2.5×10^{-2}	1.0	Flow stopped at 15 minutes
77440-3	G-47	600	0	1.0	
77440-4	G-47	800	0	1.0	
77441-1	0.5% Pd (Engelhard on	200	3.7×10^{-2}	1.0	Flow stopped at 46 minutes
77441-2	0.5% Pd activated	400	0.7×10^{-2}	1.0	
77441-3	0.5% Pd Alumina)	600	0	1.0	
77441-4	0.5% Pd	800	4.9×10^{-2}	1.0	No VPC analysis made
77441-5	0.5% Pd	750	0	0.5	
77442-1	0.5% Pd (Engelhard on	700	3.2×10^{-2}	1.0	Rate falling after 23 minutes
77442-2	0.5% Pd activated	800	4.8×10^{-2}	1.0	
77442-3	0.5% Pd Alumina)	750	28.0×10^{-2}	0.25	May be due to attempted temperature change and overshoot; no VPC analysis
77442-4	0.5% Pd	700	1.6×10^{-2}	1.0	
77442-5	0.5% Pd	650	0	0.75	
77443-1	CaO (Fisher	200	0.7×10^{-2}	1.0	
77443-2	CaO Scientific)	400	0.8×10^{-2}	1.0	
77443-3	CaO	600	0	1.0	Run terminated; trap's backed up
77444-1	0.5% Rh (Engelhard on	200	0.4×10^{-2}	0.8	Flow stopped at 17 minutes
77444-2	0.5% Rh Alumina)	400	0	0.75	
77444-3	0.5% Rh	600	0	1.0	
77444-4	0.5% Rh	800	3.2×10^{-2}	1.0	No VPC analysis made

The acid zeolite and base-type materials exhibited no activity (see Tests 77426 and 77443).

Fifteen other catalysts were evaluated before the reactor system was rebuilt. The results of these tests are given in Table XXII. The N_2O_4 input rate in these tests was 20 g/hour. The output expected for 100% conversion is 0.511 cu ft of gas (STP) consisting of 66.6 mol-% O_2 (remainder N_2). The short testing period did not allow equilibrium to be reached. However, a comparison of the evolution rates between catalysts at identical conditions is sufficient to show which catalysts are active enough to warrant more extensive testing. In this series of tests the following catalysts showed the best activity:

2% Pd on alumina

0.5% Pt on a molecular sieve base

10% CuO on alumina

G-12 nickel

C. SECONDARY CATALYST SCREENING

1. Equipment Modifications

The experimental reactor modifications had two objectives: (1) to allow continuous (overnight) operation so that catalyst activities could be evaluated over longer time periods; and (2) to allow four reactor tests to be run at identical conditions simultaneously. The first objective was considered necessary because there were definite indications that catalyst activity can vary greatly with time. For example, the precious metal catalysts appeared to improve after an initial conditioning period, while CuO catalysts appeared to deteriorate. Overnight operation was essential to reliably determine behavior. The multiple reactor design offers several advantages. Besides increasing the screening capabilities, the possibility of connecting any or all of the reactors in series would greatly expand the residence time available for characterizing a single catalyst.

A schematic of the modified equipment is shown in Figure 9. The operation of this reactor was essentially the same as for the screening reactor; however, control and instrumentation equipment were added. Since input rates are much more critical for actual catalyst characterization (as opposed to simple screening for gross activity), the flow meters were carefully calibrated by two independent methods.

Table XXII

CATALYTIC DECOMPOSITION OF N_2O_4

Run No.	Catalyst	Reactor Temp, °C	Gas Evolved, ft^3/hr	Run Duration, hr	Notes
77460-1	Cu-2501T	200	3.6×10^{-2} *	1.0	Flow stopped at 32 minutes
77460-2	6% Copper	400	0	1.0	
77460-3	Carbonate	600	0	1.0	
77460-4		800	0	1.0	
77461-1	Cu-0803T	200	1.25×10^{-2}	1.0	Flow stopped at 30 minutes
77461-2	10% Copper	400	0	1.0	
77461-3	Oxide	600	2.3×10^{-2}	1.0	
77461-4		800	9.4×10^{-2}	1.0	
77461-4 Cont.		800	12.4×10^{-2}	1.0	
77462-1	Cu-0803T	750	9.2×10^{-2}	1.0	
77462-1 Cont.	10% Copper Oxide	700	6.0×10^{-2}	0.25	
77463-1	Cu-0905T	200	2.5×10^{-2}	1.0	Flow stopped at 30 minutes
77463-2	10% Copper	400	0	0.83	
77463-3	Chloride	600	0	1.0	
77463-4		750	0.35×10^{-2}	1.25	
77464-1	Cu-0307T	200	2.6×10^{-2}	1.0	Flow stopped at 30 minutes
77464-2	99% Copper	400	0	1.0	
77464-3	Oxide	600	0		
77464-4		750	5.4×10^{-2}	1.0	
77466-1	4747 0.5%	200	0.5×10^{-2}	1.0	Flow stopped at 30 minutes
77466-2	Rhodium	400	0	1.0	
77466-3		600	0.9×10^{-2}	0.83	
77466-4		775	12.8×10^{-2}	0.25	
77467-1	G-33A Nickel	200	6.1×10^{-2}	1.0	
77467-2	Oxide	400	7.4×10^{-2}	1.0	VPC Analysis - NO
77467-3		600	0	1.0	
77467-4		800	3.7×10^{-2}	1.0	
77468-1	G-12 Nickel	200	11.4×10^{-2}	1.0	
77468-2		400	6.6×10^{-2}	0.5	
77468-3		600	0.9×10^{-2}	1.0	Flow stopped at 40 minutes
77468-4		800	32.8×10^{-2}	1.0	
77468-4 Cont.		800	26.6×10^{-2}	3.0	
77470-1	C-3884 2% Pd	200	2.4×10^{-2}	1.0	Flow stopped at 30 minutes
77470-2	Engelhard	400	0	1.0	
77470-3		600	0	1.0	
77470-4		800	11.6×10^{-2}	1.0	

Table XXII (Continued)

Run No.	Catalyst	Reactor Temp, °C	Gas Evolved, ft^3/hr	Run Duration, hr	Notes
77471-1	15% Pd	200	0.2×10^{-2}	1.0	
77471-2	MRC	400	0	1.0	
77471-3		600			Reactor blocked
77472-1	2% Pt	200	0.5×10^{-2}	1.0	Flow stopped at 30 minutes
77472-2	Engelhard	400	0	1.0	
77472-3		600	0		Reactor blacked
77473-1	0.5% Pt	200	3.4×10^{-2}	1.25	
77473-2	H_2 Reduced	400	0	1.0	
77473-3	on Molecular	600	0.8×10^{-2}	1.0	
77473-4	Sieve	800	21.0×10^{-2}	1.0	
77475-1	5% Pd on	200	2.0*	1	Flow stopped at 30 minutes
77475-2	Silica	400	0.03*	1	
77475-3	(Monsanto)	600	0.2*	0.75	
77475-4		800	0	0.75	
77476-1	Al-XL	200	1.6*		Flow stopped at 15 minutes
77476-2	No. 2247	400	0.3*		
77476-3	6% B_2O_3	600	0		
77476-4		800	0		
77477-1	Si-X-L-365	400	0.35*	0.75	Flow stopped at 30 minutes
77477-2	75% SiO	600	0	0.75	
77477-3	25% Al_2O_3	800	0	0.75	
77478-1	Al-X-L2621	200	1.85*	1.0	Flow stopped at 30 minutes
77478-2		400	1.40*	1.0	Flow stopped at 30 minutes
77478-3		600	0.2*	0.75	Flow stopped at 30 minutes
77478-4		800	0	1.0	

* Quantity of gas evolved during the entire run.

Note: System volume is $3.9 \times 10^{-2} ft^3$

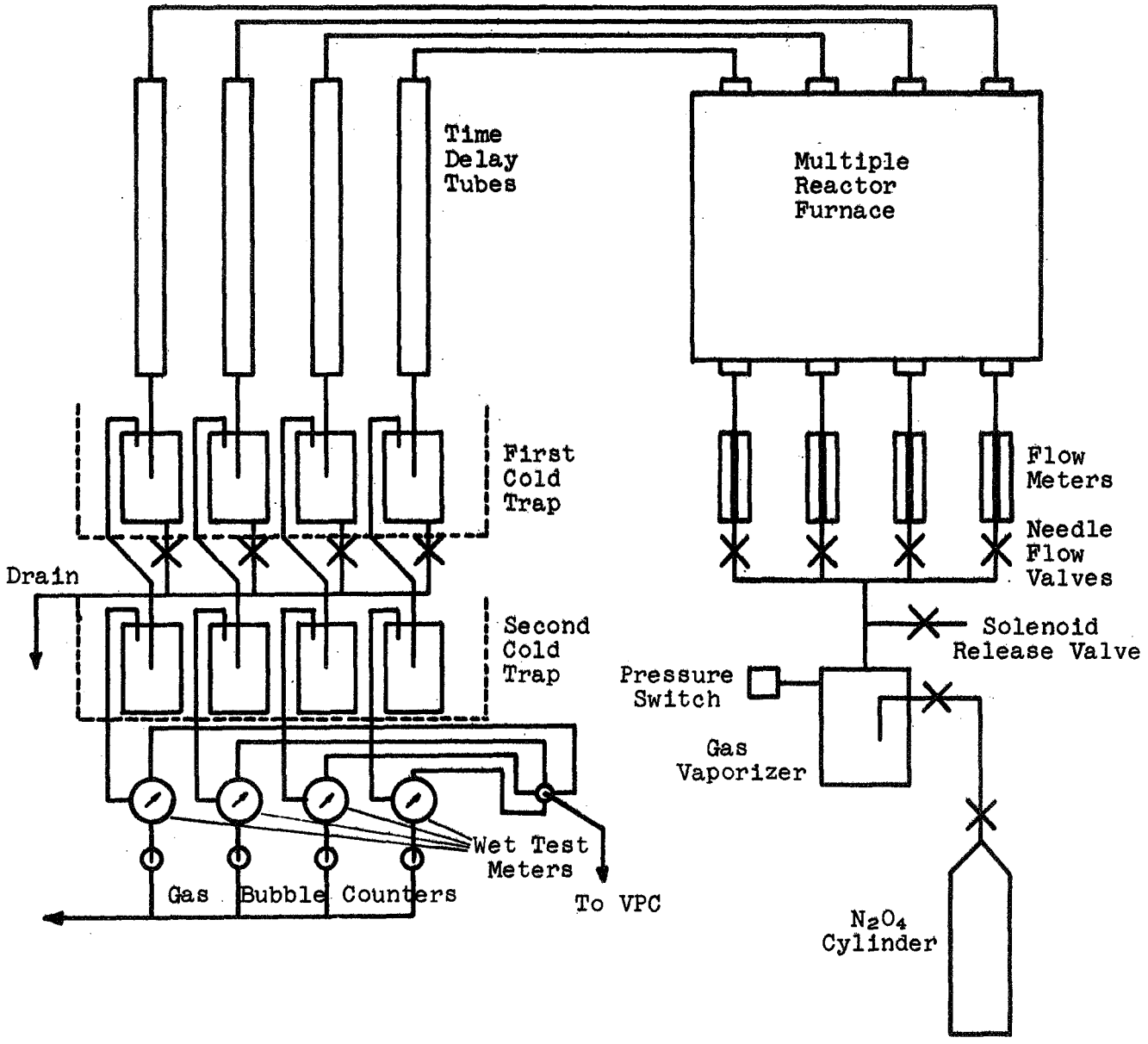

Figure 9. Multiple N_2O_4 Reactors Schematic

2. Secondary Catalyst Screening

The four catalysts listed above, the best from the screening runs, were tested continuously for times up to 13 days at 800 and 850°C. The results of these tests are summarized in Table XXIII.

Only the Pt catalyst maintained its activity over the 13-day period. This catalyst showed an initial decline in activity (69% to 53% conversion), but then maintained the same level for five days. Increasing the temperature to 850°C caused an apparent reduction in the conversion efficiency (to about 42%). However, gas chromatographic analysis of the product stream gave O_2/N_2 ratios of less than 2:1, indicating a loss of O_2 somewhere in the system. The reactor tube was fabricated from 316-stainless steel. A check of the corrosion resistance of this material shows that substantial oxidation could have occurred, explaining the apparent loss of O_2 from the product stream at 850°C. Stainless alloy 310 has much better oxidation resistance at these temperatures, and reactor tubes fabricated from this alloy were procured for further testing.

D. LONG-TERM RUNS

1. Preliminary Testing

The reactor system was modified for long-term testing. The final system used is shown schematically in Figure 10. The operation of this reactor is similar to the screening test reactor operation described in a previous section except that the residence time in this reactor was quadrupled by connecting the reactor tubes in series.

Preliminary testing was concentrated on determining the optimum operating conditions to be used with the Engelhard 2% Pt-on-alumina catalyst. Another objective was to check the operation of the system during extended continuous service. The results of these tests are shown in Figure 11.

Several conclusions can be drawn from this testing. First, it is apparent from the data that the reactor temperature cannot be reduced much below 800°C without a drop in conversion efficiency. Also, some decline in conversion efficiency with time was noted, indicating some reduction in catalytic activity.

Greater than 100% decomposition efficiencies were calculated when the feed rates were reduced. It is apparent that the system had not reached steady-state conditions when the

Table XXIII

LONG TERM TESTS OF N_2O_4 DECOMPOSITION

Run No.	Catalyst	Reactor Temp, °C	Gas Evolved, ft^3/hr	N_2O_4 Feed, g/hr	Conversion, %	Notes
77479-1	2% Pt on Alumina	800	0.5740	28.8	69.5	1st day
		800	0.4973	28.8	60.3	2nd day
		800	0.4350	28.8	52.8	3rd day
		800	0.4200	28.8	50.9	7th day
77480-1		850	0.4520	28.8	54.8	8th day
		850	0.3700	28.8	44.8	9th day
		850	0.144	11.5	42.5	13th day
77481-1	G-12 Nickel	800	0.1480	28.8	17.9	1st day
		800	0.1940	28.8	23.5	2nd day
		800	0.1680	28.8	20.4	3rd day
		800	0.2620	28.8	31.8	7th day
		850	0.2550	28.8	30.9	8th day
		850	0.2110	28.8	25.6	9th day
		850	0.0280	11.5	8.3	13th day
77483-1	2% Pd on Alumina	800	0.5600	28.8	68.0	1st day
		800	0.1160	28.8	14.1	2nd day
		800	0.1030	28.8	12.5	3rd day
		800	0.1220	28.8	14.8	7th day
		850	0.2100	28.8	35.4	8th day
		850	0.2650	28.8	31.2	9th day
		850	0.0310	11.5	9.2	13th day
77485-1	10% CuO Cu-0803T	800	0.1440	28.8	17.5	1st day
		800	0.2200	28.8	27.7	2nd day
		800	0.0950	28.8	11.5	3rd day
		800	0.1110	28.8	13.4	7th day
		850	0.1550	28.8	18.8	8th day
		850	0.1200	28.8	14.5	9th day

Test terminated after gas evolution stopped.

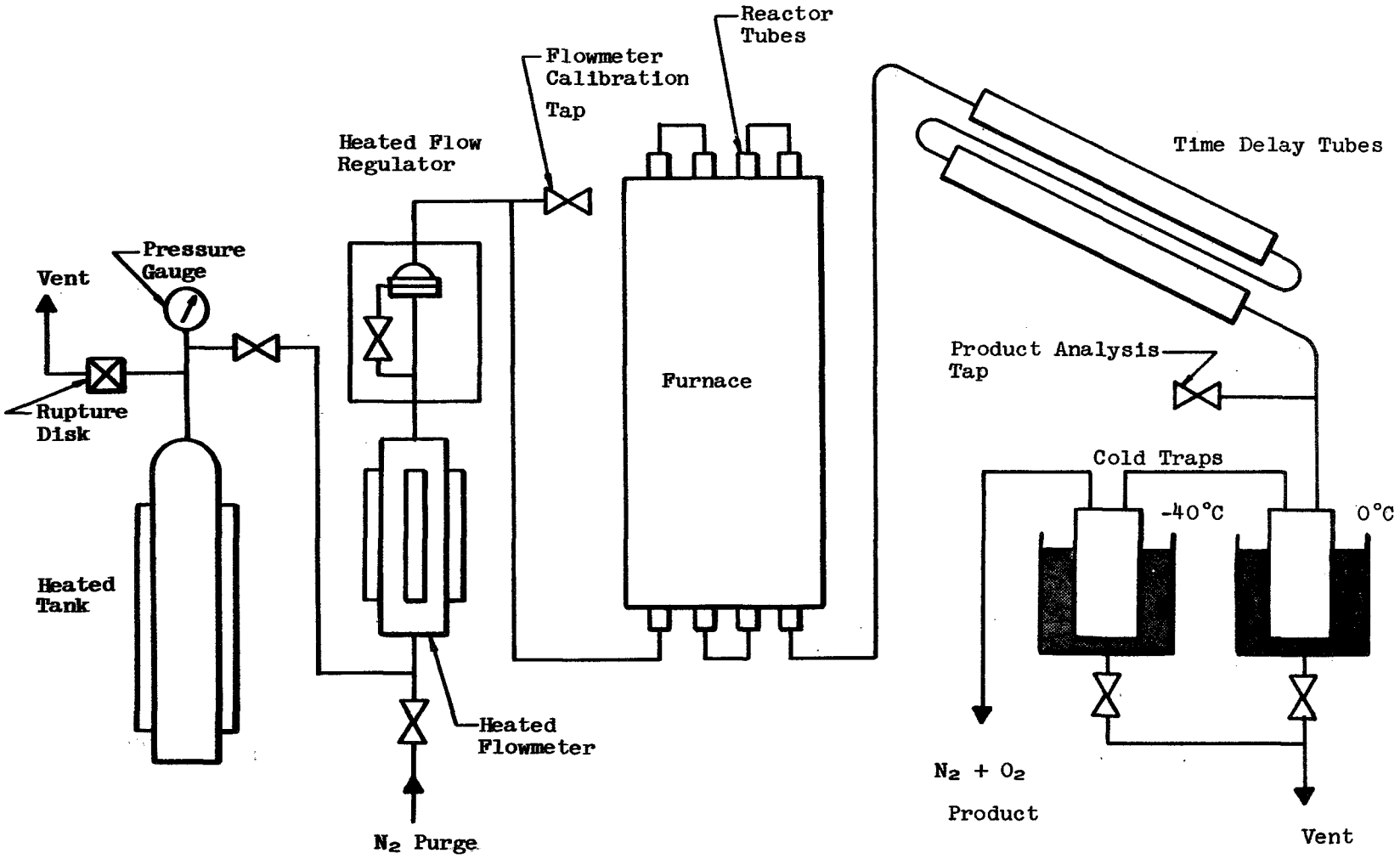

Figure 10. N_2O_4 REACTOR SYSTEM SCHEMATIC

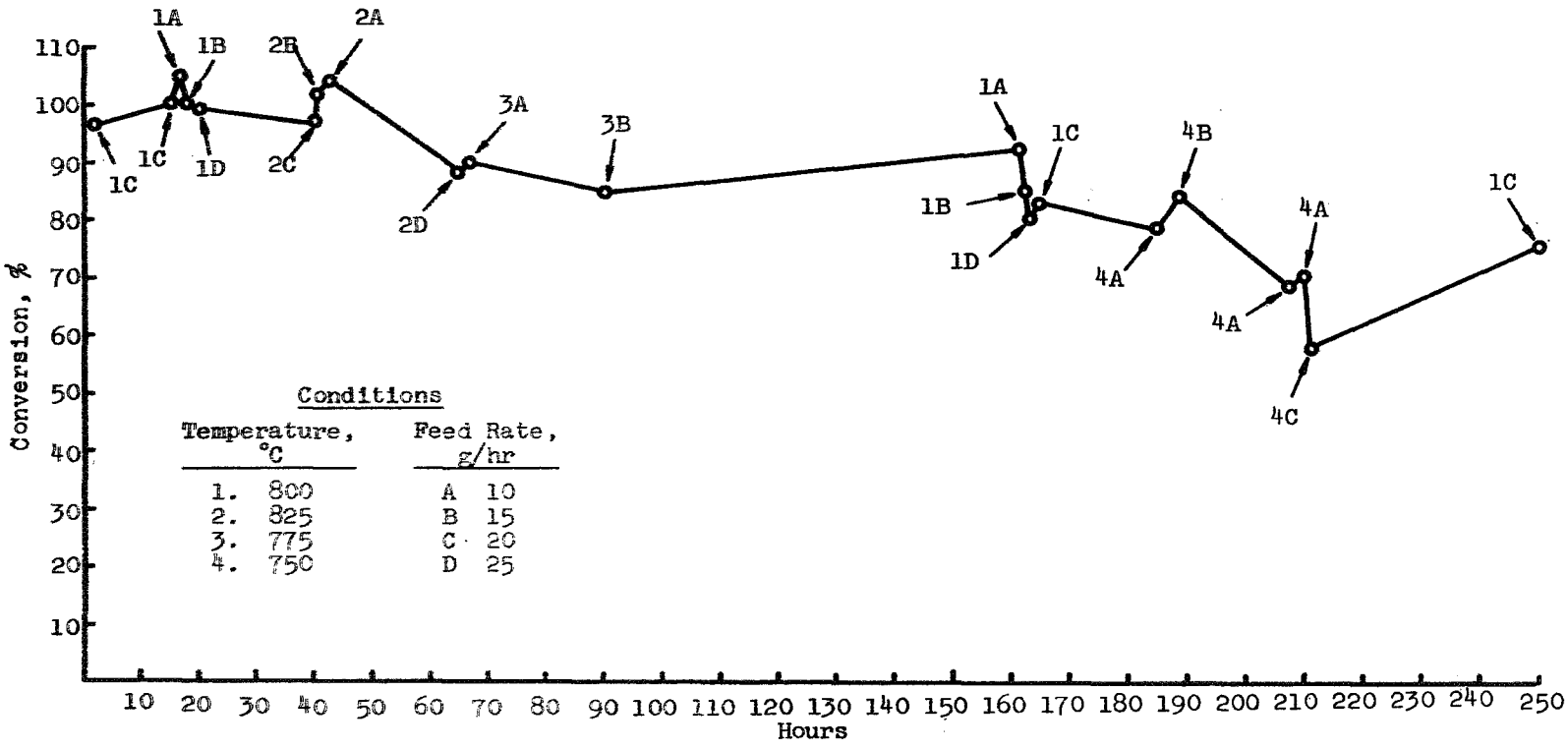

Figure 11. Conversion Efficiency versus Operating Time For 2% Pt Catalyst

measurements were made. An analysis of the operating conditions in the reactor system indicates that a long time period may be required for steady-state conditions to be attained after a change in temperature or reactant flow rate. The factors that play a major role in the slow equilibration of the system after a change in conditions are the shift in the location of the reaaction sites, changes in the gas phase and adsorbed phase composition, and changes in the catalyst activity associated with these composition changes. It is estimated that complete equilibration of the system may require as long as 16 to 24 hours after a change in operating conditions.

2. 1000-Hour Test

The 1000-hour test was started on 15 December 1965 using four reactor tubes in series containing a total of 324 grams of 2% platinum catalyst. Each reactor tube was fitted with a thermocouple in the center of the catalyst bed. The standard test conditions selected were 800°C with a feed rate of 20 g of N_2O_4 per hour. Conversion efficiencies were determined by sampling both the input and output streams and analyzing for N_2O_4 by the peroxide acid titration method. Very few mechanical problems were encountered. A thermocouple burned out in one of the tubes after 750 hours and had to be replaced. Less than one hour of down time resulted.

The conversion efficiency obtained under the standard conditions during the 1000-hour period is shown in Table XXIV.

Table XXIV

N_2O_4 REACTOR CONVERSION EFFICIENCY

800°C, 20 Grams N_2O_4 Feed/Hr

Time (hr)	N_2O_4 Converted (%)	
60	99	
80	79	
250	85	
470	79	
675	76	
750	72	(Thermocouple
900	80	replaced)
975	80	
1000	79	

After 80 hours of operation, catalyst activity declined as indicated by the decline in the N_2O_4 conversion efficiency (from 99 to 79%). Shifts in the individual reactor internal temperatures were also noted at this time. At the beginning of the test all of the reactors were within 10°C of 800°C. After 80 hours the temperature of the first reactor tube had dropped to 765°C, the second tube remained at 800°C, the third had risen to 845°C, and the fourth tube was at 810°C. It is possible that the temperature variations indicated a shift in the predominant reaction in the first reactor to simple reactant heating plus decomposition:

$$NO_2 = NO + 1/2\ O_2 \text{ (endothermic)} \qquad (24)$$

The exothermic decomposition of NO in the following sections would explain the temperature increase in these reactors.

After the conversion efficiency had stabilized, the effect of residence time was determined by varying the feed rates over the range of 6 to 29 g N_2O_4/hour. At least 16 hours were allowed for equilibration before conversion data were taken. The results of these tests are shown in Figure 12. It is apparent that much longer residence times or catalyst volumes would be required for conversion efficiencies above 85%. The two extreme points on this curve were rechecked after the 1000-hour test was completed and were within experimental error of the earlier results. The data fit a second-order plot reasonably well, indicating that the overall reaction is second order with respect to N_2O_4.

E. CONCLUSIONS AND RECOMMENDATIONS

We have demonstrated an N_2O_4 decomposer that will convert 80-85% of input N_2O_4 to a gas stream consisting of a 2:1 mole ratio of O_2 to N_2. The output stream is contaminated with unconverted N_2O_4 and probably could be used directly only in a contained-electrolyte or free-acid electrolyte fuel cell. Some HNO_3-HNO_2 will be formed in this electrolyte, but the dissolved N_2O_4 would be in equilibrium with NO in the exhaust stream and would be consumed electrochemically so that a steady state concentration would result. We have demonstrated previously that a Pt-containing H_2 anode might operate satisfactorily in such a contaminated electrolyte. However, an acid ion exchange membrane cell probably could not be used with this stream because of oxidative attack on the membrane.

For use in an alkaline or ion exchange membrane cell, the stream must be purified.

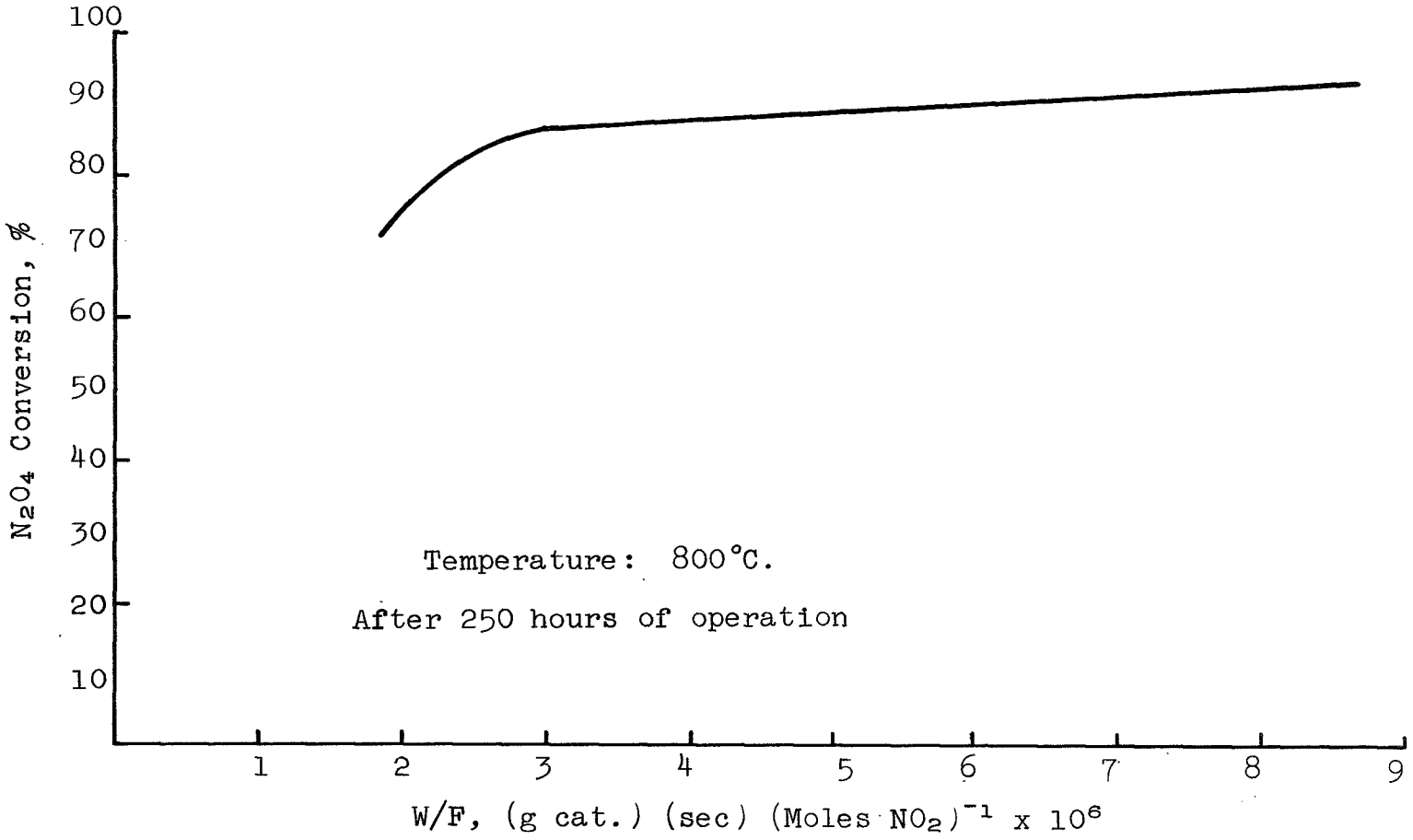

Figure 12. Conversion vs Time Factor for N_2O_4 Reactor

We had expected to demonstrate greater than 97% conversion efficiency by providing increased residence time in the reactor. This would have demonstrated the feasibility of scrubbing the stream with a column containing molecular sieves or KOH pellets. At 80-85% conversion, however, this method is not feasible for any reasonable operating time because the weight of the scrubber would be too high. Figure 12 indicates that the weight of catalyst required to reach 97% conversion would also be prohibitive. For example, at an 80% conversion only 16.4 lb of catalyst would be required to supply a 1 KW fuel cell module with O_2. For 97% efficiency, this figure is over 100 lb of catalyst.

Our first recommendation was to develop a capability to remove residual N_2O_4 from the reactor product stream. This program was undertaken as a part of the current contract and is reported in a later section of this report.

Beyond this, much could be done to optimize the reaction. Specifically, the loss in performance with time should be investigated, particularly with respect to the effects of impurities in the tank N_2O_4. The effects of higher Pt loadings, catalyst pellet size, higher pressure operation, and higher temperature operation with more resistant reactor materials, all should be investigated so that trade-offs can be made in final system design.

V. ELECTROCHEMICAL DEVELOPMENT FOR DIRECT REACTANT USE AND OPERATION ON REFORMER PRODUCT STREAMS

A. BACKGROUND

Work on the previous contract (Ref. 2) had demonstrated long-term operation of a full cell operating on gaseous N_2O_4 and N_2H_4 dissolved in H_3PO_4 electrolyte. The cathode used in this work was a proprietary, hydrophobic but vapor-permeable carbon-PTFE* electrode (termed the "MRD" electrode). The anode was a noble-metal-catalyzed (no carbon) version of this electrode that was made sufficiently porous to operate as a flow-through electrode. A special multicomponent separator-electrolyte combination completed the cell assembly.

In these tests the N_2O_4 coulombic efficiencies were low with a single pass of reactant gas (7.7% based on reduction to NO). The dissolved fuel, pumped electrolyte configuration could have caused added complexities in systems designed for zero gravity operation. Also, operation on Aerozine-50 with the UDMH component of the fuel included was not documented extensively.

With the foregoing considerations in mind, the objectives of this task were to develop electrode structures and techniques that would allow the direct utilization of gaseous N_2O_4 and Aerozine-50 (50 wt % N_2H_4, 50 wt-% UDMH) as reactants in a fuel cell. A further requirement was that these reactants be used efficiently in a single pass through the electrode chamber of the fuel cell. Finally, the operation of fuel cells on the reformer product streams were to be investigated.

B. CATHODE OPTIMIZATION

1. Background

Although the MRD carbon-PTFE cathode has demonstrated adequate polarization characteristics, the coulombic efficiencies must be improved. Three areas were investigated to achieve this:

(a) Improved gas manifold design to minimize N_2O_4 purging losses.

(b) Attempts to limit and control diffusion of N_2O_4 through the carbon-PTFE electrode and prevent losses by solution in the electrolyte.

(c) A catalyst study aimed at electro-reducing N_2O_4 completely to N_2.

---

* Polytetrafluoroethylene

2. Design of Electrode Holders and Manifolding

a. Design Consideration

In the actual operation of a cathode with N_2O_4 supplied to the back of the electrode via appropriate manifolding, several processes must be taken into account. In practice, product NO or N_2 diffuses back through the electrode from the catalytically active sites to the bulk of the reactant stream, with a consequent dilution effect on the N_2O_4 (NO_2) concentration. H_2O formed can enter the electrolyte or back-diffuse to the reactant stream, depending on temperature and electrode properties. Where H_2O does go to the NO_2 stream in the vapor state, some reaction with the NO_2 undoubtedly occurs, although the exact extent of this reaction is uncertain. Its effect on cell performance is probably highly dependent on flow rate, diffusion of H_2O in the gas stream, and concentrations.

It has been previously reported (Ref. 2) that the performance of MRD carbon cathodes was influenced to a considerable extent by N_2O_4 flow rates. A flow rate of 22 mg N_2O_4/min-cm^2 was found necessary for current densities in the range of 100 amp/ft^2. Such a flow rate represents a N_2O_4(NO_2) utilization efficiency of only about 8%. It was believed that the excessive N_2O_4 rates were necessary to remove back-diffused water of reaction, which tended to condense on the electrode surface due to transfer limitations. Such condensed water could block NO_2 diffusion to active sites either mechanically or through favoring the reaction

$$3NO_2 + H_2O \longrightarrow 2HNO_3 + NO \text{ (warm concentrated solution)} \quad (25)$$

thus producing the more slowly diffusing HNO_3 as the active oxidant.

In the cell holders used, the flow rate of 22 mg N_2O_4/min-cm^2 corresponds to an average Reynolds Number,

$$\frac{(\text{equiv dia})(\text{vel})(\text{density})}{\text{viscosity}} = N_{Re} \quad (26)$$

of approximately 40, which is still well within the laminar flow range and suggests H_2O transfer limitations due to poor film coefficients.

A further set of experiments was run to evaluate N_2O_4 cathode performance as a function of flow rate or average N_{Re}. Results are shown in Figure 13.

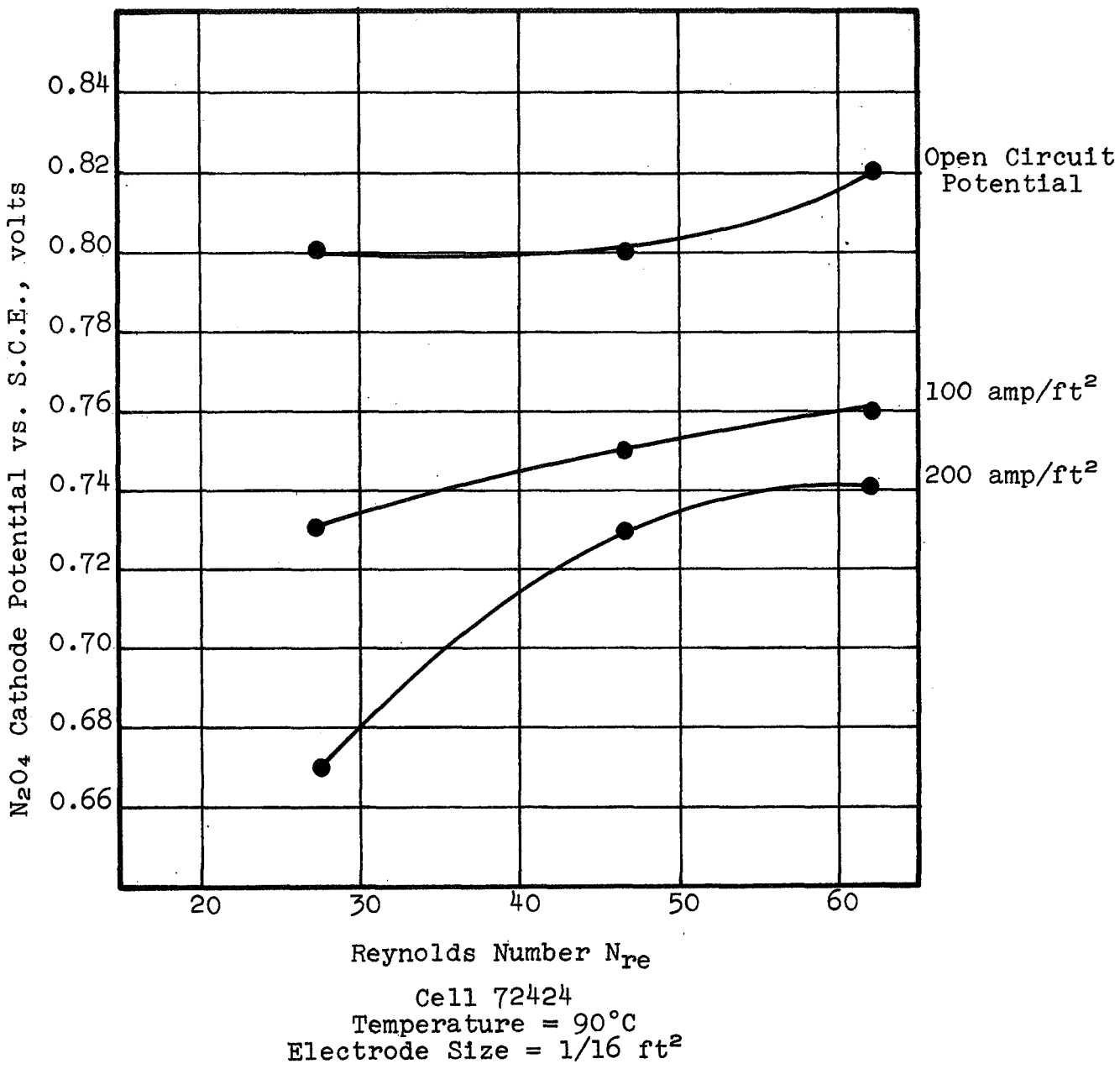

Figure 13. Effect of N_2O_4 Flow Rate (as Reynolds Number) on Cathode Polarization at Various Current Densities

N_2O_4 flow rates were varied from approximately 10 to 30 mg N_2O_4/min-cm^2 so that N_{Re} varied over the relatively narrow laminar flow range of 25 to 70. Again, dependence of cathode potential on N_2O_4 flow (expressed as Reynolds Number) was shown to exist, particularly at the higher current densities.

It is not suggested that the N_2O_4 cathode potential is solely a function of Reynolds Number, but it is apparent that flow, expressed as N_{Re}, is an important factor, as evidenced by the relatively large potential variations seen in Figure 13 over a very small span of N_{Re}. It is concluded that, in general, Reynolds Numbers greater than about 50 should be maintained in grooving and manifolds of N_2O_4 cathodes.

A long NO_2 flow path is also indicated to cause maximum contact of the continuously degradating NO_2 stream with the electrode surface and obtain as high a NO_2 utilization as is possible. Multiple passes of the NO_2 stream will best produce this extended contact, but care must be taken to prevent excessive pressure drops with resulting areas of high static pressure sufficient to cause gross transfer of NO_2 through the permeable electrode. Furthermore, reasonable distribution of "strong" and "weak" pass streams is required to ensure relatively even current densities across the electrode surface.

The grooving geometry that appeared to best meet the above requirements is illustrated in Figure 14.

Experience has shown that the MRD carbon cathode performs well with a 1/8-inch groove, 1/8-inch land support and distribution system. Polarization curves for small, unsupported half-cell electrodes and for 1/16 ft^2, 1/8-inch land-groove supported electrodes were essentially identical. Mechanically, wider grooves and/or narrower lands usually cause excessive extrusion of the MRD electrodes into the flow channel with higher possibility of eventual electrode rupture.

For the grooving detail shown in Figure 14, as applied to the 1/3-ft^2 square geometry electrode shape, an overall flow length of approximately 19 inches per parallel path was obtained. Width of the repeating element was 3/4 inch, requiring nine such elements for the 48-in.^{2} square electrode. This configuration always placed the weakest (No. 3) NO_2 concentration pass of each element adjacent to a strongest concentration (No. 1) pass except for the last element. A single pass from inlet to exhaust manifold at the end of the nine multi-pass repeating groove elements would eliminate the exception.

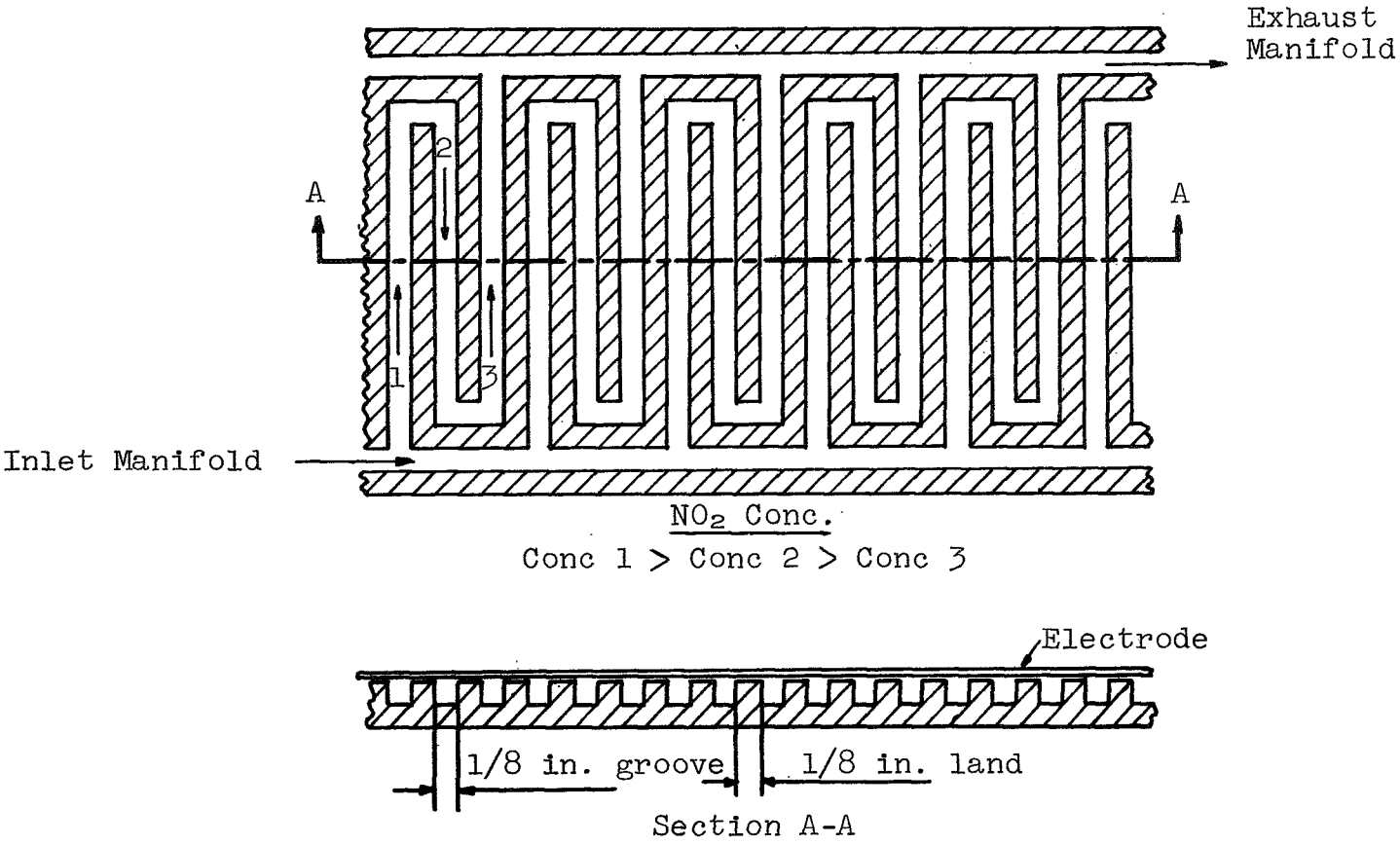

Figure 14. Grooving Detail

This flow pattern should provide a reasonably even distribution of NO_2 over the entire electrode area, though a slight overall NO_2 concentration gradient from inlet to exhaust manifold will inevitably exist.

Pressure drops in the 19-inch long, multi-pass, parallel paths should be slight (<0.5-in. H_2O gauge if gas flows result in Reynolds Numbers less than 100). Figure 15 illustrates pressure drops in MRC fuel cell designs as determined in test fixtures with 1/8-in. wide grooves on 1/4-in. centers, 0.050-in. or 0.030-in. deep grooves, with air as the test fluid.

From a mechanical standpoint, this multi-pass groove construction with 1/8-inch land, 1/8-inch groove will provide a land-to-groove ratio of approximately 0.7 when inlet and exhaust manifolds are considered. This value has been shown in previous proprietary work in our laboratory to provide adequate mechanical support with negligible internal electrical resistance losses due to contact area for current collection purposes at current densities up to at least 200 amp/ft^2.

A 1/3-ft^2 test cell design was made to evaluate the grooving and flow arrangements previously discussed. A 7 x 7 in. active electrode area unit was selected with construction similar to that of the 3 x 3 in. cells that had been well tested in our laboratory. The principal feature of the large-size test cell was a replaceable flow plate permitting testing with various groove arrangements and depths.

Details of the frame and insert are shown in Figure 16. The center exposed electrode area was 7 x 7 in. Sealing between the electrode and frame was provided by a 0.25-in. wide 0.020-in. thick lip around the perimeter of the electrode. Insert-to-frame sealing was provided by an O-ring as shown. Reactant flow passages across the face of the electrode were in the form of slots cut in a removable plate.

The design of the initial flow plate is shown in Figure 17. Shown also in Figure 17 is the way in which the flow plate pattern mates with the insert manifolds providing inlet and outlet for the pattern. Due to the replaceability of this flow plate, different flow patterns and groove depths can be accommodated by fabrication of additional plates.

b. Electrochemical Evaluation

The holder-manifolds were evaluated with MRD carbon electrodes in the cell construction illustrated in Figure 18.

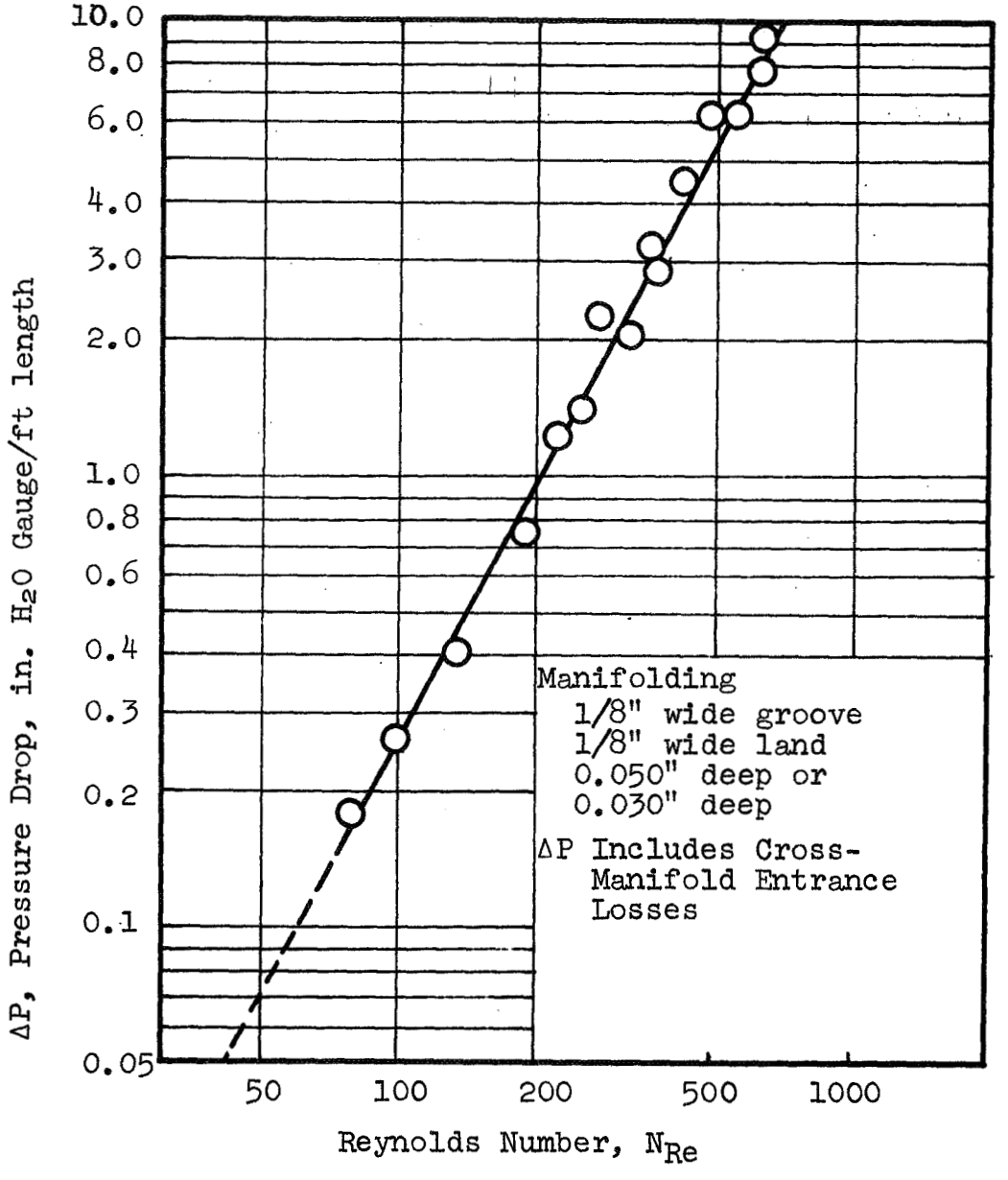

Figure 15. Pressure Drop in 1/8 in. Wide Gas Manifold Grooving; MRC Fuel Cell Designs

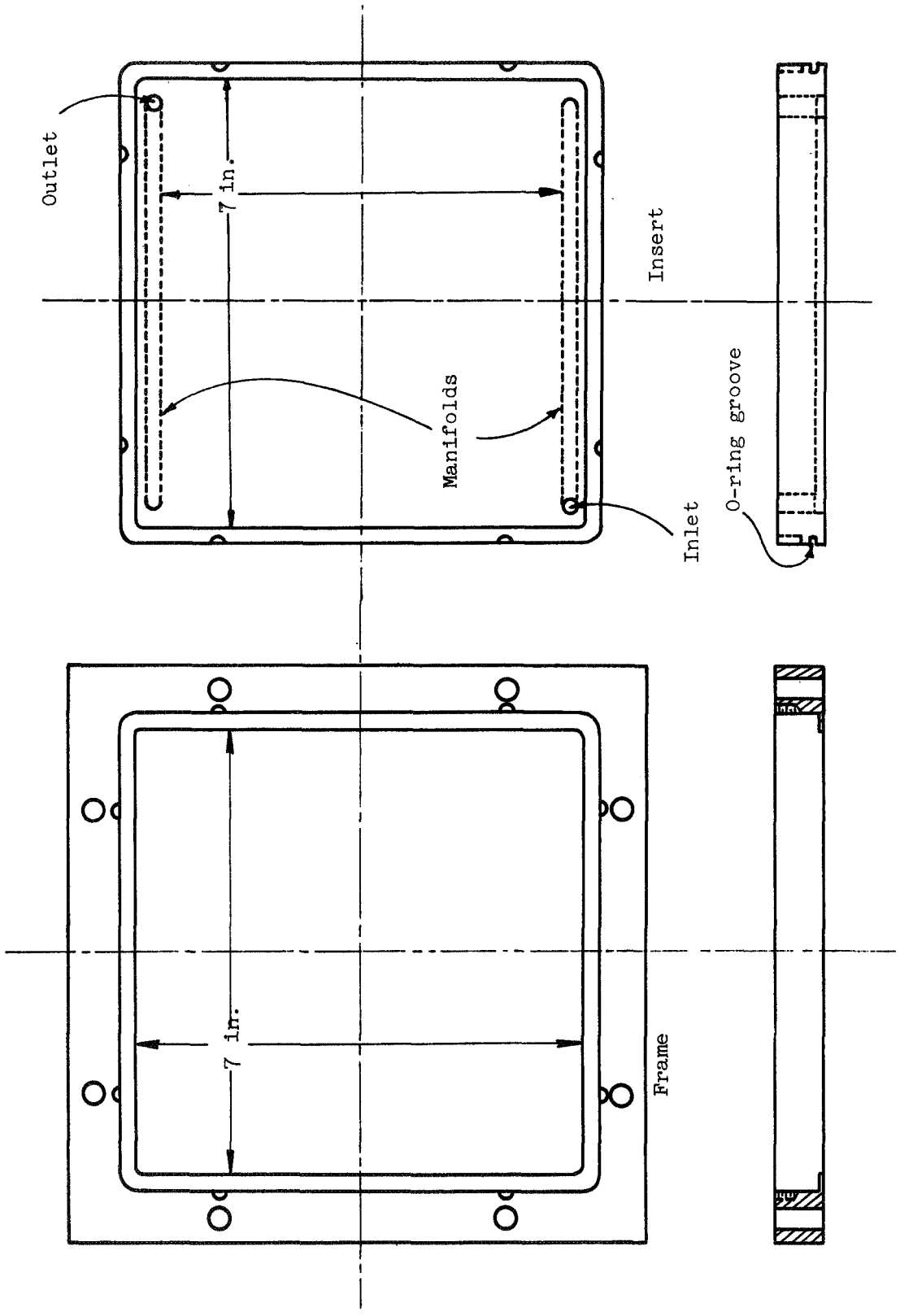

Figure 16. Test Cell Endplate Construction

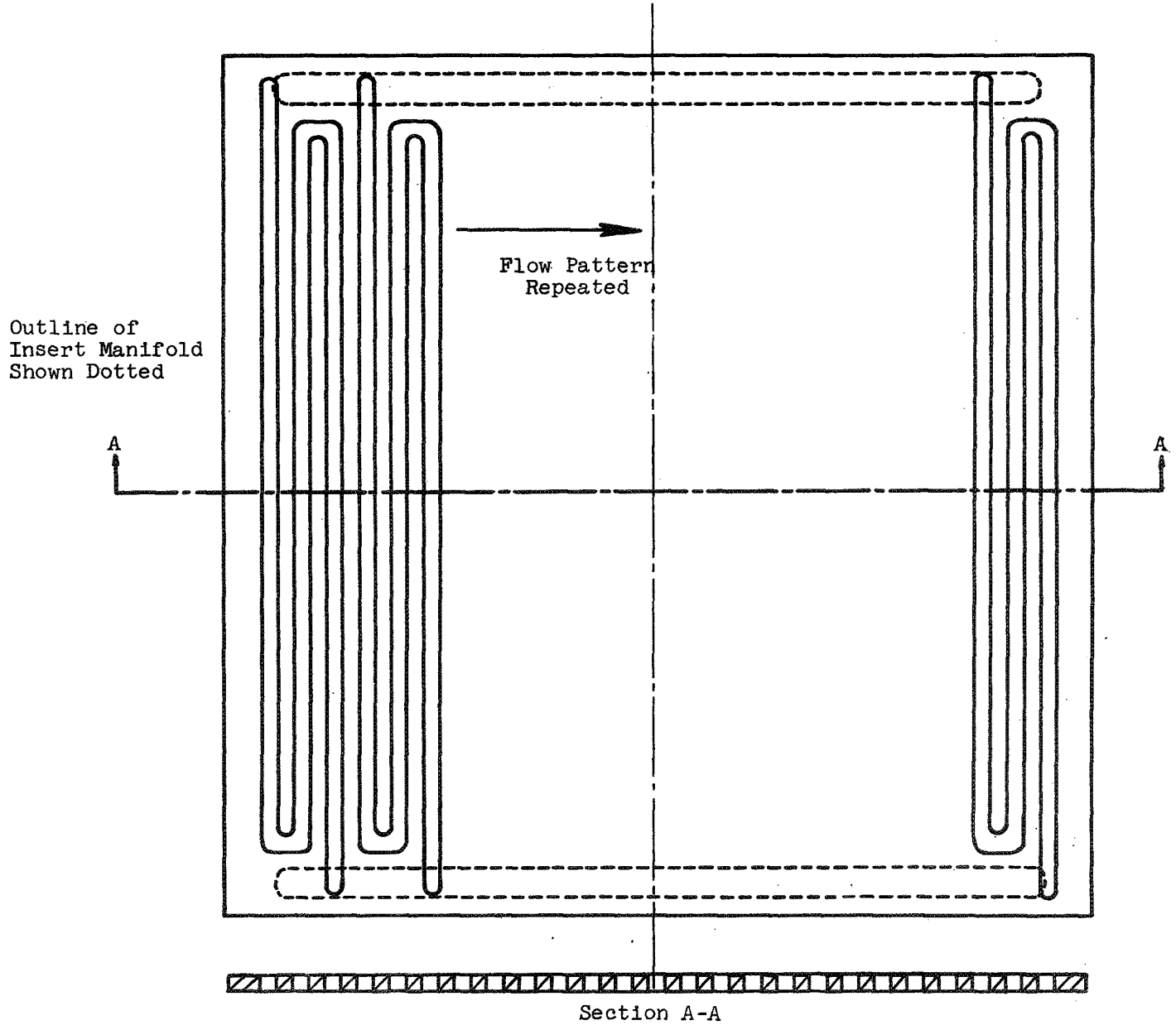

Figure 17. Reactant Flow Plate

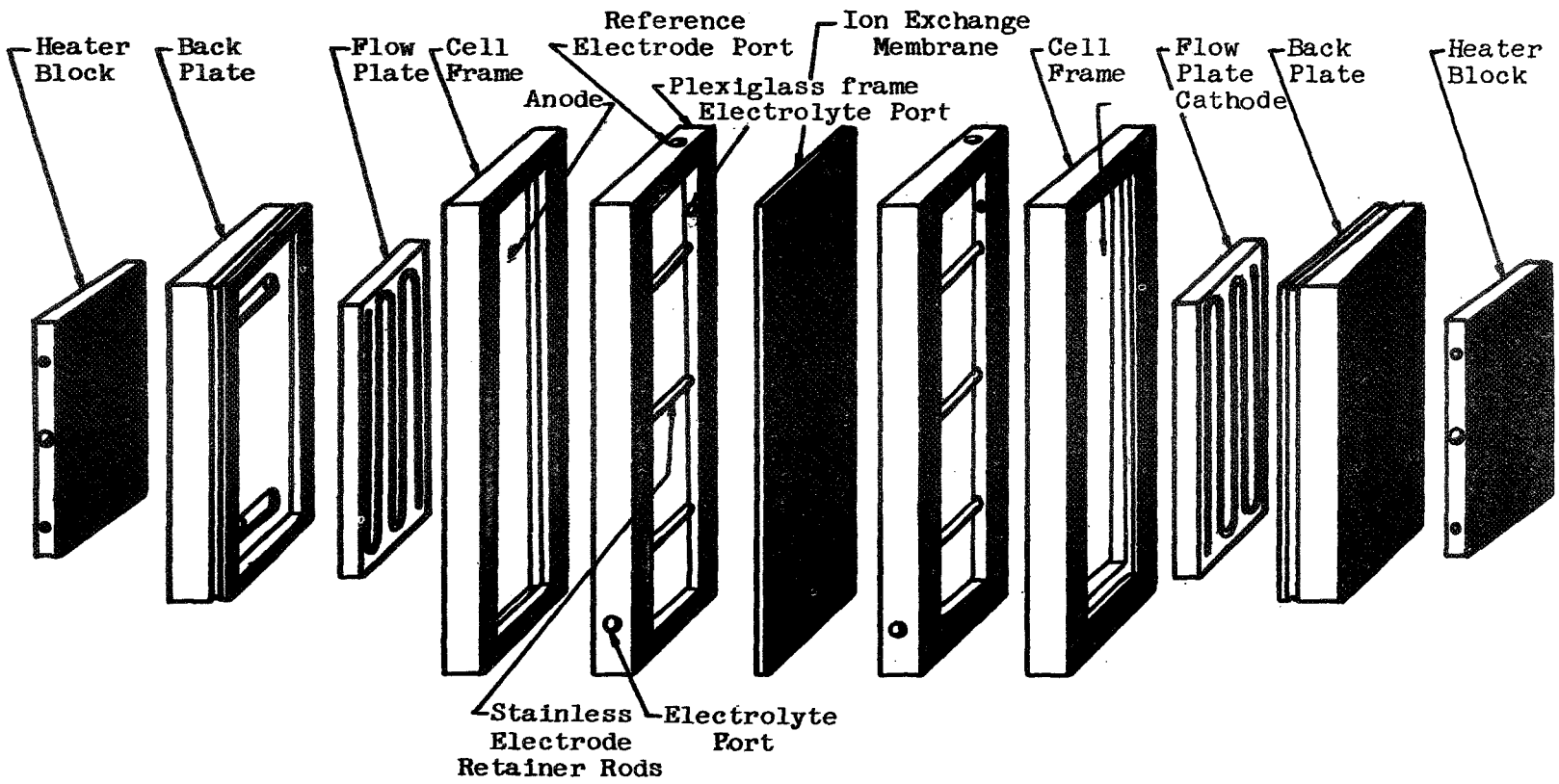

Figure 18. 1/3 Ft^2 Test Cell

This cell was a "free electrolyte" cell in which 5M H_3PO_4 electrolyte was circulated between the two electrodes. A strong acid ion exchange membrane (Ionics 61AZL183) was used to separate the cell into anode and cathode compartments so that cathode product analysis and operation could be determined free from any effects due to anode operation. In order to measure IR-free cathode potentials, a Luggin capillary salt bridge consisting of a small plastic tube containing a fiberglass wick saturated with electrolyte was affixed to the cathode face. The tube articulated externally with a reservoir of electrolyte containing a reference electrode.

The anode was an MRD carbon-Pt-PTFE electrode operated on gaseous H_2. The unit was operated with a large-capacity constant-current power supply.

The gaseous products of the cell reaction exited the cell in both the electrolyte and cathode exhaust stream. Both of these streams were analyzed to obtain a complete material balance. The electrolyte stream contained nitrogen and nitric oxide. Quantitative tests were not made on the gases but the qualitative tests performed indicated that mostly nitrogen and very little nitric oxide was present.

The stream exiting from the back side of the operating cathode contained N_2O_4, NO, N_2, and H_2O and proved extremely difficult to analyze. However, the overall coulombic efficiency of the electrode could be determined because both the N_2O_4 input rate and the total electrical current withdrawn from the electrode were known accurately. Since there was some evidence that N_2 is the predominant reaction product, the coulombic efficiencies were calculated on the basis of complete reduction to N_2.

A pumped electrolyte cell constructed as described above was assembled with a 0.050-in. thick cathode flow plate and mounted in the test stand. Over a period of a week this cell was operated intermittently at various temperatures and N_2O_4 flow rates. Table XXV summarizes the results of these tests.

Table XXV

N_2O_4 CATHODE HALF CELL ELECTRICAL PERFORMANCE

	Current Amp	Voltage Volts vs SHE	N_2O_4 Used, %	Watts	N_2O_4 Input*
60°C	10	1.04	9.2	10	3.7x
	20	0.49	18.2	9.8	
	30	-0.20			
70°C	10	0.12	9.2	11	3.7x
	20	0.90	18.2	18	
	30	0.72	27.3	22	
70°C	10	1.03	13.7	10	2.5x
	20	0.35	27.3	7.0	
	30	-0.13	41.0		

* Times stoichiometric amount for complete reduction to N_2 at 30 amp.

The results given in Table XXV are representative of the cathode performance that can be expected after one hour at each of the test conditions and therefore were assumed to be steady state conditions. It may be noted that the performance at 70°C was much better than at 60°C at the same current densities. This difference was noted on many occasions and is thought to be due to changes in the diffusion rate of water and reaction products through the cathode. There was also a considerable reduction in performance when the N_2O_4 feed rate was reduced from 3.7 to 2.5 times the stoichiometric amount for 30-ampere operation. The data points were rechecked on several occasions and found to be reproducible.

The calculated coulombic efficiency based on complete reduction to N_2 was 27% for 30-ampere, 20-watt operation. This compares to an efficiency reported in the previous contract (Ref. 2) of 3.8%, calculated on the same basis.

3. Permeation of N_2O_4 through the MRD Carbon PTFE Electrode

N_2O_4 dissolves in aqueous solutions as:

$$N_2O_4 + H_2O \rightleftharpoons HNO_2 + HNO_3 \text{ (Ref. 14)} \qquad (27)$$

The effect of this reaction in our work is clear; any N_2O_4 that diffused through the electrode and was not consumed electrochemically could dissolve in the electrolyte. In a pumped electrolyte cell, in which "fresh" electrolyte is continually brought to the electrode surface, the amount dissolved in a given time would be determined by the diffusion rate through the electrode and the current drawn from the cell. The effects would be a loss of coulombic efficiency at the cathode, and a gradual poisoning of the anode as the HNO_3-HNO_2 concentration builds up in the electrolyte.

The most direct approach to this problem was to control the diffusion rate through the cathode so that the N_2O_4 supply was balanced with the stoichiometric requirements.

A program was undertaken to determine the effect of easily controlled external parameters of temperature and pressure on the diffusion rate. The details of this work are reported in Ref. 3a. In brief, a standard two-compartment cell was used with the cathode clamped between halves. N_2O_4 gas was purged through one side with a stagnant H_2SO_4 solution on the other. The amount of N_2O_4 diffusing was determined by a permanganate titration. The results are illustrated in Table XXVI.

Table XXVI

N_2O_4 DIFFUSION RATE - ELECTRODE 55-67229

Electrolyte: 2M H_2SO_4 (0.2N in $KMnO_4$)
Temperature: 25°C
N_2O_4 Flow Rate through Cell: 1.6-2.0 g/min.
Electrode: Standard MRD Carbon-PTFE

N_2O_4 Pressure, in. H_2O	Diffusion Rates in g N_2O_4/hr/cm^2 Exposure Times, min.		
	0.5	1.0	2.0
0	0.34	0.19	0.18
5.4	0.28	0.46	0.55

Mean Values:

0 in. H_2O pressure: 0.24 g N_2O_4/hr/cm^2
5.4 in. H_2O pressure: 0.43 g N_2O_4/hr/cm^2
0.5 min exposure: 0.31 g N_2O_4/hr/cm^2
1.0 min exposure: 0.33 g N_2O_4/hr/cm^2
2.0 min exposure: 0.36 g N_2O_4/hr/cm^2

Stoichiometric Requirement for 100 ma/cm^2:

0.089 g N_2O_4/hr/cm^2 for reduction to NO
0.045 g N_2O_4/hr/cm^2 for reduction to N_2

The data show that the N_2O_4 diffusion rate responded to pressure differences but that the rate was quite high compared to stoichiometric requirements.

A second series of tests corroborated the pressure effect but also indicated that the effect of temperature was not as pronounced (Ref. 3b). Attempts to modify the permeability of the electrode by inclusion of "pore fillers" ($MnPO_4$, Kel-F® oils) and by densification of the carbon-PTFE matrix produced inconclusive results.

4. Electro-Reduction of N_2O_4 Completely to N_2

On a previous contract (Ref. 2) the electrochemical reaction of HNO_3 on carbon was shown to produce NO as the exclusive reaction product. The reaction for N_2O_4 should be analogous since the mechanisms proposed in the literature all involve common reactants (cf. Refs. 15, 16). Thus, N_2O_4 should electroreduce as:

$$N_2O_4 + 4H + 4e^- = 2NO + 2H_2O \qquad (28)$$

which yields 107 ampere-hours/mole N_2O_4. The preferred reaction

$$N_2O_4 + 8H^+ + 8e^- = N_2 + 4H_2O \qquad (29)$$

yields 214 ampere-hours/mole N_2O_4.

The apparatus constructed to screen electrodes with various catalysts consisted of a standard 3 x 3 in. cell with an ion exchange membrane, silica gel-H_3PO_4 separator (to isolate the cathode and the cathode reaction products), and a gas analysis train. This train consisted simply of two cold traps, to remove all N_2O_4, followed by a gas sampling bulb. VPC analysis of the contents of the bulb detected any NO, N_2O, or N_2 produced in the cell reaction. The whole system was purged with either argon or helium prior to a run.

The details on the electrodes and catalysts tested are given in Ref. 3c. These basically consisted of different carbon types, borohydride-precipitated Ag, Au, Ir, and Pd, as well as a commercial Pt black.

The results of tests with these electrodes showed that nitrogen was produced in every test where a VPC analysis was made, regardless of catalyst used. This was true for the uncatalyzed control electrode as well. The clear indication is that the standard carbon electrode, whether catalyzed or not, is (and most likely has been) producing substantial quantities of N_2 as a product of the electroreduction of N_2O_4. These results are in conflict with the original work on carbon, as referenced above. However, both the type of carbon and the type of electrode were different; porous block carbon electrodes were used in the early work. The present results are not considered conclusive proof that N_2 is formed under all conditions with these electrodes, but do indicate that substantial N_2 can be produced in the off-gas under some conditions.

A detailed investigation of possible explanations clearly indicated the results were not caused by failures or abnormalities in the test equipment used (Ref. 3c).

C. AEROZINE-50 ANODES

1. Background

The objectives of this task were to develop an electrode that would operate on Aerozine-50 as a direct electrochemical fuel with:

(a) High electrochmical activity and little polarization,

(b) High coulombic efficiencies with a single pass of reactant through the electrode chamber, and

(c) Little or no contamination of the electrolyte from unreacted fuel or from products of the reaction.

The first requirement dictated a catalyst selective for the reactions involved in the electro-oxidation of the components of the fuel. A catalyst screening program was undertaken to determine the activity of both UDMH and Aerozine-50 on a variety of prospective catalysts.

The achievement of the second objective hinged on two factors:

(a) Minimization of the catalytic decomposition of N_2H_4 on the electrode which causes a loss of fuel efficiency.

(b) Maximization of the ampere-hours output per gram of fuel.

The catalytic decomposition problem was susceptible to solution by electrode design; that is, by preventing direct contact of the catalytic surface of the electrode with large volumes of fuel. The coulombic capacity of the fuel could be greatly increased if some portion of the UDMH fraction could be utilized, as follows:

1.67 amp-hr/g of Aerozine-50 if only N_2H_4 is utilized.

2.12 amp-hr/g of Aerozine-50 if N_2H_4 is utilized and UDMH is utilized in a $2e^-$ oxidation.

3.00 amp-hr/g of Aerozine-50 if N_2H_4 is utilized and UDMH is utilized in a $6e^-$ oxidation.

However, the desirability of promoting the electro-oxidation of UDMH depended on whether the reaction products are deleterious or difficult to accommodate in operating cells. Thus, the catalyst screening program had dual objectives:

(1) To find a catalyst that would electro-oxidize both UDMH and N_2H_4 at a reasonably good mixed potential.

(2) To find a catalyst that would electro-oxidize N_2H_4 efficiently but that was inert with respect to UDMH.

2. Catalyst Screening Program

After some experimentation, an electrode screening half cell was designed that used dissolved fuel, with a stream of fuel-electrolyte solution pumped across the electrode surface to sweep away gas bubbles. This had the additional effect of reducing concentration polarization in the cell. With these modifications the true activity of the catalysts could be determined. A representation of the cell is shown in Figure 19. A Kordesch-Marko bridge was used to obtain IR-free potentials.

The catalyst powders were either commercially available or made in-house by borohydride reduction of metal salts in solution. The latter process produced powders with very small particle size and high surface areas; they generally possessed high catalytic activity. Test electrodes were made by incorporating the catalyst powders into MRD-PTFE-type electrodes supported on Pt screen.

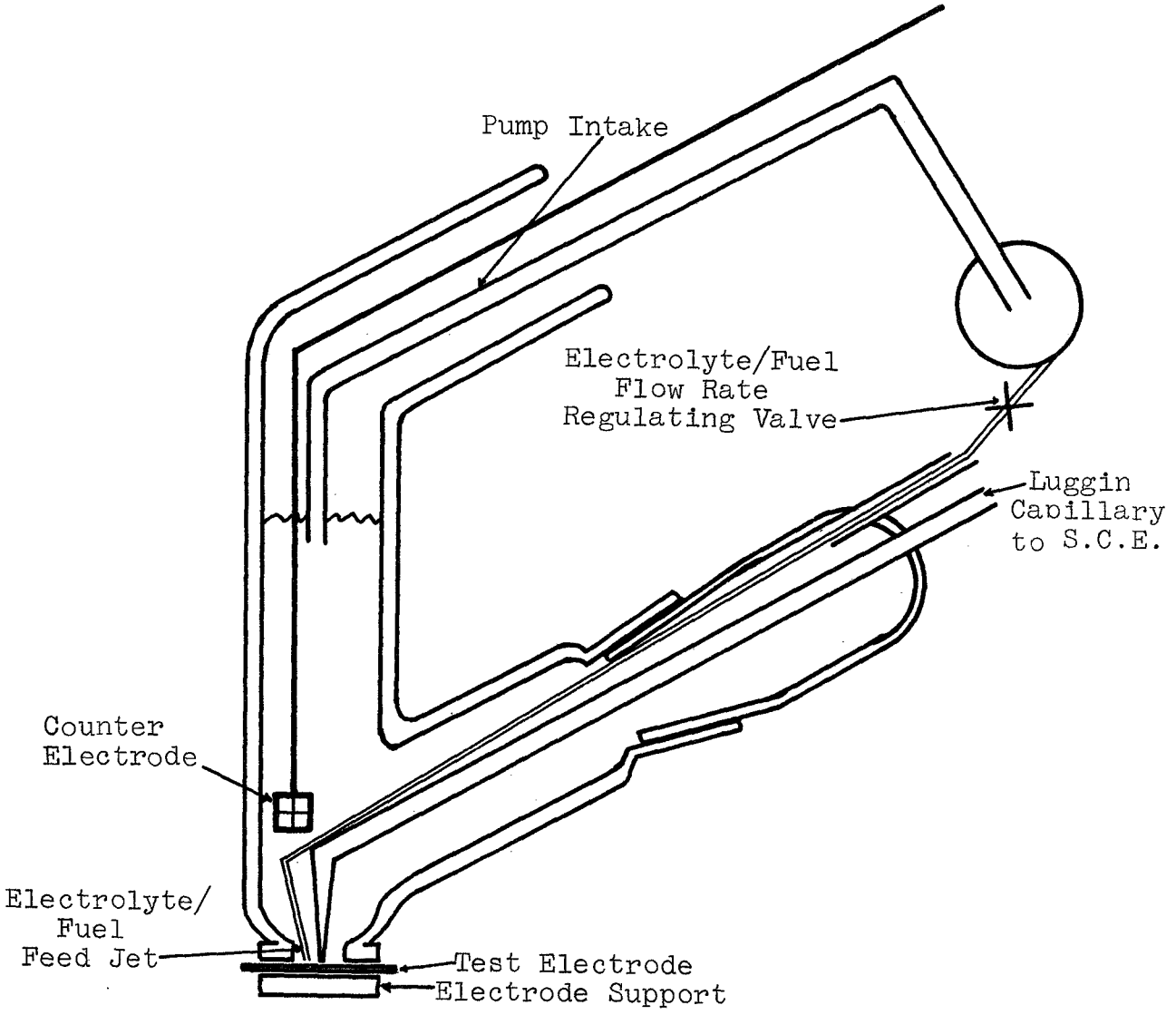

Figure 19. Fuel Catalyst Screening Cell

Thirteen catalysts were tested initially (Ref. 3a). The two that showed the best activity on UDMH fuel were Rh powder (Engelhard) and a proprietary MRC quaternary noble metal alloy catalyst (both gave 0.56 V vs SHE at 100 mA/sq cm and 60°C). The best catalyst in short-term testing on Aerozine-50 fuel was the same Rh powder (0.13 V vs SHE, 100 mA/sq cm, 60°C).

In further tests, 17 new catalysts were evaluated and several of the original 13 were retested on Aerozine-50. The results of these tests are presented in Table XXVII. Two catalysts that performed as well as Rh on UDMH fuel were Ru-Rh alloys (50-50 and 75-25% composition by weight); they yielded 0.54 V vs SHE at 100 mA/sq cm, 60°C. These catalysts also were active on Aerozine-50 (0.06 V vs SHE, 100 mA/sq cm, 60°C). Ru, Ir, Ni_2B, Ru-Rh (25-75), and a proprietary five-component alloy (electrode 77628) all showed relatively poor activity on UDMH, and fair-to-good activity on Aerozine-50, making them candidates for the second objective of the screening program discussed above. The best of these appears to be Ru (0.69 V with UDMH, 0.11 V on Aerozine-50, both vs SHE at 100 mA/sq cm, 60°C).

3. Cell Tests

In order to characterize promising electrodes by determining fuel coulombic efficiencies and long-term electrode performance, a test stand and 3 x 3 in. cell configuration were designed, constructed, and tested. The object of these designs was to trap and measure off-gases from the electrode reactions. Analysis of these gases is a preferred method of determining fuel efficiency. The reactions that can occur with the hydrazine component are:

Catalytic decomposition: $N_2H_4 \longrightarrow N_2 + 2H_2$ (30)

Electro-oxidation: $N_2H_4 \longrightarrow N_2 + 4H^+ + 4e^-$ (31)

The only likely reaction that might have upset this analysis was the decomposition to ammonia:

$$3N_2H_4 \longrightarrow 4NH_3 + N_2 \quad (32)$$

The extent of this reaction could be determined by checking H_2/N_2 ratios in the off-gases from open circuit testing; substantial deviations from a 2:1 ratio would indicate that reaction 32 was a significant factor.

Table XXVII

AEROZINE-50 ELECTRODE CATALYST TEST RESULTS

Temperature: 60°C
Electrolyte: 5M H_3PO_4
Fuel: 3M in all cases, dissolved in electrolyte
Electrodes: Catalyst/Teflon mixtures cured on Pt Screen, MRC laboratory made catalysts made by borohydride reduction of salts

Electrode Code	Catalyst Description	Fuel	Electrode Potential (volts) vs SHE at Indicated Current Density, ma/cm²				
			0	50	100	150	200
50-67226	Rh (Engelhard) - Standard Catalyst	UDMH	0.34	0.51	0.55	0.59	0.63
		A-50	0.00	0.04	0.08	0.09	0.12
71221-1	Ru (MRC laboratory made)	UDMH	0.39	0.59	0.69	0.77	0.79
		A-50	0.05	0.08	0.11	0.13	0.16
71221-3	Rh (MRC laboratory made)	UDMH	0.46	0.52	0.59	0.62	0.65
		A-50	0.09	0.12	0.15	0.16	0.16
71221-6	Ru-Rh (25-75) Alloy Catalyst (MRC made)	UDMH	0.51	0.57	0.64	0.72	0.77
		A-50	0.09	0.11	0.12	0.13	0.14
71221-7	Ru-Rh (50-50) Alloy Catalyst (MRC made)	UDMH	0.35	0.47	0.54	0.57	0.61
		A-50	0.04	0.05	0.06	0.07	0.08
71221-8	Ru-Rh (75/25) Alloy Catalyst (MRC made)	UDMH	0.33	0.47	0.54	0.60	0.64
		A-50	0.04	0.05	0.06	0.06	0.07
71221-2	Ir (MRC laboratory made)	UDMH	0.39	0.74	0.84	0.95	1.00
		A-50	0.08	0.14	0.20	0.26	0.30
71221-4	Os (MRC laboratory made)	UDMH	0.42		No Activity		
		A-50	0.04		No Activity		
71221-5	Mo (MRC laboratory made)	UDMH	0.41		No Activity		
		A-50	0.11		No Activity		
71221-9	Au (MRC laboratory made)	UDMH	0.10		No Activity		
		A-50	0.11		No Activity		

Table XXVII (Continued)

Electrode Code	Catalyst Description	Fuel	Electrode Potential (volts, vs SHE at Indicated Current Density, ma/cm^2) 0	50	100	150	200
56838	MRC Chelate Catalyst on Carbon Substrate	UDMH			No Activity		
		A-50	0.33	0.57	0.65	-	-
68729-3	Raney Nickel on Carbon on SS Screen	UDMH	0.35		No Activity		
		A-50	0.13		No Activity		
73233-29	Ni_2B Catalyst	UDMH			No Activity		
		A-50	-0.02	0.25	0.29	0.30	0.30
73233-1a	Co_2B Catalyst	UDMH	0.36	0.58	0.87	-	-
		A-50	-0.05	0.46	0.50	0.58	0.62
77628	5-Component Precious Metal Alloy Proprietary Catalyst on Carbon	UDMH	0.53	0.69	0.78	-	-
		A-50	0.09	0.17	0.20	0.21	0.23
77605	Pt-1% Mo Alloy Catalyst (MRC made)	UDMH	0.53	0.75	0.84		
		A-50	0.25	0.33	0.40	0.44	0.49
70449-52	Pt-Rh (90-10) Alloy (MRC made)	UDMH	0.55	0.69	0.75		
		A-50	0.21	0.38	0.50	0.56	0.60
73354-9	5-Component Precious Metal Alloy	UDMH	0.47	0.55	0.61	0.65	0.66
and -10	Proprietary Catalyst	UDMH	0.43	0.61	0.64	0.65	0.64
73354-6	4-Component Precious Metal Alloy	UDMH	0.45	0.63	0.64	0.65	0.64
and -7	Proprietary catalyst	UDMH	0.41	0.62	0.63	0.62	0.63
and -8		UDMH	0.41	0.62	0.67	0.69	0.71
73354-4	Pt-Ru (30-70) Alloy (MRC made)	UDMH	0.36	0.57	0.66	0.74	0.81
77604-1	5-Component Precious Metal Alloy	UDMH	0.41	0.58	0.61	0.63	0.65
and -2	Proprietary Catalysts	UDMH	0.45	0.61	0.62	0.63	0.64

The reactions of UDMH are more complex, with many more products involved. However, N_2 is the only gaseous product likely to be formed. In addition, our work on low-temperature decomposition of Aerozine-50 showed UDMH self-decomposition was minimal at temperatures of interest in this work. Thus, the participation of UDMH in the anodic reaction would be indicated by the volume of N_2 produced per ampere-hour of cell electrical output.

Calculation details on the effect of UDMH on the volume of N_2 produced per ampere-hour are reported in Ref. 3b. In general, this factor will be a maximum at 7.4×10^{-3} ft^3 of N_2/ampere-hour. This will occur only when N_2H_4 is the sole reactant at the electrode (UDMH an inert diluent). The participation of UDMH in the electro-oxidation in any mode will decrease this factor. Thus values substantially below 7.4×10^{-3} are a strong indication of UDMH reaction. In practice it is necessary to account for N_2 produced by catalytic decomposition of N_2H_4 in calculating the factor. This can be accomplished by analyzing the off-gases for H_2 and back calculating and subtracting the corresponding amount of N_2.

The Aerozine-50/O_2 acid electrolyte cell design used to conduct these tests is shown in Figure 20. This was a free electrolyte cell with the electrolyte pumped across the anode surface. An ion exchange membrane (Ionics Inc. cation exchange membrane 61AZL-183) was used to prevent O_2 from the cathode from entering the electrolyte, and to prevent exit of anode gases through the cathode.

The test stand used with this cell is shown in Figure 21. Provision was made for trapping anode off-gases whether from the fuel side of the electrode or from the electrolyte itself. The gas volume was measured accurately with a wet-test meter and analytical samples were taken for VPC analysis. A controlled power supply and associated equipment were used to determine electrode performance and ampere-hour output.

Initial tests with a Rh MRD electrode indicated that liquid Aerozine-50 could not be pumped directly to the back of the electrode. The spontaneous decomposition of the N_2H_4 component was so rapid and exothermic that permanent damage to the electrode resulted from the sudden temperature rise and no useful electric power could be drawn from the electrode. A capillary membrane type of electrode was then tried in which an MRC carbon electrode served as the membrane. This electrode reduced the spontaneous decomposition by several orders of magnitude, but the polarization characteristics were poor. The capillary membrane should pass only vapors and the composition of the vapors above Aerozine-50 were known to be 92% UDMH

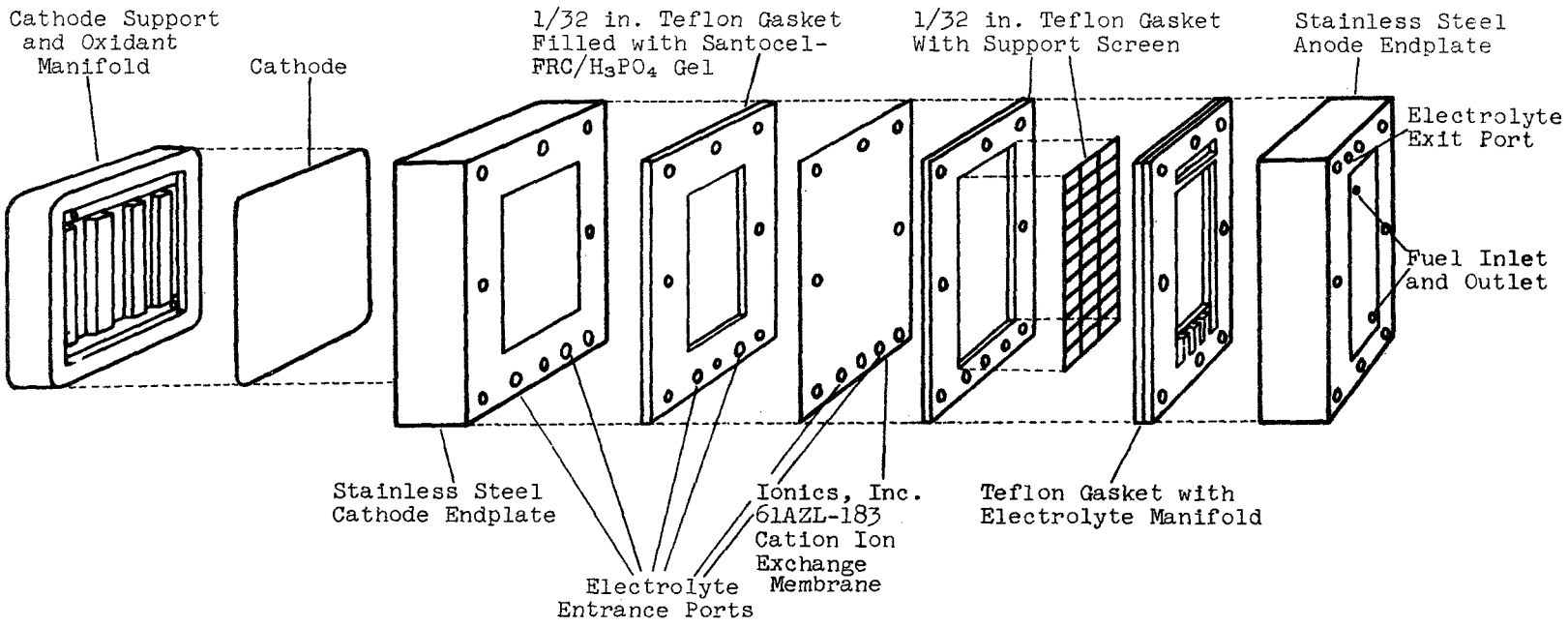

Figure 20. Aerozine-50 Anode Test Cell Construction

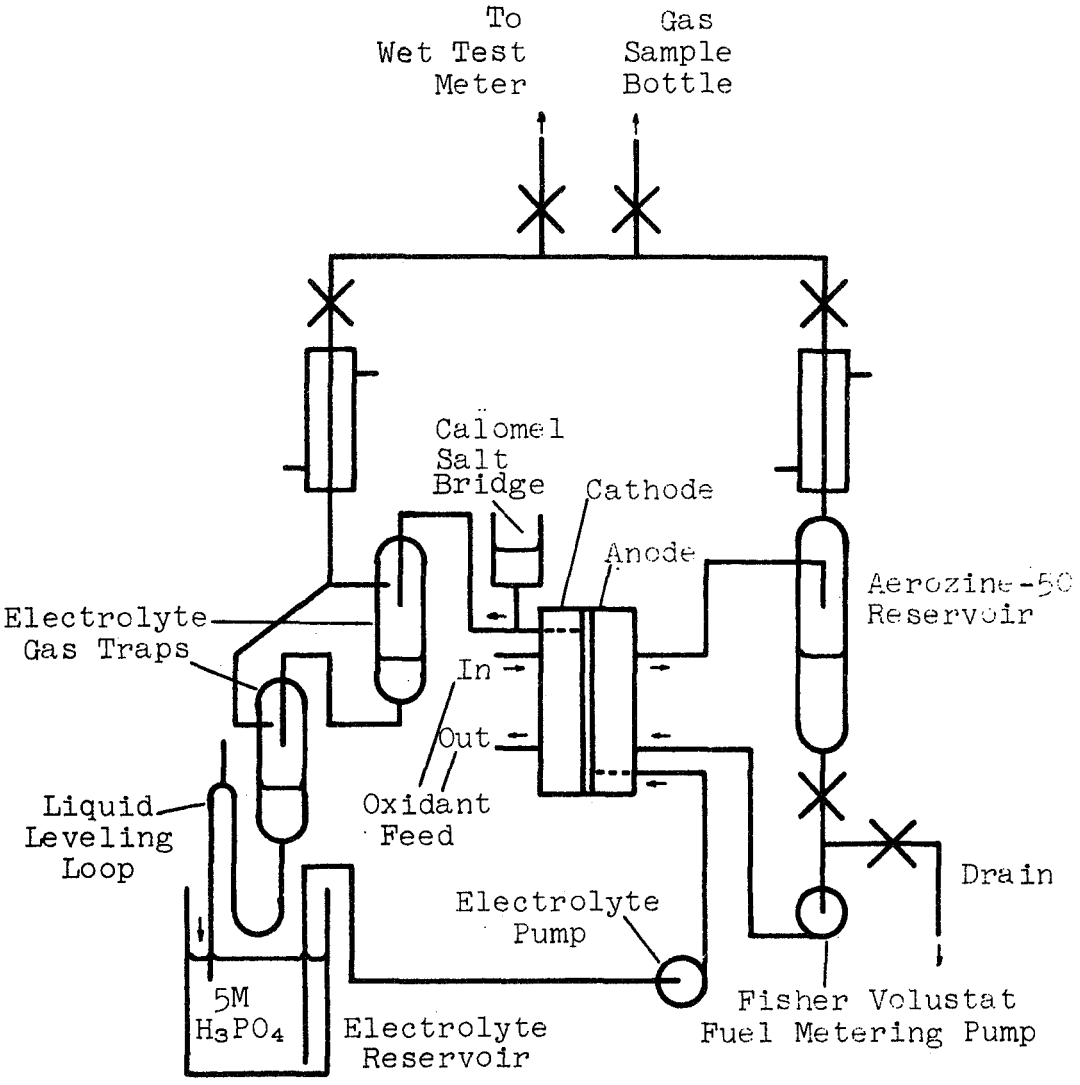

Figure 21. Aerozine-50/O_2 Cell Test Stand

by weight at 70°C (Ref. 17). Thus, the major reactant at the catalytic surface of the electrode may have been UDMH, which would account for the less anodic potentials found.

Other types of permeation barriers were also tried. The results of some of these tests are outlined in Table XXVIII. The object in these tests was to allow enough liquid diffusion to keep the N_2H_4 concentration at the catalytic surface high enough to support a reasonable current density. The vermiculite-Teflon barrier appeared to act as a capillary membrane (similar to the carbon electrode). The silica gel-glass wool-Teflon barrier allowed too much diffusion and the electrode was damaged by local high temperatures. The stainless steel plaque also did not perform as expected. It is theorized that the high internal surface area of the plaque catalyzed the decomposition of N_2H_4 and very little could diffuse through intact to the catalytic surface.

Other types of electrodes and membranes were tried. The results of these tests are given in Table XXIX. None of these electrodes performed satisfactorily on Aerozine-50 and none was considered worth following up.

Another approach was taken to this problem. Theoretically, Aerozine-50 can be fractionally distilled to separate its components. If even a partial distillation could be accomplished to obtain a relatively enriched N_2H_4 feed stock, the carbon/Pt electrode (or an equivalent) might be feasible. The major problem would be separation of phases (liquid N_2H_4 and vapor UDMH) under zero-gravity conditions.

Liquid anhydrous N_2H_4 was therefore also tried as a fuel with an MRD carbon Pt electrode. The results of the tests are shown in Table XXX. To characterize the self decomposition rate, the liquid N_2H_4 was pumped into the electrode chamber at a rate greatly in excess of electrochemical requirements. Alternately, H_2 gas was purged slowly into the electrode chamber and comparable data were taken with this fuel. The potential of the electrode was measured with a Luggin capillary salt bridge consisting of a supported Teflon spaghetti tube inserted into the electrolyte chamber. A slow flow of electrolyte was maintained through the tube to prevent gas bubbles from blocking the electrolyte path. This arrangement ensured minimum IR contribution to the measured potentials and gave a truer indication of electrode performance. Data were taken at 25 and 45°C; however, irreversible electrolyte leakage occurred at 60°C and above.

Table XXVIII

TEST RESULTS OF Rh ANODE -- DIFFUSION BARRIER COMBINATIONS

Cell Description

3 x 3 inch standard endplates

A-50 fuel / diffusion barrier / Rh anode // 5M H_3PO_4 electrolyte pumped / ion exchange membrane / gelled electrolyte // MRD-C Pt cathode / O_2

Fuel: metered at 10.0 ml per minute

Temperature: 60°C in all cases

O_2 and Electrolyte: metered at moderate rates, high enough to insure adequate cell performance

Electrode-Barrier Descriptions

No. 1 Electrode 67267-3: MRD Rh/Vermiculite laminar on 60 mesh stainless steel screen with 0.17 g Rh/in.^{2} Vermiculite layer made by mixing powdered vermiculite and Teflon dispersion and curing.

No. 2 Electrode 67267-4: MRD Rh electrode mated to silica gel, glasswool, Teflon diffusion barrier. Rh anode has 0.55 g Rh/in.^{2} on 60 mesh stainless steel screen. Diffusion barrier made by mixing ingredients in a Waring blender, sheeting, and curing (Notebook reference 5080).

No. 3 Electrode 67267-0 and -2: Double MRD Rh electrode mated to porous stainless steel plaque. Rh anode has 1.10 g Rh per in.^{2} on 60 mesh stainless steel screen. Stainless steel plaque from Clevite Corp., 60-65% porous, 0.030 in. thick.

Test Results

Electrode-Barrier	Open Circuit Gas Evolution, ca. ft/hr	Anode Potential at Indicated Current Density, volts versus SHE		
		0 ma/cm^2	50 ma/cm^2	100 ma/cm^2
No. 1	0.002	-0.32	+1.18	-
No. 2	0.367	+0.38	+0.54	+0.84
No. 3	0.090	+0.14	+0.49	+1.04

Table XXIX

RESULTS OF ELECTRODE TESTS WITH AEROZINE-50

Electrode	Description	Results of Tests on Aerozine-50	Electrical Performance
MRD-carbon/Pt	Proprietary electrode consisting of 40mg Pt/cm^2 on carbon-teflon substrate, supported on stainless steel screen.	Will operate as a vapor diffusion electrode for 20-30 min, then completely wetted with Aerozine-50 and operates as liquid diffusion anode Pt layer disrupted and blistered.	Poor-heavy polarization.
Chemcel-hydrophobic	9mg Pt/cm^2 on a Ta mesh screen, Teflon hydrophobic layer applied by unspecified "new method".	Too porous - allows direct mixing of fuel and electrolyte with precipitation of hydrazine phosphates.	Could not be tested.
Chemcel + added porous Teflon	Above electrode mated with a sheet of porous Teflon - 0.050 in thick, 6.6μ average pore size.	Operated immediately as liquid diffusion anode - demonstrated for circa one hour - some physical degradation evident after test.	+0.32v vs SHE at 50 ma/cm^2, 30°C.
American Cyanamide LAF 1	Pt-RH catalyst deposited on a porous Teflon backing.	Delaminated and physically degradated (blistered) due to effects of decomposition of fuel.	Could not be tested.

Table XXX

TEST RESULTS ON LIQUID ANHYDROUS N_2H_4 FUEL

Cell Description

3 x 3 inch Standard Endplates

Anhydrous N_2H_4 / MRD-C/Pt Electrode // 5M H_3PO_4 Electrolyte Pumped / Ion Exchange Membrane / Gelled Electrolyte // MRC-C/Pt Dummy Electrode

Fuel:	99+% N_2H_4 metered at 10 ml/min or tank H_2 metered at 3 in. H_2O pressure, slight purge
Reference Electrode:	"Luggin Capillary" constructed from a Teflon spaghetti tube inserted into electrolyte cavity in cell and positioned against the anode face.
Electrolyte:	Pumped through cell at a rate sufficient to insure adequate cell performance.
Electrode:	Standard MRD-C/Pt with 0.050 g Pt/in.^{2}

Data

1. Polarization Curve - N_2H_4

Temp, °C	Fuel	Anode Potential at Indicated Current Density (volts vs SHE), ma/cm^2 0	50	100	150	200
25	N_2H_4	0.03	0.13	0.20	0.28	0.30
25	H_2	-0.04	0.07	0.20	0.32	-
45	N_2H_4	0.02	0.08	0.11	0.17	0.22
45	H_2	-0.01	0.07	0.14	0.23	0.34

2. Open Circuit Gas Evolution - N_2H_4 Fuel

Temp, °C	Measured Gas Evolution, ft^3/hr	N_2H_4 Decomposed, g/hr	Equivalent N_2H_4 Current Density, ma/cm^2
25	0.000	0.00	0
45	0.015	0.19	10.6

3. 30-minute Run, 45°C, 100 ma/cm^2, N_2H_4 Fuel

Initial electrode potential: +0.12 v vs SHE

Electrode potential after 30 minutes: +0.14 v vs SHE

Volume of gas evolved: 0.030 ft^3

Theoretical gas volume: 0.0075 ft^3 from decomposition
0.0242 ft^3 from electrochemical reaction
0.0317 ft^3 TOTAL

The following statements can be made on the basis of these tests:

(a) The polarization characteristics of liquid N_2H_4 with the carbon/Pt electrode (even at lower temperatures) are sufficient to ensure a high power output. For example, a power density of 85 mW/cm^2 is possible if the results at 45°C, 100 mA/cm^2 are combined with the results of N_2O_4 cathode testing (60°C, 100 mA/cm^2, 1.00 V vs SHE).

(b) The performance of N_2H_4 with this electrode compares favorably with H_2 fuel performance at the same temperature.

(c) The self-decomposition rate measured in this test would limit the N_2H_4 current efficiency to circa 90% at 100 mA/cm^2. However, there is some indication that the self-decomposition rate decreases as current is drawn from the electrode.

D. ONE-THIRD SQUARE FOOT CELL OPERATION ON REFORMER STREAMS

1. Background

The objective of this work was to determine electrode performance on the decomposed propellant streams in a 1/3 ft^2 half cell. Both the power densities and coulombic efficiencies of the possible combinations of electrode, electrolyte, and reactant stream compositions were of interest.

The test cell set-up used was identical to that described for the N_2O_4 cathode characterization in Section V.B.2.b, and Figure 18 is applicable to this section. The test procedure was identical except that tests were also run with 5M KOH electrolyte.

2. Initial Testing

Electrodes used in these tests were standard MRD carbon/Pt laminar electrodes, with 50 mg of Pt/$in.^2$ on a 0.025-in. thick carbon/Teflon matrix supported by a stainless steel screen.

The unit was assembled and run on tank O_2 and H_2 to characterize the electrode performance before reformer streams were used. The results of these tests are shown in Table XXXI.

Table XXXI

INITIAL H_2/O_2 1/3 FT^2 CELL TESTING

Electrodes: MRD-C Carbon/Pt laminar electrodes on stainless steel screen, 40-50 mg Pt/in^2.

Electrolyte: 5M H_3PO_4 or 5M KOH (as noted), pumped through cell (IEM Separation)

Reactants: Tank O_2 and tank H_2 supplied at near atmospheric pressure.

Temperature	Electrolyte	Feed Rate	Current	Electrode Potential, volts vs SHE	
			ASF	Anode	Cathode
60°C	5M H_3PO_4	1 SCFH H_2 + O_2	0	0.01	0.99
			30	0.10	0.71
			60	0.18	0.57
			90	0.27	0.46
80°C	5M H_3PO_4	1 SCFH H_2 + O_2	0	0.03	0.99
			30	0.10	0.75
			60	0.19	0.16
			90	0.27	0.49
80°C	5M KOH	1 SCFH - H_2 1 SCFH - O_2	0	-0.86	+0.11
			30	-0.84	+0.09
			60	-0.80	-0.24
			90	-0.79	-0.37

Anode performance was reasonably satisfactory at both 60°C and 80°C in both acid and alkaline electrolytes. However, cathode polarization was severe at both temperatures and in both electrolytes. The performance appeared to be independent of O_2 feed rate, and there were indications that IR losses were the major source of polarization. Since the reference electrode was a Luggin capillary the IR losses due to electrolyte resistivity should have been quite small. The main resistance must then have been in the electrode itself and in the current collector on the reverse side of the electrode. This consisted of the electrode support screen and the reactant flow plate, both of which were stainless steel. Several other tests were run that tended to confirm these results. The electrode was removed from the cell and several small (ca. 3 cm^2) sections were tested in a glass half cell using a Kordesch-Marko bridge to obtain IR-free potentials. At 80°C using 5M H_3PO_4 electrolyte, IR-free potentials of 0.81-0.83 V vs SHE electrode were obtained at a current equivalent to 90 ASF.

The cell was subsequently rebuilt with the stainless steel electrode screen, the reactant flow plate, and the cell backing plate all gold plated over a nickel plate strike. The test results on this rebuilt cell are shown in Figure 22. The cathode polarization characteristics were much better and confirmed the importance of low-resistance current collection in a cell of this size. We estimate that the total resistivity of the electrode and current collector combination in the original tests was 14 milliohms. However, at 30 amperes, this resistance will produce 0.4 V of IR polarization.

3. H_2 Half Cell Testing

Using the Au-plated components, the operation of the electrode on H_2 was more full characterized. The results are summarized in Table XXXII. In Table XXXII(A) the results of testing on tank H_2 at various flow rates are shown. The limiting stoichiometric currents were calculated based on the reaction:

$$H_2 = 2H^+ + 2e^- \qquad (33)$$

For this reaction, one standard cubic foot (SCF) of H_2 is equivalent to 62.5 ampere-hours. Thus 1 SCF per hour (SCFH) will support 62.5 amperes. The results show that the H_2 utilization is near stoichiometric with these electrodes and that polarization will be less than 0.10 volt up to the stoichiometric current.

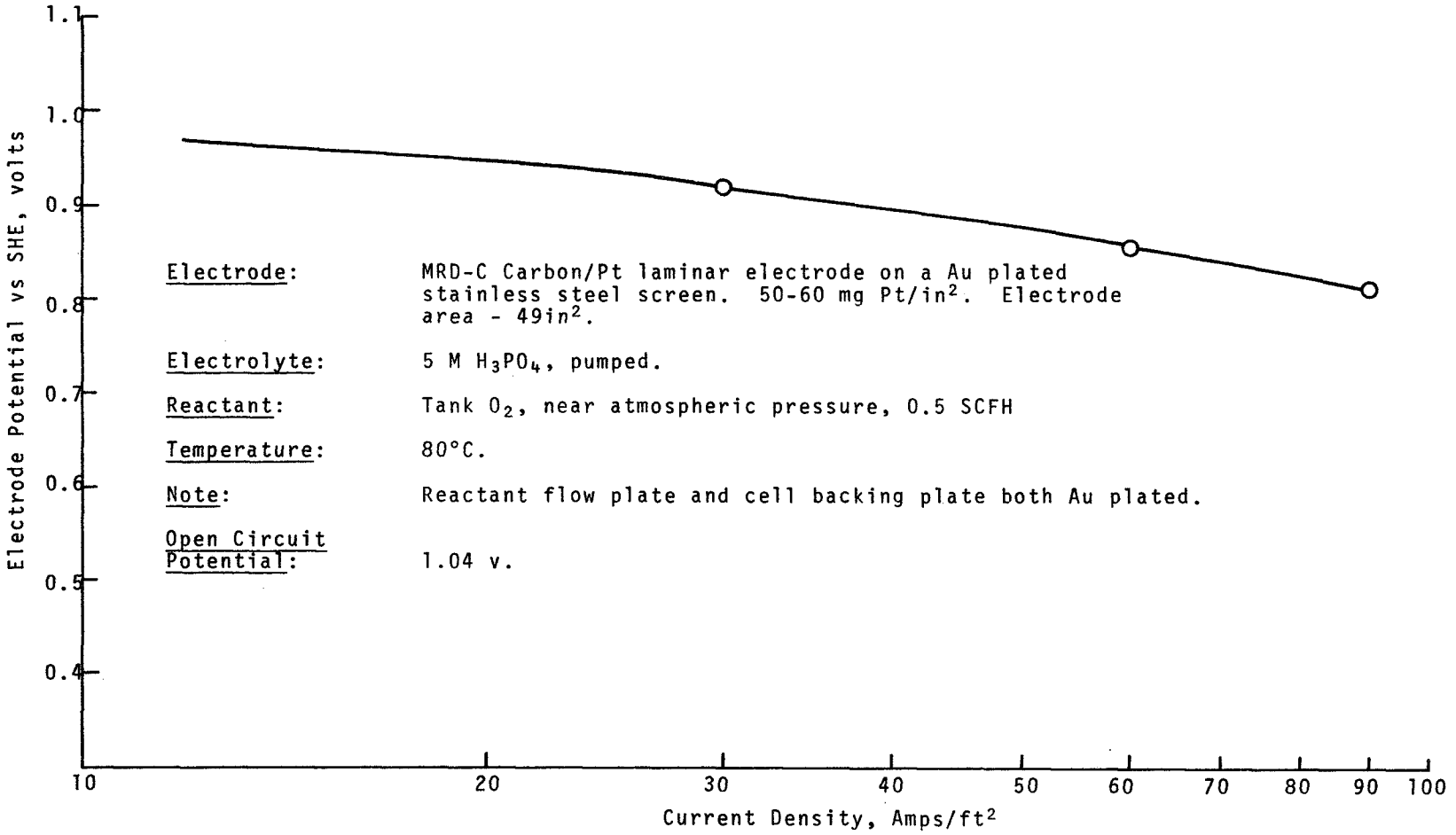

Figure 22. O_2 Cathode Tests With Au Plated Components

Table XXXII

H_2 HALF CELL TESTS

Electrode: MRD Carbon/Pt laminar, 50 mgPt/in^2 60 mesh s.s. screen Au plated over Ni strike. Electrode Area = 49in^2

Electrolyte: 5 M H_3PO_4, pumped

Temperature: 80°C

A. OPERATION ON TANK H_2

Measured H_2 Flow Rate SCFH	Limiting Stoichiometric Current for This Flow Rate (100% efficiency) Amperes	Electrode Potential, volts vs SHE, at indicated current, Amperes, from 1/3ft^2 Electrode				
		0	10	20	30	40
0.30	19	0.06	0.09	heavy polarization		
0.40	25	0.07	0.10	0.12	heavy polarization	
0.50	31	0.06	0.08	0.10	0.15	----
0.60	38	0.05	0.08	0.10	0.14	----

B. OPERATION ON H_2 FROM REFORMER-PD DIFFUSER COMBINATION

Ultrapure H_2 measured rate: 0.312 SCFH

Amperage Equivalent: 19.4 Amp

Current From* Cell, amperes	Electrode Potential,**Volts to SHE
0	0.05
19	0.10
20	0.10
21	Heavy polarization
20	0.25
19	0.10

* Values in chronological order

** Steady state values after 10 minutes at indicated current.

In Table XXXII(B) the results of coupling the Aerozine-50 stream reformer-Pd diffuser combination to the cell are shown. More exact measurements of flow rates and limiting currents were made. These results indicate that the H_2 utilization efficiency was greater than 95% in these tests.

4. O_2 Half Cell Testing

The results of similar testing on tank O_2 are given in Table XXXIII. Although near stoichiometric utilization was realized before heavy polarization occurred, the magnitude of polarization up to this point was generally much higher than was found with H_2. In addition, the values were sometimes difficult to reproduce exactly and it was found that the electrode potential depended to some extent on pretreatment. A period of slow cathodization without O_2 flowing seemed to have a beneficial effect. These results are completely in agreement with the well-documented fact (both in our work and that of others in the field) that a Pt-catalyzed O_2 electrode is not reversible in acid electrolytes. Larger polarizations and difficulty in exact reproduction of data are to be expected.

5. Half Cell Testing on Unscrubbed N_2O_4 Decomposer Stream

The objective of this test was to determine if higher electrochemical utilization of N_2O_4 could be realized by partially decomposing the reactant first. In a previous section the results of testing 1/3 ft^2 cells on pure N_2O_4 were reported. Coulombic efficiencies of 27% were measured in those tests.

The product stream from the N_2O_4 decomposer was fed directly to the cell through a heated line (to prevent condensation of the unreacted N_2O_4). The results of the subsequent tests are summarized in Table XXXIV. Very unstable electrode potentials were found; there seemed to be a slow cycling of the potential that was independent of current density and reactant feed rate.

This type of behavior had not been found in prior testing with pure N_2O_4. The data are very difficult to interpret and no reliable conclusions can be made about utilization efficiency of this stream.

Table XXXIII

O_2 HALF CELL TESTS

Electrode: MRD Carbon/Pt laminar, 50mgPt/in^2 60 mesh s.s. screen Au plated over Ni strike. Electrode Area = 49in^2

Electrolyte: 5 M H_3PO_4, pumped

Temperature: 80°C

Reactant: Tank O_2

Measured O_2 Flow Rate SCFH	Limiting Stoichiometric Current for this Flow Rate (100% efficiency) amperes	Electrode Potential, volts vs SHE, at indicated current, amperes, from 1/3ft^2 Electrode				
		0	10	20	30	40
0.08	10	0.98	0.78	heavy polarization		
0.16	20	0.99	0.79	0.72	heavy polarization	
0.25	31	0.99	0.80	0.74	0.69	heavy polarization

Table XXXIV

HALF CELL TESTS ON UNSCRUBBED
N_2O_4 DECOMPOSER STREAM

Electrode: MRD Carbon/Pt laminar, 50mgPt/in^2 60 mesh s.s. screen Au plated over Ni strike. Electrode Area = 49in^2

Electrolyte: 5 M H_3PO_4, pumped

Temperature: 80°C

Reactant: Product stream from N_2O_4 Decomposer Measured Rates: 0.268 SCFH of gas of composition 67.6% O_2 and 32.4% N_2 (by VPC) plus 4g/hour of unreacted N_2O_4.

Stoichiometric Limiting Currents: For O_2 alone: 23 amps
For total stream: 32 amps

Current From Cell amperes*	Electrode Potential vs SHE** volts
10	0.77 - 0.94
15	0.51 - 0.78
10	0.60 - 0.94
11	0.63 - 0.93
12	0.59 - 0.90
13	0.53 - 0.90
14	0.59 - 0.86
15	0.48 - 0.74
16	0.45 - 0.50

* Chronological order
** Values are lowest and highest potentials recorded during 20-30 minutes at each current.

E. CONCLUSIONS AND RECOMMENDATIONS

We successfully obtained a greatly improved N_2O_4 cathode coulombic efficiency primarily as a result of the design of an efficient reactant flow plate. The efficiencies reported here are nearly an order of magnitude better than those reported on our previous contract (Ref. 2). The cathode was demonstrated in a 1/3 ft^2 size at practical current densities.

The same degree of success was not realized with the Aerozine-50 anode despite testing of a variety of electrode structures for this service. Those electrodes with satisfactory electrical characteristics invariably also caused excessive self-decomposition of the fuel and/or precipitation of hydrazine phosphates due to mixing of fuel and electrolyte.

An electrode operating from pure anhydrous N_2H_4 has been successfully demonstrated and could be developed for fuel cell service with an N_2O_4 cathode. A more promising system, however, is a H_2/N_2O_4 cell with the H_2 supplied by the Aerozine-50 steam reformer. We have previously shown that the H_2 anode is compatible with this cathode.

Half cells of 1/3 ft^2 size were operated on H_2 and O_2. The H_2 half cell polarized less than 0.10 V at 90 ASF and operated at a coulombic efficiency above 95% on the stream from the Pd membrane diffuser. The O_2 electrode appeared to operate at nearly the same coulombic efficiency. However, it polarized more under load. Operation of the unscrubbed N_2O_4 decomposer stream was attempted, but unstable electrode potentials were found. It is recommended that scrubbing of residual N_2O_4 from this stream be included in system considerations.

VI. REMOVAL OF UNREACTED N_2O_4 FROM THE N_2O_4 DECOMPOSER STREAM

A. BACKGROUND

The experimental results on the decomposition of N_2O_4 reported in section IV indicate that conversion efficiencies above 80-85% will probably require prohibitively high residence times in the reactor. This means prohibitive size and weight of equipment would be required to increase conversion efficiencies to the point where an in-line caustic scrubber would be feasible for any but the shortest mission times. The solution to this problem lies in the development of a regenerable scrubber.

After preliminary experimentation with several alternates, the concept settled upon as most promising was a dual column adsorption unit.

A conceptual design of one configuration of the proposed unit is diagrammed in Figure 23. The adsorption unit consists of two columns packed with adsorbent, one of which adsorbs N_2O_4 from the reactor gas stream while the other column desorbs to space vacuum. When the adsorber becomes saturated, the functions of the two columns are reversed.

Each of the packed columns contains a central heat exchanger (indicated by the spiral line) to effect heat exchange between the packing and the boiling liquid N_2O_4 during the adsorption cycle, and a separate heat exchanger attached to each column to provide for cooling of the reactor gas stream prior to its entering the bed. Another heat exchange function is indicated by the outer coiled tube providing for the preheating of the columns by the reactor gas stream during desorption. A porous walled core tube in each column provides open access of space vacuum to the column packing during desorption.

The general operating principles of this unit are as follows. The column entering the desorption part of the cycle is initially heated by the hot reactor gases to some temperature at which (after the heating is discontinued and the column is opened to space vacuum) the column will be adiabatically returned to near its initial temperature by the evaporative cooling of the desorbing N_2O_4 in the unit. The adsorbing unit is fed initially with the reactor gases partially cooled by the desorbing column and later in the cycle directly with the hot gases. The liquid N_2O_4 from tankage is fed continuously to the adsorbing column heat exchanger.

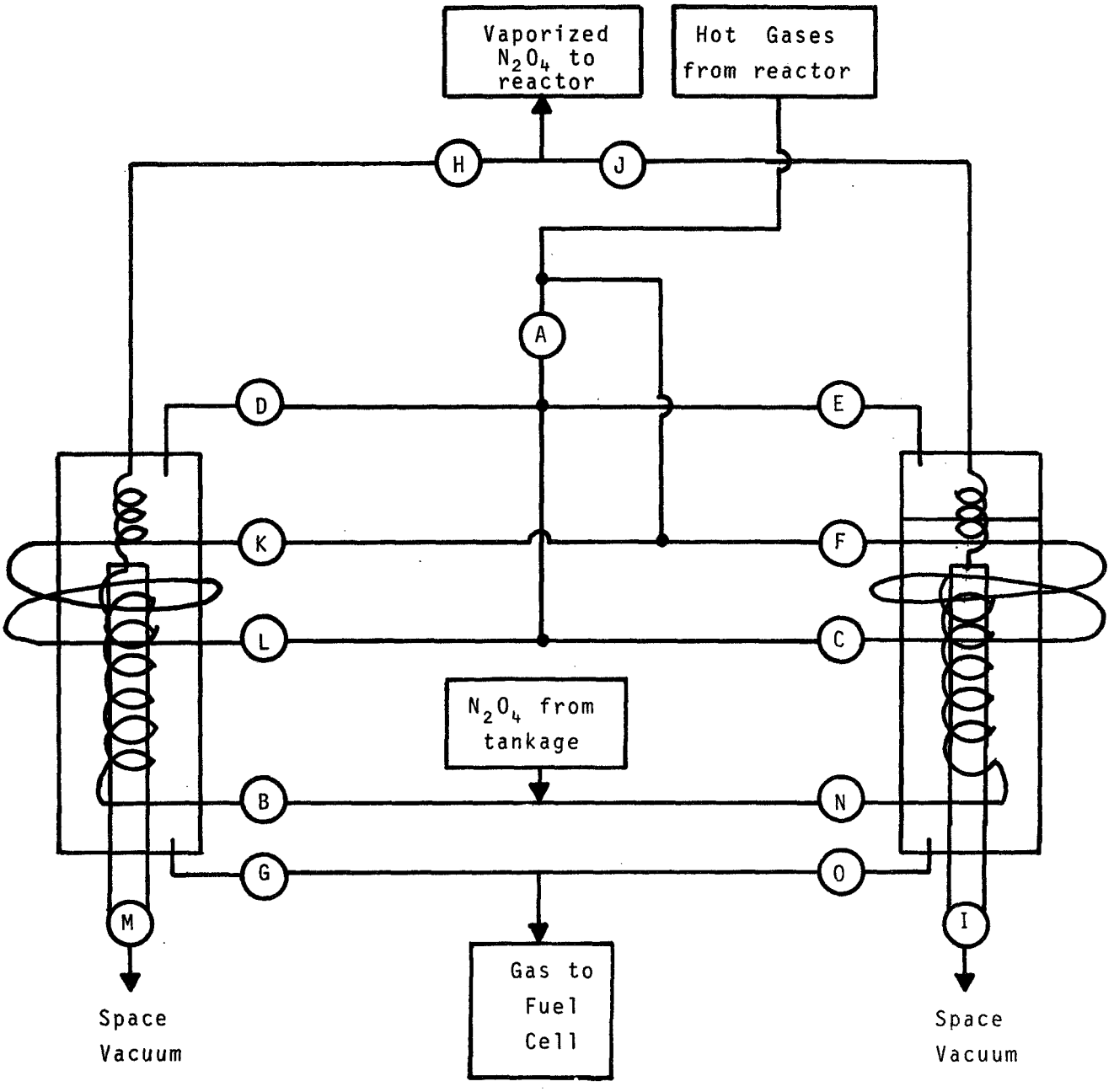

Figure 23. Schematic for Non-Steady-State N_2O_4 Scrubber

In more detail, the system would operate as follows, starting at a point in which column II in Figure 23 is just completing an adsorption cycle and column I a desorption cycle. The completion of this cycle is indicated by the initial show of N_2O_4 gas in the purified N_2O_4 product mixture. At this point in the cycle, before N_2O_4 gas appears in the product, valve I is open to vacuum and valves B, D, G, and H are open to supply reaction product gas and the liquid N_2O_4 stream to the adsorbing column. All valves not indicated as open are closed. When the operation of the unit is switched so that column II is starting the desorption cycle and column I the adsorption cycle, the open valves are F and C. This provides for the preheating of column II by the reactor product gases, the adsorption of the N_2O_4 on the packing in the vacuum cleaned column I, and the cooling of column I by the liquid N_2O_4. When sufficient energy is supplied to column II to provide for the evaporation of the N_2O_4 adsorbed in it, valves F and C are closed and valve A is opened, until the completion of adsorption cycle in column I and the desorption in column II at which time the operations are again switched.

A development program was initiated to screen possible adsorbents and determine the sorption characteristics of the optiminal adsorbent.

B. INITIAL STUDIES

1. Screening of Adsorbents and Sorption Experiments with Molecular Sieve

a. Apparatus and Methods

Small adsorption units were constructed for the adsorption of N_2O_4 from a carrier gas mixture consisting of 34 mol % N_2 and 66 mol % O_2. These adsorption units were made of Pyrex glass. They had an inside diameter of 1.2 cm and an effective length of 8 cm. The flow rates of the gas mixture and of N_2O_4 were monitored with separate flow meters. The flow meter for the gas mixture was calibrated with a wet test meter, while that for the N_2O_4 was calibrated by bubbling the stream through 10% H_2O_2 solution and titrating the resulting solution with a standard NaOH solution. The amount of N_2O_4 adsorbed was determined by weighing the adsorption tube and sorbent with an analytical balance both before and after adsorption. The breakthrough time was determined both by visual observation of the brown color appearing in the exit stream from the adsorption bed and by the change of color of a wet litmus paper.

b. Screening of Sorbents

Five sorbents were screened for the adsorption of N_2O_4. They were: (1) molecular sieve 13X, 1/16 in. pellets; (2) molecular sieve 4A, 1/16 in. pellets; (3) silica gel, 14 x 20 mesh; (4) activated carbon BPL, 13 x 30 mesh; and (5) chromosorb, acid washed, 30 x 40 mesh. The N_2O_4 flow rate was 3.1 to 3.7 g/hr and the carrier gas flow rate was 10 l/hr. The screening runs were conducted at room temperature (25-27°C). The results are given in Table XXXV. Among the five sorbents tested, molecular sieve 13X showed the highest N_2O_4 adsorption capacity at break point, 0.24-0.29 g N_2O_4/g sorbent. The adsorption capacity of the other sorbents evaluated was 0.04 g/g for silica gel; 0.03 g/g for activated carbon; 0.007 g/g for molecular sieve 4A; and 0.003 g/g for chromosorb.

The fact that the adsorption capacity of activated carbon was an order of magnitude lower than that of molecular sieve 13X was surprising. Measurement of the bed temperature during the run with activated carbon showed that the bed reached 305°C. This indicates evolution of a large amount of heat and suggests that the adsorption is chemisorptive in nature. The resulting high temperature of the bed may be responsible for the low adsorption capacity of activated carbon.

c. Adsorption Experiments

Adsorption experiments were continued with molecular sieve 13X as the sorbent. Runs were made at five temperature levels, 26°, 72°, 100°, 150°, and 200°C; and at three different N_2O_4 flow rates, 2.0, 3.2, and 10 g/hr. The carrier gas was composed of 34 mole % N_2 and 66 mole % O_2. The flow rate of the carrier gas was fixed at 10 l/hr (25°C, 1 atm) in all cases. The N_2O_4 contents of the sorbent at the break point are given in Table XXXVI. These data are plotted in Figure 24 as a function of temperature and N_2O_4 flow rate. The N_2O_4 content at the break point decreased as the temperature was increased. This is expected because adsorption is an exothermic process and is, therefore, favored by low temperatures. At high N_2O_4 flow rates, the N_2O_4 content at the break point decreased considerably at 26°C to 72°C, but only slightly at 100°C to 200°C.

Table XXXV

ADSORPTION DATA FOR N_2O_4

	Molecular Sieve 13X		Molecular Sieve 4A	Activated Carbon BPL		Silica Gel	Chromosorb, Acid-Wash
Run No.	10	11	6	8	19	5	9
Temperature, °C	25	25	27	26	70	27	25
Gas Flow Rate,* l/hr	10	10	10	10	10	10	10
N_2O_4 Flow Rate, g/hr	3.6	3.7	3.6	3.7	3.1	3.2	3.7
Wt. of Sorbent, g	4.65	3.51	5.13	3.52	3.86	4.12	2.49
Bed Height, cm	4.3	4.1	4.5	4.2	5.0	3.3	3.8
Break-through Time, min	16.79	15.89	0.54	2.26	1.54	4.32	0.36
N_2O_4 adsorbed, g	1.125	1.002	0.036	0.113	0.092	0.178	0.007
g N_2O_4/g sorbent	0.242	0.286	0.007	0.032	0.024	0.043	0.003
Max. Temp. of Bed During the Run, °C	------	------	-----	305	-----	51	-----

*34 vol-% nitrogen, 66 vol-% oxygen

Table XXXVI

ADSORPTION OF N_2O_4 WITH MOLECULAR SIEVE 13X

N_2O_4 Flow Rate* g/hr	N_2O_4 Content at Break Point, g/g				
	26°C	72°C	100°C	150°C	200°C
2.0 - 2.4	0.290	0.194	0.154	0.078	0.052
	0.255				
3.0 - 3.7	0.286	0.202	0.128	0.072	0.049
	0.242				
9.7 - 11.4	0.160	0.121	0.106	0.062	0.043
	0.177				

* Carrier Gas (1/3 N_2 + 2/3 O_2) flow rate = 10 ℓ/hr, @ 25°C, 1 atm

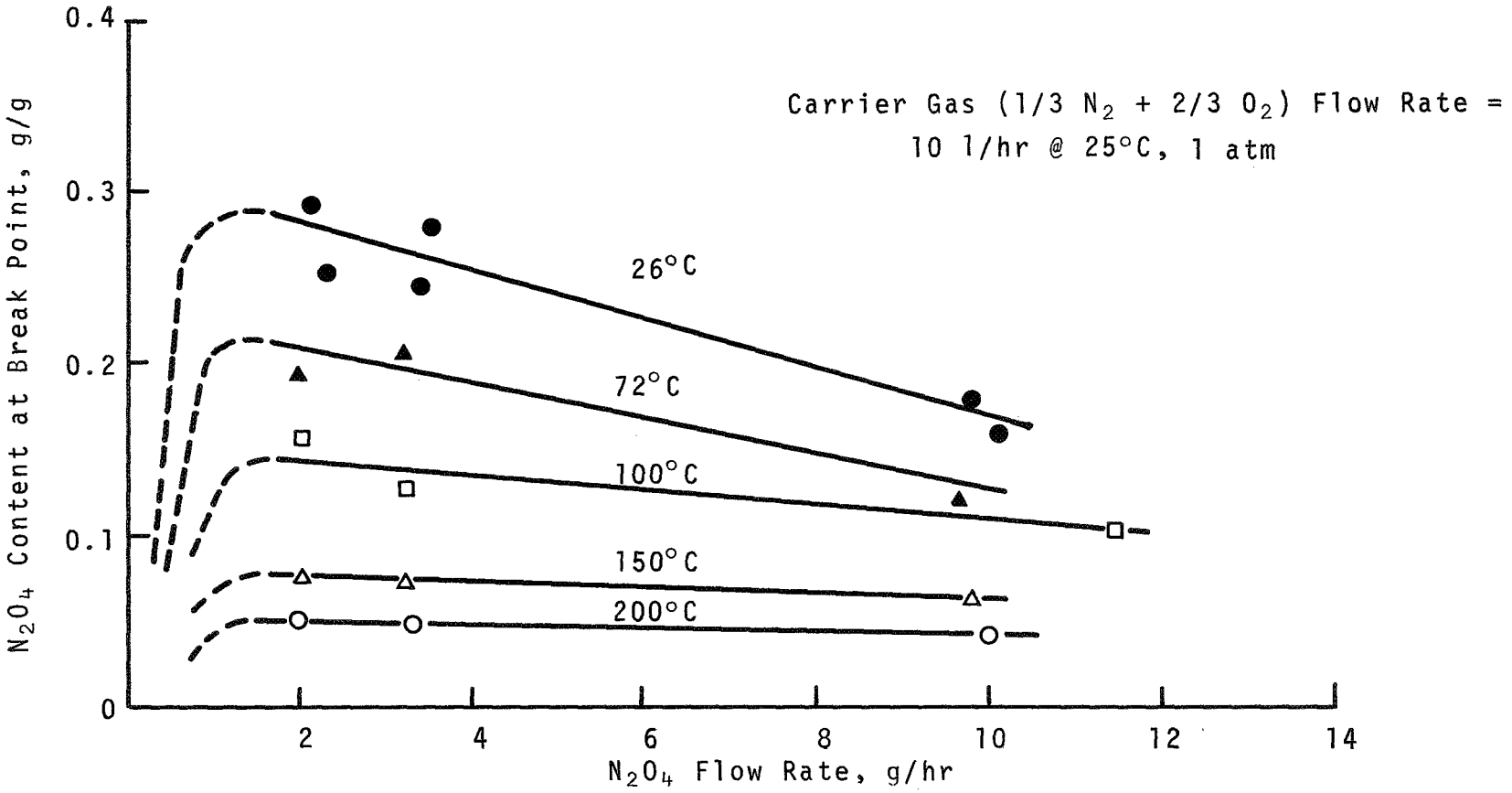

Figure 24. Adsorption of N_2O_4 with Molecular Sieve 13X

d. Desorption Experiments

Desorption experiments were also carried out at five temperature levels, 26°, 72°, 100°, 150°, and 200°C. A vacuum of 30 in. Hg was used for the desorption. Molecular sieve 13X was the only sorbent used in this study.

During the desorption run, the N_2O_4 content, X, expressed in grams of N_2O_4 per gram of sorbent, was followed with time, t, in minutes. The integral curve, X versus t, was differentiated by plotting $\Delta X/\Delta t$ versus X. The instantaneous rate of desorption dX/dt, in g N_2O_4/g sorbent-minute, was obtained from the plot as a function of N_2O_4 content, X. Figure 25 presents the rates of desorption at five temperature levels. It is seen that the rate increased rapidly with the temperature, and that, at each temperature level, the rate decreased linearly with the N_2O_4 content of the sorbent. This relationship continued until a certain N_2O_4 content was reached. Beyond this point the slope of the curve reduced drastically, and the rate was extremely slow. This critical N_2O_4 content varied with the temperature of desorption. At 26°C the critical N_2O_4 content was about 0.18 g/g, while at 200°C, it was about 0.08 g/g.

e. Adsorption-Desorption Cycling

Two adsorption-desorption cycling experiments were conducted. In one experiment the adsorption was done at 26°, the desorption at 72°C. In the other experiment the adsorption was also done at 26°C, but the desorption at 100°C. Both experiments were carried out to 10 cycles. The results are presented in Figures 26 and 27. At 72°C desorption cycling (Figure 26), the efficiency of the sorbent gradually decreased as indicated by the approaching of the adsorption and desorption curves. At 100°C desorption cycling (Figure 27), the adsorption and desorption curves remained parallel and the sorbent showed no signs of deterioration up to 10 cycles.

f. Discussion of Initial Results with 13X Molecular Sieve

Figure 24 shows data for the adsorption of N_2O_4 obtained by allowing a mixture of N_2O_4 in a carrier gas consisting of 34 mole % N_2 and 66 mole % O_2 to flow through a packed bed containing molecular sieve 13X. The amount of N_2O_4 adsorbed was determined by weighing the tube and sorbent

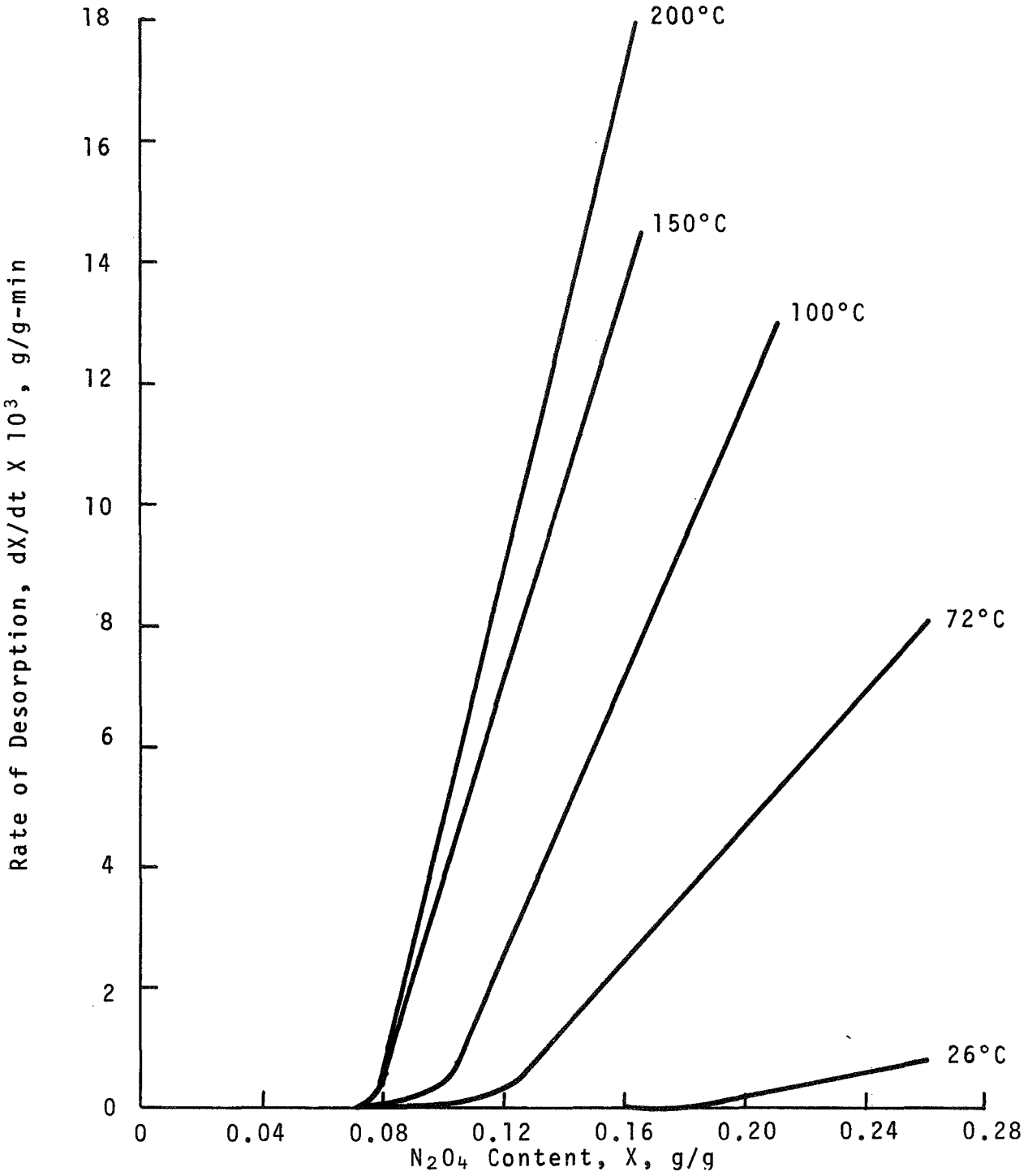

Figure 25. Desorption of N_2O_4 from Molecular Sieve 13X with 30" Hg Vacuum

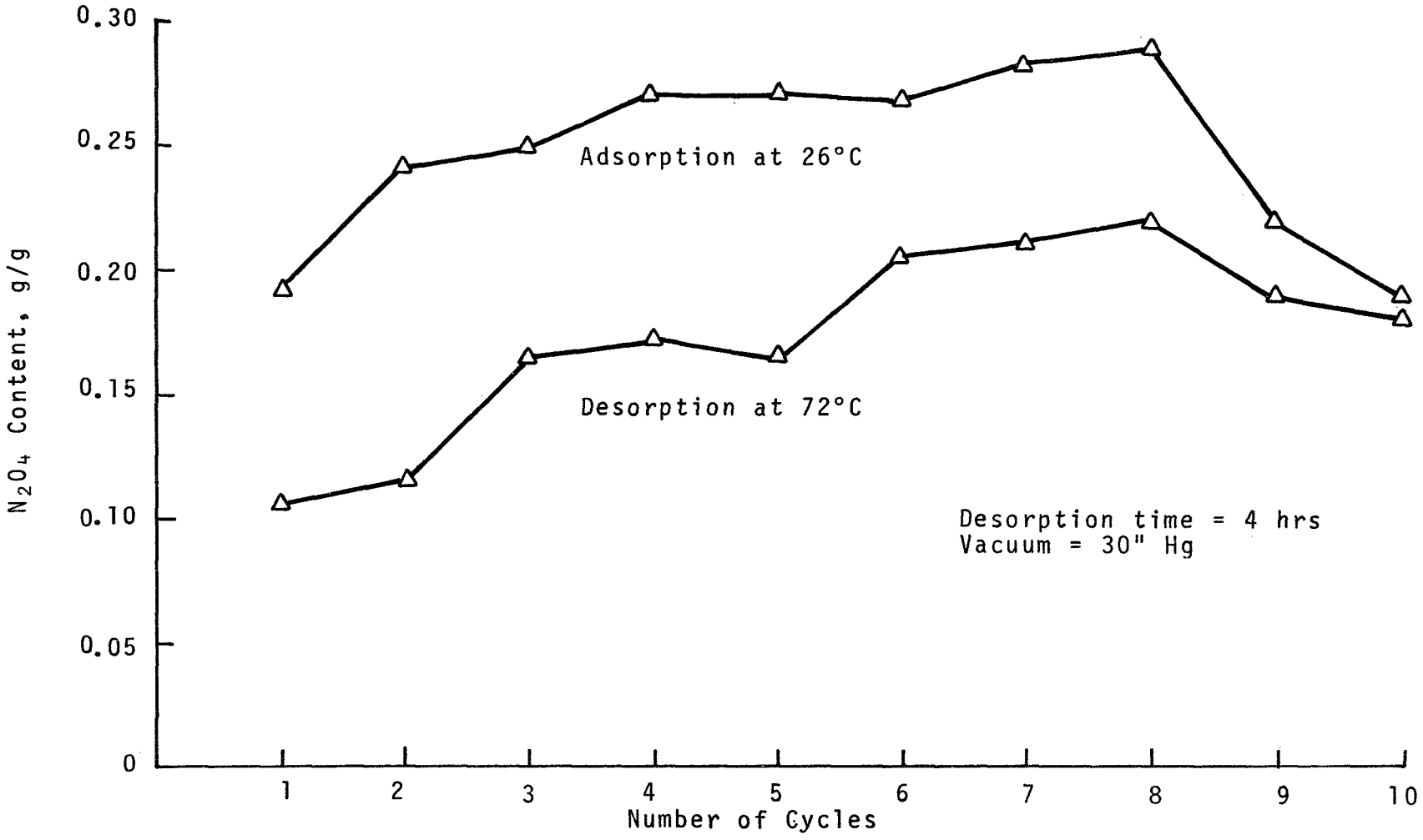

Figure 26. Adsorption-Desorption Cycling of N_2O_4-Molecular Sieve 13X System (desorption temperature = 72°C)

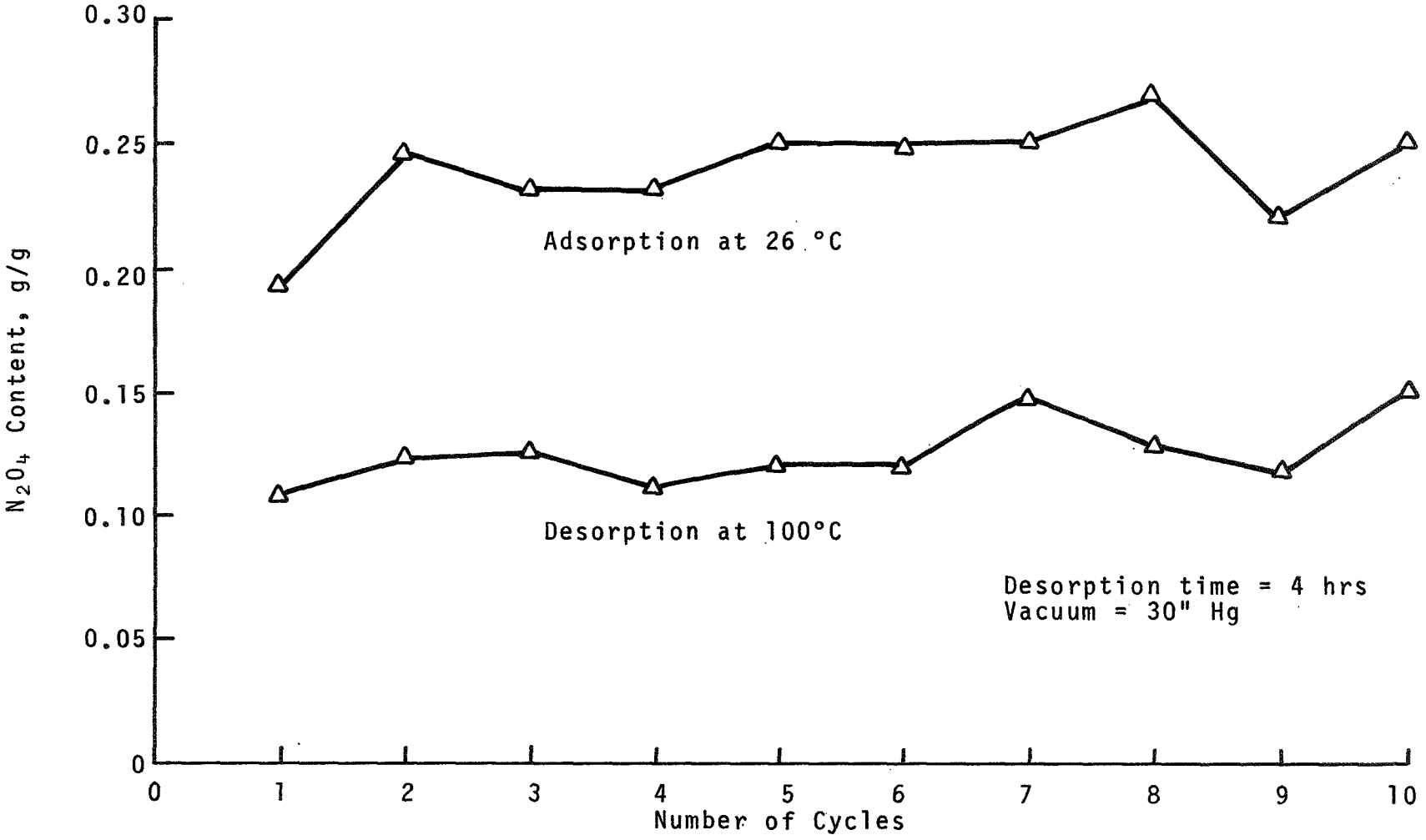

Figure 27. Adsorption-Desorption Cycling of N_2O_4-Molecular Sieve 13X System (desorption temperature = 100°C)

with an analytical balance both before and after adsorption. The breakthrough time was determined both by visual observation of the brown color appearing in the exit stream from the adsorption bed and by the change of color of a wet litmus paper. Since the carrier gas flow rate was constant, an increase in the N_2O_4 flow rate, as shown on the figure, is equivalent to an increase in the concentration of N_2O_4 in the entering gas stream. Specifically, on this plot, three grams per hour of N_2O_4 is equivalent to 19.1 wt % of N_2O_4 in the inlet stream and 10 grams per hour to 44 wt % N_2O_4. Although not shown on the plot, 19 grams per hour would be equivalent to 69 wt % N_2O_4, a concentration studied later by a simple spring balance method.

The slopes of these lines are not consistent with the data that would be expected to be obtained under equilibrium conditions. If the content of N_2O_4 in the 13X sieve increased with vapor-phase concentration, as would normally be expected, these curves should slope upwards to the right. Even if the content in the adsorbed phase were independent of gas-phase concentration the curves should be horizontal. The fact that the opposite occurs, namely, an upward slope to the left, especially at low temperatures, means that some extraneous phenomena occurred and that true equilibrium was not being observed.

The degree of separation of N_2O_4 from the carrier gas obtained upon flow through a packed bed can be affected by a wide variety of factors. A good review of the problems that may be encountered is given by T. Vermeulen (ref. 18). Such factors as change in Reynolds number and in pressure drop with a change in flow conditions can affect the degree of axial dispersion and, hence, the breakthrough curves. However, it appears much more likely here that the phenomena are caused by the highly exothermic nature of the adsorption process. The heat released by adsorption causes the development of a "hot spot" that grows in peak height as it moves downstream because of the continual displacement of heat of adsorption from upper portions of the bed to lower portions of the bed as adsorption continues. A quantitative analysis of this

situation is highly complex, but the nature of this phenomenon qualitatively is shown below:

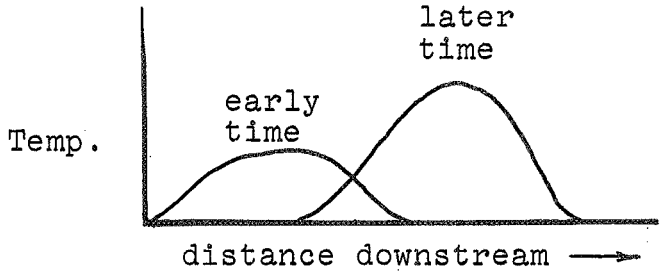

More details are given by K. Denbigh (ref. 19). This reinforcing effect occurs in continuous flow-through packed beds but not in simple contact of a gas with a sorbent held on a pan balance. Hence, here one obtains much higher peak temperatures and much more prolonged temperature gradients than one would obtain in a simple spring balance experiment.

The curves in 24 are completely consistent with the above hypothesis. At higher N_2O_4 concentrations, the heat effect would be expected to be greater and this would therefore greatly decrease the quantity of N_2O_4 that could be adsorbed before breakthrough. At relatively low temperatures the amounts of N_2O_4 adsorbed are greater and the hot spot phenomenon would be expected to be more significant. This in fact is shown in the figure. The curves at low temperatures show a much more pronounced slope than those at high temperatures.

At flow rates below those actually studied one would expect the curves to turn downwards and go through the origin, as indicated on the figure by the dashed lines, since with no N_2O_4 in the carrier gas, none would be adsorbed on the sieve.

It should be noted that the temperatures on the curves represent the reading of a thermocouple on the outside wall of the bed and this could be far different than the actual point temperature distribution inside the bed.

The results from the packed bed studies seem to be fairly reliable at temperatures of the order of 100°C and above and at N_2O_4 flow rates of 2 to 3 grams per hour. The only concentration at which the packed bed data can be directly compared to the pan balance data (reported in a later section) is 20 wt % (equivalent to slightly over 3 grams per hour). The data obtained at 75 and 100°C on the pan balance compare closely with those obtained in the packed bed.

2. Initial Test of Sorption Unit

a. Design Considerations for Adsorption-Desorption Unit

The time required for desorption from X_1 to X_2 can be obtained from the rate equation.

$$R = - \frac{dX}{dt} \tag{1}$$

where R = rate of desorption, g/g-min
X = N_2O_4 content, g/g
t = time, minutes

Integration of Equation (1) gives:

$$\int_0^t dt = - \int_{X_1}^{X_2} \frac{dX}{R} \tag{2}$$

Since R is a linear function of X, logarithmic mean rate, R_m, can be used in Equation (2).

$$t = \frac{X_2 - X_1}{R_m}$$

$$t = \left(\frac{X_1 - X_2}{R_1 - R_2}\right) \ln \left(\frac{R_1}{R_2}\right) \tag{3}$$

The amount of sorbent required to adsorb N_2O_4 from X_1 to X_2, during the same time period can be expressed by the following expression:

$$(t)(F) = (X_1 - X_2)S \tag{4}$$

where F = N_2O_4 flow rate, g/min
S = wt of sorbent, g

Eliminating t from Equations (3) and (4):

$$S = \left(\frac{F}{R_1 - R_2}\right) \ln \left(\frac{R_1}{R_2}\right) \tag{5}$$

An isothermal unit, constructed for the 24-watt nominal system utilizing the available experimental N_2O_4 reactor, was designed as follows:

Based on the experimental desorption curves for 100°C (Figure 28), the sieve loading was taken as X_1 = 0.10 g N_2O_4/g sieve as an upper value, desorption time of 4 hours was arbitrarily chosen, which set the lower limit at X_2 = 0.083 g N_2O_4/g sieve. The formula for calculating sieve weight is:

$$S = \frac{(t)\ (F)}{(X_1 - X_2)} \qquad \text{(Equation 4)}$$

where: S = weight of molecular sieve in g
t = desorption time in hours
F = N_2O_4 mass flow rate in stream from reactor in g N_2O_4/hr
X_1 and X_2 sieve loading factors

The N_2O_4 mass flow rate from the reactor, selected to produce 24 watt-equivalents of oxygen at 80% reactor conversion efficiency, calculates to be 3.2 g N_2O_4/hr.

Inserting the values into the equation:

$$S = \frac{(4)(3.2)}{(0.100-0.083)} = 750 \text{ g-mole of sieve}$$

A safety factor of 2X was used to allow for variable flow rates and possible long term changes in sieve capacity or reactor efficiency. The design is conservative in that the value of X_1 chosen was below the maximum demonstrated ($\sim$0.13 g N_2O_4/g sieve). This is justified in the isothermal scrubber, since complete equilibration can probably never be attained. In the non-steady state design, the attainment of an X_1 value this high can be assured simply by adjusting adsorption temperature by fuller use of the liquid N_2O_4 stream cooling capacity.

The N_2O_4 purification unit was constructed and assembled. The unit consisted of a converter section and an adsorption-desorption section.

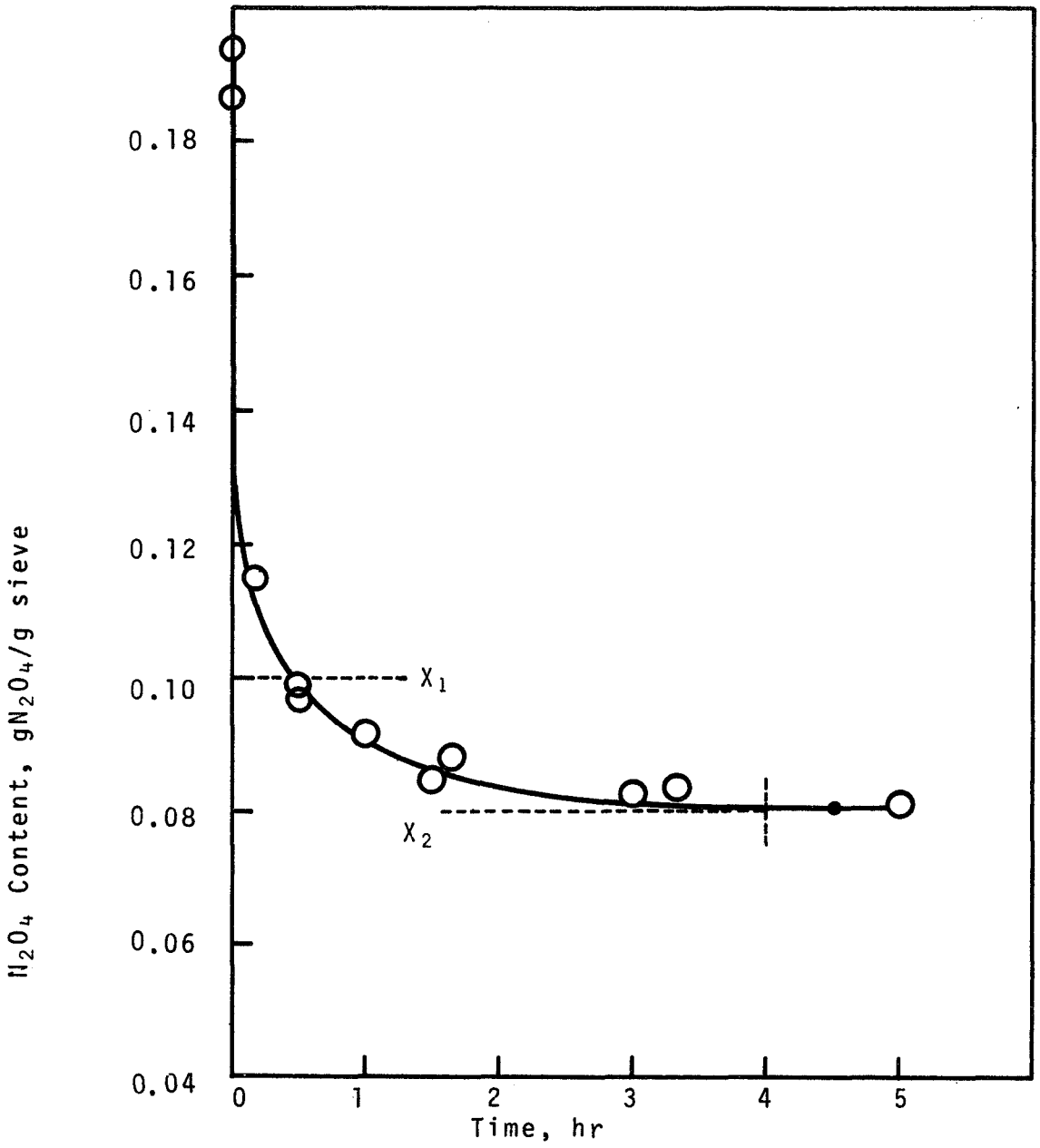

Figure 28. N_2O_4 Desorption at 100°C from Molecular Sieve 13X into 30" Hg Vacuum.

The converter section consisted of N_2O_4 cylinders, a flow meter, a catalytic converter, and a cooling tube. The function of this section was to decompose the N_2O_4 and to provide a feed stream of O_2, N_2, and undecomposed N_2O_4 for the adsorption-desorption section. The catalyst used 2% Pt on activated alumina (1/8 inch pellets). The converter was operated at 800°C.

The adsorption-desorption section included two parallel adsorber-desorbers, two traps, two gas bubblers, two vacuum pumps, and appropriate valves. The sorbers were made of stainless steel and were 10 cm in diameter and 30 cm long. They were electrically heated and were used alternately for adsorption and desorption. The product stream leaving the adsorber was metered and analyzed.

b. Test Results and Discussion

The unit could not be operated successfully on initial trials on the decomposer stream. Typical behavior consisted of a very rapid rise in internal temperature (to over 300°C) of the adsorber beds upon exposure to the stream and a subsequent loss of adsorptive capacity for N_2O_4.

An analysis of possible causes resulted in the following conclusions:

(1) The heat transfer through the packed molecular sieve bed was obviously insufficient, and much better heat exchange is required. The isothermal design loses much of its attractiveness in this case, since, if extra equipment weight and volume must be added for increased heat exchange, a non-steady-state operation mode is a more optimum solution.

(2) The N_2O_4 used was shown to be contaminated both with H_2O and with an iron-containing compound that probably arose from attack on the steel storage tanks. The significance of the H_2O content lies in the high affinity of 13X molecular sieve for H_2O. Water would contribute to the heat effects by adding its heat of adsorption.

Subsequent work on the adsorption problem took the following course:

(1) Nonsteady-state operation was emphasized and a design study was undertaken to delineate the possibilities and determine desired equipment characteristics and possible operating configurations. A great deal of attention was paid to heat balances and interfaces with the other components of the system. The details, results, and conclusions of the study are presented in Appendix II.

(2) A more fundamental study of the sorption of N_2O_4 on 13X molecular sieve was undertaken, including a determination of the heat effects associated with adsorption in a column with a flowing stream. Particular attention was paid to ensuring a pure N_2O_4 supply for these studies. The results are presented in the following sections.

C. PURIFICATION AND ANALYSIS OF AS-RECEIVED N_2O_4 AND CHARACTERIZATION OF 13X MOLECULAR SIEVE

1. Analytical Methods

Procedures, methods and apparatus as specified in MSC-PPD-2A, published 1 February 1966 by the Manned Spacecraft Center for the analysis of N_2O_4, were followed as closely as possible. The only difficulties encountered were in determining the exact end-point of the water equivalent determination and in establishing a transmittance calibration curve for the NOCl determination. In the latter case, supposedly identical samples varied by as much as 100% in measured transmittance values.

The problems with the H_2O determination can be illustrated with actual results obtained with material from the purification unit described in the next section.

The value we obtained for the H_2O equivalent of tank N_2O_4 was 0.90 to 0.11, which corresponds to 1.6 to 2.1 ml of sample left in the evaporation tube. The purified N_2O_4 has a H_2O equivalent of 0.00343, which corresponds to less than 0.1 ml of sample left in the tube. But even with these limitation H_2O contents below maximum specifications can be determined.

In the initial work on the NOCl determination, seven standards varying from 0 to 0.6 mg NaCl/l were made up according to the specification procedure and transmittancy readings taken at 535μ. The values plotted as $\log(\frac{1}{T})$ vs mg NaCl did not give a smooth curve. To check reproducibility, five samples, all at 0.6 mg NaCl/l, were made up and checked. Transmittancy values varied from 0.378 to 0.572 on these supposedly identical samples, indicating a definite lack of reproducibility. A partial parametric study was undertaken in which stirring, temperature, rate and sequence of solution additions, washing of glassware, time of transmittancy readings were all varied without much success. Finally, a series of 17 determinations were made with extreme attention to control of the parameters, and better reproducibility was obtained. Although the results were still somewhat variable, a statistical analysis was made to set confidence limits on the variability of the standard curve. Two samples of N_2O_4 were run by the procedure and the results are compared in Figure 29. It can be seen that the samples are quite low in NOCl content and that the probability that the NOCl content is within specifications is very high (>99% based on this data). No further work on this problem was done other than routine periodic checks of the sample N_2O_4.

2. Purification Unit

A schematic of the N_2O_4 purification and metering unit is shown in Figure 30. The function of each component and the operation of the system in brief was as follows.

- Vaporizer: liquid N_2O_4 under pressure by N_2 gas was fed into a heated, welded stainless steel pressure boiler, emerging as a vapor at 47°C. The vaporizer allowed for optional higher pressure operation of the entire system, as well as serving a pre-purification function via distillation.

- Porcelain Chip Reactor: the vaporized N_2O_4 was fed to a tubular reactor containing porcelain chips, heated to 300°C and then through a glass wool and stainless steel screen particulate trap. The purpose of this reactor was to thermally decompose contaminants, particularly $Fe(NO_3)_3 \cdot 6N_2O_4$, which decomposes to Fe_2O_3 at this temperature.

- Molecular Sieve Column: the purpose of this component was to remove contaminants that could selectively adsorb on molecular sieve and displace adsorbed N_2O_4, primarily H_2O although higher boiling potential contaminants such as N_2O_5 (47°C with decomp.) and HNO_3 (86°C) or those with

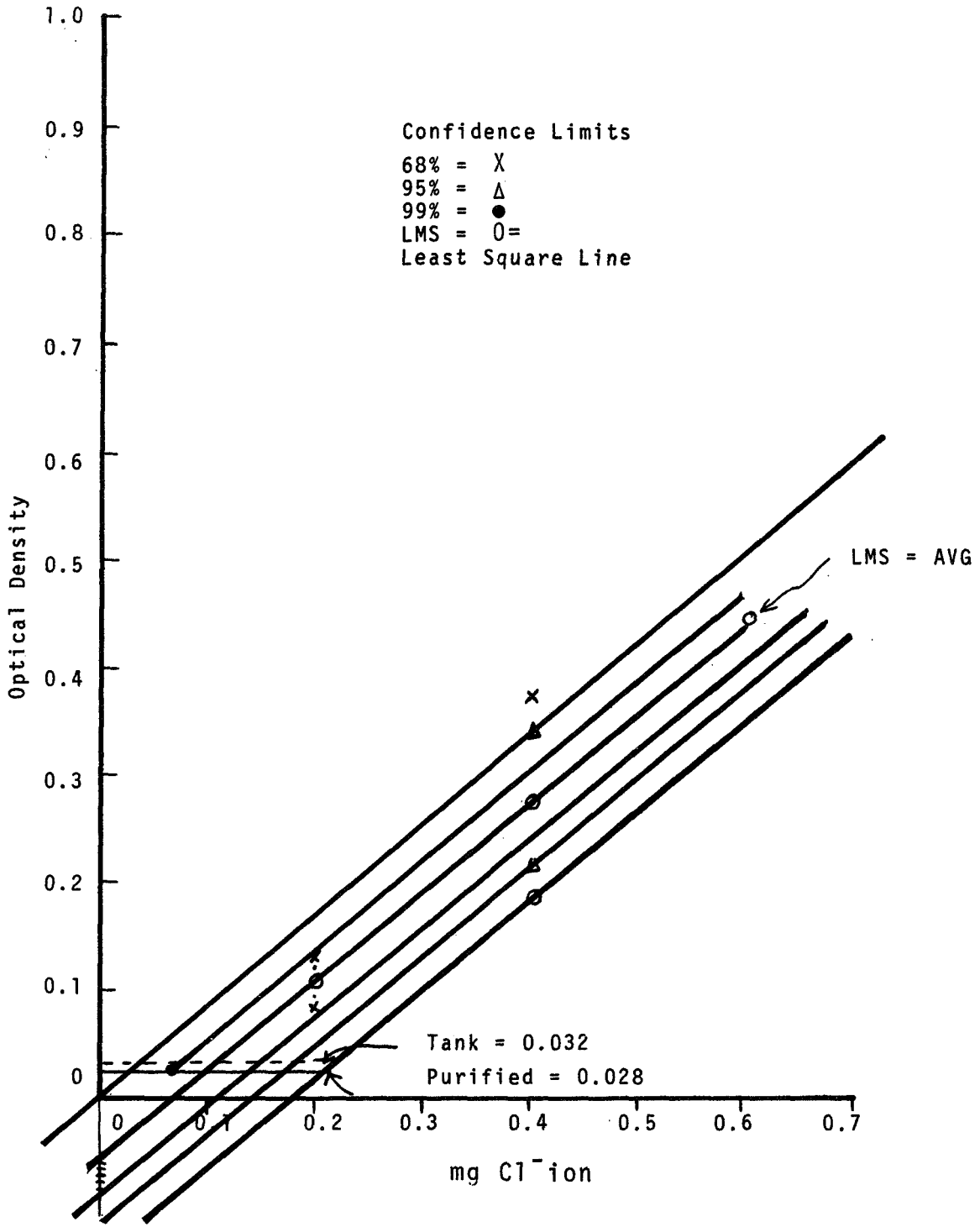

Figure 29. Calibration Curve for NOCl Assay

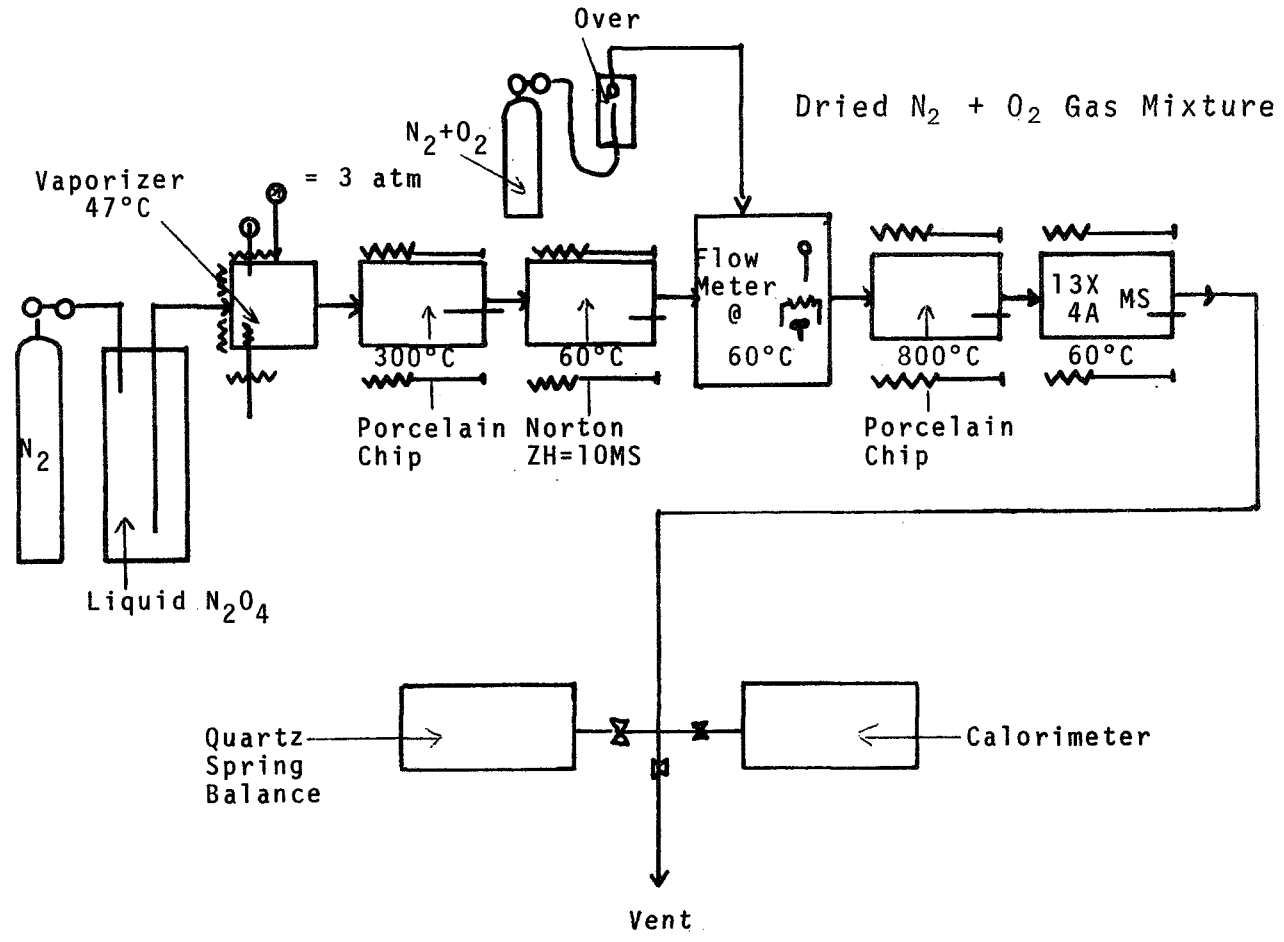

KEY:

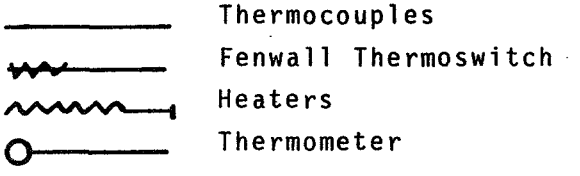

Figure 30. N_2O_4 Flow System

boiling points near N_2O_4, such as NOCl (-5.5°C) and N_2O_3 (3.5°C) can be expected to adsorb. Because of the expected relatively high H_2O content, a special acid washed molecular sieve (Norton ZH-10MN) was used.

- Flow Meter and Mixer: the purified N_2O_4 vapor was temperature equilibrated in an air thermostat to at least 60.0 ± 0.5°C, and metered through an adjustable fluorine flowmeter-flow regulator and subsequently mixed with an N_2/O_2 stream previously dried to at least a -73°C (-100°F) dew point in molecular sieve columns.

- 800°C Porcelain Chip Reactor: this tubular unit was included simply to simulate the 800°C reactor that would be part of the final system. Any residual thermally labile impurities would be decomposied.

- Final Molecular Sieve Scrubber: this unit contained an equal weight mixture of Linde 4A and 13X molecular sieve and served as a final purification unit for the total gas mixture.

The purification unit was put into operation. After 28 days of continuous running time at 15-30 g/hr N_2O_4, the output stream was analyzed. The data, presented in Table XXXVII indicate:

- The moisture content of the as-received N_2O_4 ("Tank N_2O_4") was indeed out of spec as anticipated, but the purification unit was very effective in reducing the H_2O level.

- The $\Sigma NO + N_2O_4$ values at the terminus were below specs, but were within specs prior to entry into the 800°C reactor. Either slight decomposition of N_2O_4 occurred on the porcelain chips or slight oxidation of the stainless steel tubing removed a small amount of N_2O_4. In either case, compensation was possible by slightly enriching the N_2O_4 content of the gas stream entering the reactor.

- All other values were within specs.

The unit was run for an additional 40 days with little change. Then the reactor and adsorber tubes were repacked.

Table XXXVII

N_2O_4 ANALYTICAL RESULTS

% by Weight	Tank N_2O_4	Purified N_2O_4 I	Purified N_2O_4 II	Specifications
NO	0.55	0.66	0.66	0.6 ± 0.2
N_2O_4	98.38	98.88	98.39	98.70 min
$\Sigma NO + N_2O_4$	98.93	99.54	99.05	99.5 min
H_2O_4	0.90-0.11	-	0.0034	0.10 max
NOCl	0.0285*	0.0278*	0.0278*	0.08 max
Particulate	0.1 mg/l	-	-	-

I = before 800°C reactor

II = after 800°C reactor + 13X/4A M.S. Scrubber

* = 99% probability

3. X-Ray Diffraction Study of Molecular Sieve Samples

a. Introduction

This study was undertaken to fulfill two objectives:

1) To determine if molecular sieves samples from different parts of a given batch were identical.

2) To measure and record a physical property of this lot of molecular sieves for possible comparison with that measured on subsequent lots.

b. Experimental

The molecular sieves were obtained from the Linde Division of Union Carbide, taken from lot #M1371003 and supplied in a ten-gallon drum. Approximately 400 cc was removed from the top, middle, and bottom of the drum and small quantities were withdrawn from each sample. These aliquots were labelled I, II, and III, respectively. The remainder of the three 400-cc samples was thoroughly mixed together, and three small samples were arbitrarily removed from this mix. These samples were labelled Composite I, Composite II, and Composite III. X-ray diffraction patterns were then obtained with these six samples.

The diffraction patterns were obtained using a JEOLCO X-ray Diffractometer (Model JDX5B). Copper K_α radiation was passed through a nickel filter before impinging on the sample. Preparation of the sample consisted in thoroughly grinding the molecular sieves using a mortar and pestle and then pressing the powder into a glass holder to form a planar surface. X-ray scans were recorded between 2θ angles, 10° and 60°.

c. Results and Discussion

Numerous diffraction peaks ($\sim$20) were observed between 2θ angles 10° and 60°, and are listed in Table XXXVIII. For each of the six samples of 2θ angles at which the five most intense peaks were found are recorded in Table XXXIX.

Table XXXVIII

2θ ANGLES AT WHICH DIFFRACTION PEAKS WERE OBSERVED

Sample I	Sample II	Sample III	Composite I	Composite II	Composite III
11.7	11.7	11.7	11.7	11.7	11.7
15.5	15.5	15.5	15.5	15.5	15.5
18.5	18.5	20.1	18.5	18.5	18.5
20.1	20.1	23.3	20.1	20.1	20.1
23.3	23.3	26.7	23.3	23.3	23.3
26.7	26.7	29.2	26.7	26.7	26.7
29.3	29.3	30.3	29.3	29.3	29.3
30.3	30.3	31.0	30.3	30.3	30.3
31.0	31.0	32.0	31.0	31.0	31.0
32.1	32.1	33.6	32.1	32.1	32.1
32.8	32.8	34.2	33.6	33.6	33.6
33.6	33.6	37.4	34.2	34.2	34.2
34.3	34.3	40.9	37.4	37.4	37.4
37.4	37.4	41.3	40.9	40.9	40.9
40.9	40.9	42.7	41.3	41.3	41.3
41.3	41.3	47.1	42.7	42.7	42.7
42.7	42.7	51.7	46.5	46.5	46.5
46.5	46.5	53.2	47.2	47.2	47.2
47.2	47.2	57.4	51.1	51.1	51.1
51.1	48.2		51.7	51.7	51.7
51.7	48.8		53.2	53.2	53.2
53.3	49.9		57.5	57.5	57.4
57.5	51.0				
	51.7				
	53.3				
	57.4				

Table XXXIX

2θ ANGLE

Relative Peak Intensity	Sample I	Sample II	Sample III	Composite I	Composite II	Composite III
100%	31.0	31.0	26.7	31.0	31.0	31.0
90-99	26.7 23.3	26.7 23.3		26.7 23.3	26.7 23.3	26.7 23.3
80-89						
70-79			31.0 23.3			
40-69	15.5 33.6	15.5 33.6	15.5 33.6	15.5 33.6	15.5 33.6	15.5 33.6

D. SORPTION STUDIES WITH A MASS ADSORPTION BALANCE

1. Equipment and Procedure

The system used was a quartz spring balance sold as a complete unit by Worden Quartz Products, Inc., Houston, Texas. It consisted of a fused quartz tube mounted vertically and closed at the bottom, with a side arm inlet tube and dual outlet ports in the O-ring sealed, flanged top. A non-rotating fused quartz spring was suspended from the top and articulated with a quartz-fiber-suspended quartz sample pan. The spring excursions were followed by a cathetometer. The sections of the tube adjacent to the spring proper were jacketed to allow thermostating of the spring, thus ensuring no change in the spring constant.

Besides providing valving and piping to channel and control the gas streams and the evacuation, we modified the Worden unit by:

- Replacing the mounted cathetometer with a precision, pole mounted unit placed some 6 feet away.

- Replacing the tube furnace type heater with a wrapping of heating tape around the tube, thus extending the isothermal zone much further along the tube; and

- Mounting a second weighing pan, fixed in position below the suspended weighing pan. This pan was filled with the same amount of molecular sieve as the other, but a calibrated thermistor buried in the bed was used to check bed temperatures during a run.

Gas compositions were adjusted by regulation of flows as indicated by the appropriate flow meters, and were checked by adsorption into alkaline peroxide solutions with subsequent titration of remaining alkali.

Approximately 0.3 g of molecular sieve was weighed carefully and placed in the pan after heating it overnight to 350°C in a dry argon stream to remove moisture.

2. Sorption Test Plan

a. Equilibrium Sorption Cycles

(1) Test Plan

The test plan used is illustrated in Table XL on the following page.

With all the samples except sample III (that taken from the bottom of the shipping container) the most intense peak occurred at $2\theta = 31.0°$ and the order of relative intensity of the 5 most intense peaks are the same. With sample III, however, the most intense peak is at $2\theta = 26.7°$ and the relative intensity of the 3 most intense peaks is different than that observed with the other five samples. Furthermore, three peaks of low intensity at $2\theta = 18.5, 46.5°$ $51.1°$ are missing in the pattern determined with sample III.

From these results we conclude that except for the molecular sieves taken from the bottom of the shipping container, the composition of the molecular sieves in the remainder of the container and those taken elsewhere in the container were not large. Indeed, when the bottom sample was mixed with those obtained from the top and middle of the container, any differences were not detectable.

Since molecular sieves consist of alkali metal alumino-silicates compounded together with an inert clay binder, X-ray diffraction peaks are obtained for both materials. The different relative peak intensities found with sample III compared with all other samples suggests that a different ratio of clay to alumino-silicate exists in this sample.

It is possible that during packing and shipment the softer of the two materials divides from the molecular sieves and falls to the bottom of the container. This would result in a higher concentration of the softer material in the sample taken from the bottom of the container and result in different relative peak intensities than those found with the other samples.

Table XL

SORPTION TEST PLAN EQUILIBRIUM SORPTION CYCLES

(Body of Table = Desorption Temperatures)

Adsorption Temp → / Gas Composition ↓	50°C	75°C	100°C
20% N_2O_4	200°C	150°C	100°C
60% N_2O_4	100°C	200°C	150°C
80% N_2O_4	150°C	100°C	200°C

Duplicate runs for each combination

(2) Procedure

The experimental procedure that was used follows:

1. Apparatus was temperature equilibrated at adsorption temperature with dry N_2 purge.
2. A sample of gas stream was taken for analysis of N_2O_4 content.
3. The valve was opened to admit the gas stream at a controlled rate to the apparatus, (time zero = time of valve opening).
4. Weight changes were followed and plotted vs time until constant ($\pm$0.5%). Stop N_2O_4 flow; the vent on the chamber was left open; the chamber was heated to desorption temp.
5. A second sample of the gas stream was taken for analysis of N_2O_4 content.
6. The apparatus was temperature equilibrated at desorption temperature with weight changes followed during this period.
7. The vacuum line was opened slowly and apparatus pumped down to 29 in. Hg.

8. Weight changes were followed and plotted vs time until constant (±0.5%).

9. The apparatus was temperature equilibrated at 200°C under 29 in. vacuum until constant weight (±0.5%) was achieved.

10. A new cycle was started.

b. Nonsteady State Cycles

(1) Plan

The cycle endpoints were determined by weight capacities calculated from the equilibrium data so that adsorption started at a sieve loading of $0.25Q^{\infty}$ and ended (i.e., desorption started) at $0.75Q^{\infty}$ regardless of other conditions, where Q^{∞} = the equilibrium adsorption capacity for the temperature and gas composition under study.

(2) Procedure

1. The apparatus temperature was equilibrated at adsorption temperature under dry N_2 purge.

2. A sample of gas stream was taken for analysis of N_2O_4 content (at 3rd and 10th cycles).

3. A valve was opened to admit the gas stream to the apparatus at a controlled rate.

4. Weight changes were followed and plotted vs time until $0.75Q^{\infty}$.

5. The N_2O_4 valve was closed, leaving the vent open. Heat was started, then stopped at weight reading = $0.25Q^{\infty}$.

6. The next cycle was started, beginning from (3) above, allowing apparatus to cool at the same time.

3. Results

The shape and general configuration of both the equilibrium and non-steady-state curves were the same for all runs. A representative run is illustrated Figures 31 and 32.

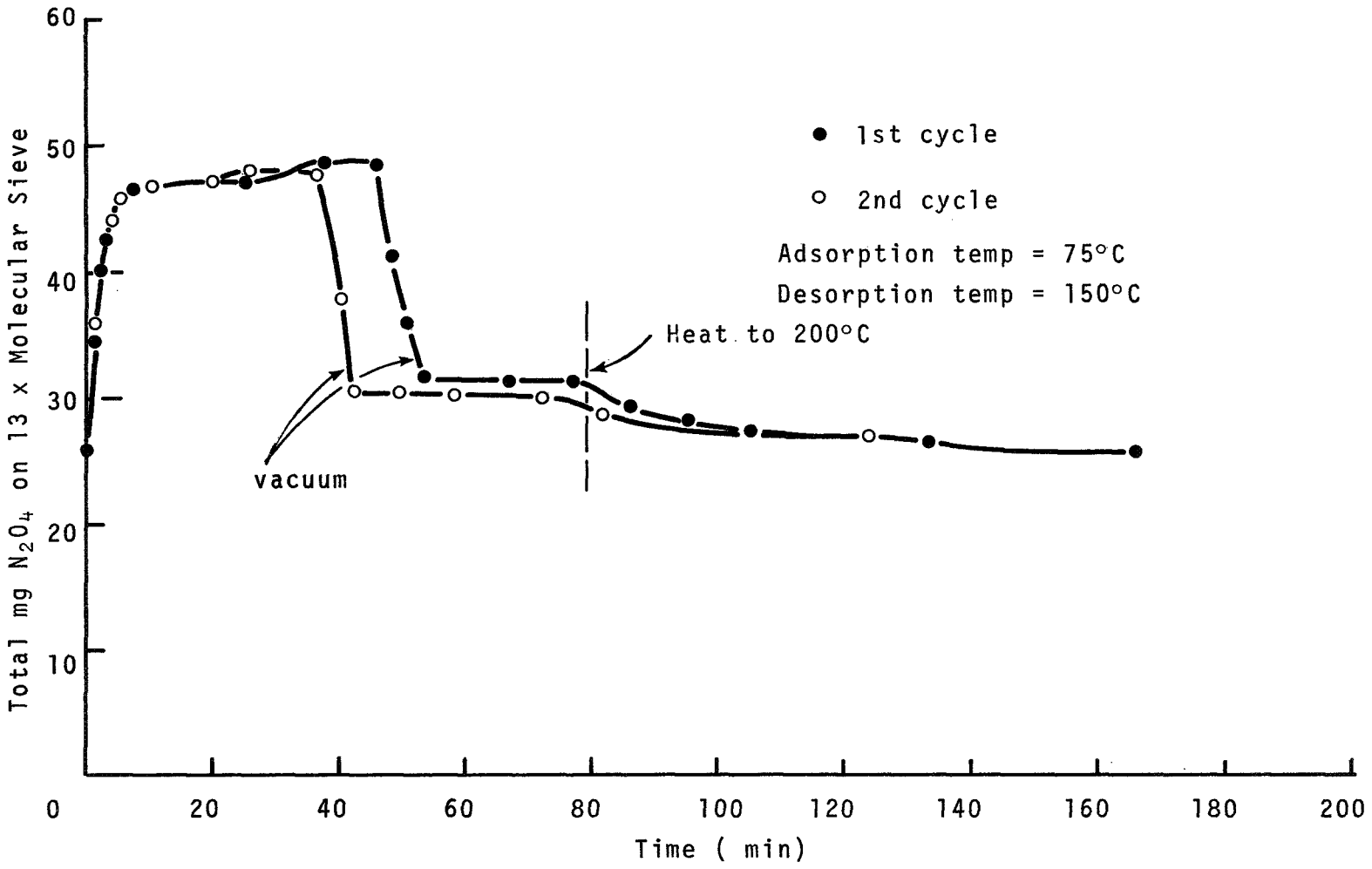

Figure 31. Steady State Sorption of 20% N_2O_4 on 305 mg of 13X Molecular Sieve

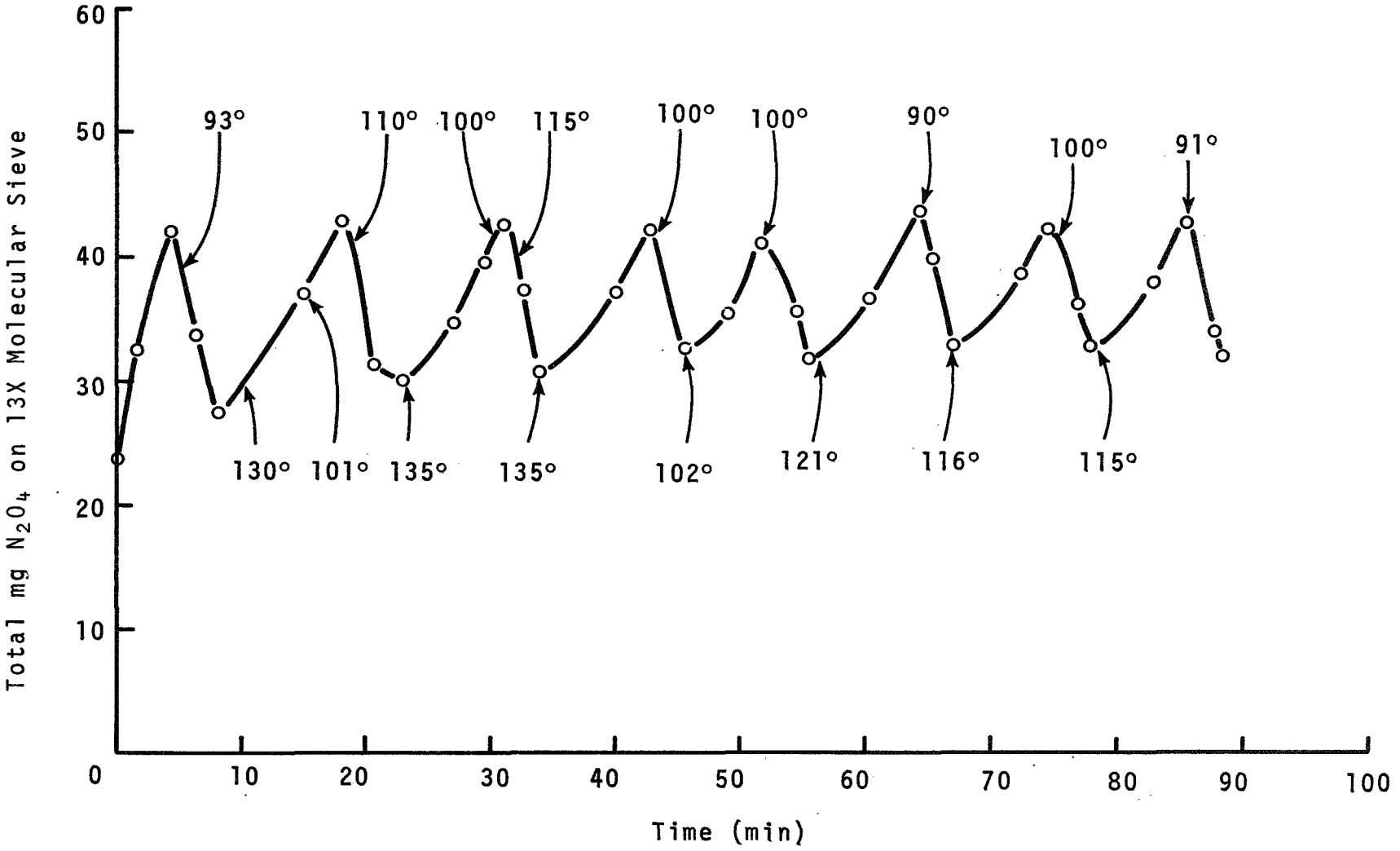

Figure 32. Unsteady State Cycles Corresponding to Figure 31.
20% N_2O_4 - 305 mg 13X Molecular Sieve

Data for all runs with gas composition ≥20% N_2O_4 are compiled in Tables XLI and XLII.

Subsequently, sorption data were obtained for 5%, 1%, and 1/2% N_2O_4 (by weight) in the N_2 + O_2 carrier gas stream. The data obtained at 1/2% were extremely variable. The limits of control for the apparatus had apparently been exceeded, and randomly varying compositions with time resulted. Better control was maintained with 5% and 1% gas streams. The data are presented in Table XLIII.

Other properties not evident from the foregoing tables and figures are:

(1) There is a definite initial conditioning effect with the 13X sieve, both with respect to the bed temperatures measured (Figure 33) and adsorption (Figure 34)

(2) All of the residual N_2O_4 left on the sieve at 200°C, 29 in. vacuum can be removed by increasing the temperature to about 300°C (Figure 34).

(3) The residual amount (200°C, 29 in. vacuum) apparently varies from sieve sample to sample. (Compare residuals for 80, 60, and 20% runs with those for 5 and 1% runs.)

4. Discussion

Figures 35 and 36 show the total adsorption and adsorption capacity of N_2O_4 on 13X sieve as a function of gas composition and of temperature. The interpretation of data such as this is more clearly understood in terms of the ratio P/P_O (the ratio of the partial pressure of the N_2O_4 to the vapor pressure that would exist above the liquid-phase at the temperature of interest). Data on physical properties of NO_2 and N_2O_4 are given in references 20 and 21. To assign specific property values is somewhat difficult in this case because N_2O_4 and NO_2 exist in equilibrium with one another, and the ratio of NO_2 to N_2O_4 varies greatly with temperature over the temperature range studied here. The term "N_2O_4" as used here refers to the particular mixture of NO_2 and N_2O_4 that exists under the experimental conditions specified. The most useful information is a set of values from Gmelin (ref. 21) for the vapor pressure above equilibrium mixtures of NO_2 and N_2O_4 at pressures above atmospheric. These data have been plotted on Figure 37 on the coordinates of log of the vapor pressure vs the reciprocal of the absolute temperature, a procedure which gives a nearly linear relationship that can be readily extrapolated.

Table XLI

STEADY STATE N_2O_4 SORPTION ON 13X MOLECULAR SIEVE

(Average of 2 Runs)

Conditions				
Composition (wt% N_2O_4)	Ads. Temp. (°C)	Des. Temp. (°C)	Adsorption* Capacity (gN_2O_4/g sieve)	Desorption** Residual (gN_2O_4/g sieve)
20	50	200	0.067	0.088
20	75	150	0.072	0.101
20	100	100	0.052	0.113
60	50	100	0.096	0.111
60	75	200	0.078	0.094
60	100	150	0.067	0.095
80	50	150	0.115	0.107
80	75	100	0.085	0.123
80	100	200	0.069	0.095

* Adsorption Capacity = Wt N_2O_4 adsorbed at steady state minus initial wt N_2O_4 remaining on sieve before adsorption (after 200°C, 29 in. vacuum exposure)

** Desorption Residual = Wt N_2O_4 remaining on sieve after attainment of steady state during desorption under 29 in. vacuum at the specified desorption temperature

Table XLII

SORPTION CYCLE DATA FOR N_2O_4 ON 13X MOLECULAR SIEVE

Conditions		Fraction of N_2O_4 on Sieve (gN_2O_4/g sieve)		
I. 20% N_2O_4				
Run	Sequence	Start	Cycle Range	End*
1	After 50°C ads/200°C des.	0.095	0.099 - 0.78	0.088
2	After 75°C ads/150°C des	0.078	0.090 - 0.141	-----
3	After 100°C ads/100°C des.	0.088	0.123 - 0.139	0.082
II. 60% N_2O_4				
Run	Sequence			
1	After 50°C ads/100°C des.	0.092	0.147 - 0.174	0.088
2	After 75°C ads/200°C des.	0.093	0.110 - 0.155	0.082
3	After 100°C ads/150°C des.	0.089	0.115 - 0.140	0.089
III. 80% N_2O_4				
Run	Sequence			
1	After 50°C ads/150°C des.	0.092	0.138 - 0.191	0.098
2	After 75°C ads/100°C des.	0.095	0.138 - 0.182	0.088
3	After 100°C ads/200°C des.	0.093	0.121 - 0.151	-----

* Steady state after 29 in. vacuum at 200°C all tests

Table XLIII

STEADY STATE SORPTION DATA FOR LOWER N_2O_4 CONTENTS

Composition (wt % N_2O_4)	Ads. T. (°C)	Des. T. (°C)	Ads. Capacity* (gN_2O_4/g sieve)	Desorption** Residual (gN_2O_4/g sieve)	200°C - 29 in. Vacuum Desorption Residuals (gN_2O_4/g sieve)	
					Start	End
5	75	100	0.070	-----	0.043	0.040
5	100	150	0.045	-----	0.040	0.045
5	125	200	0.022	0.035	0.037	0.035
1	75	200	0.026	0.046	0.045	0.046
1	100	100	0.0095	0.063	0.055	0.057
1	125	150	0.008	0.057	0.054	0.053

* Ads. Capacity - Wt N_2O_4 adsorbed at steady state minus initial wt N_2O_4 on sieve (start column -200°C- 29 in. vacuum)

** Desorption Residual - Wt N_2O_4 remaining on sieve at steady state under 29 in. vacuum at specified desorption temperature

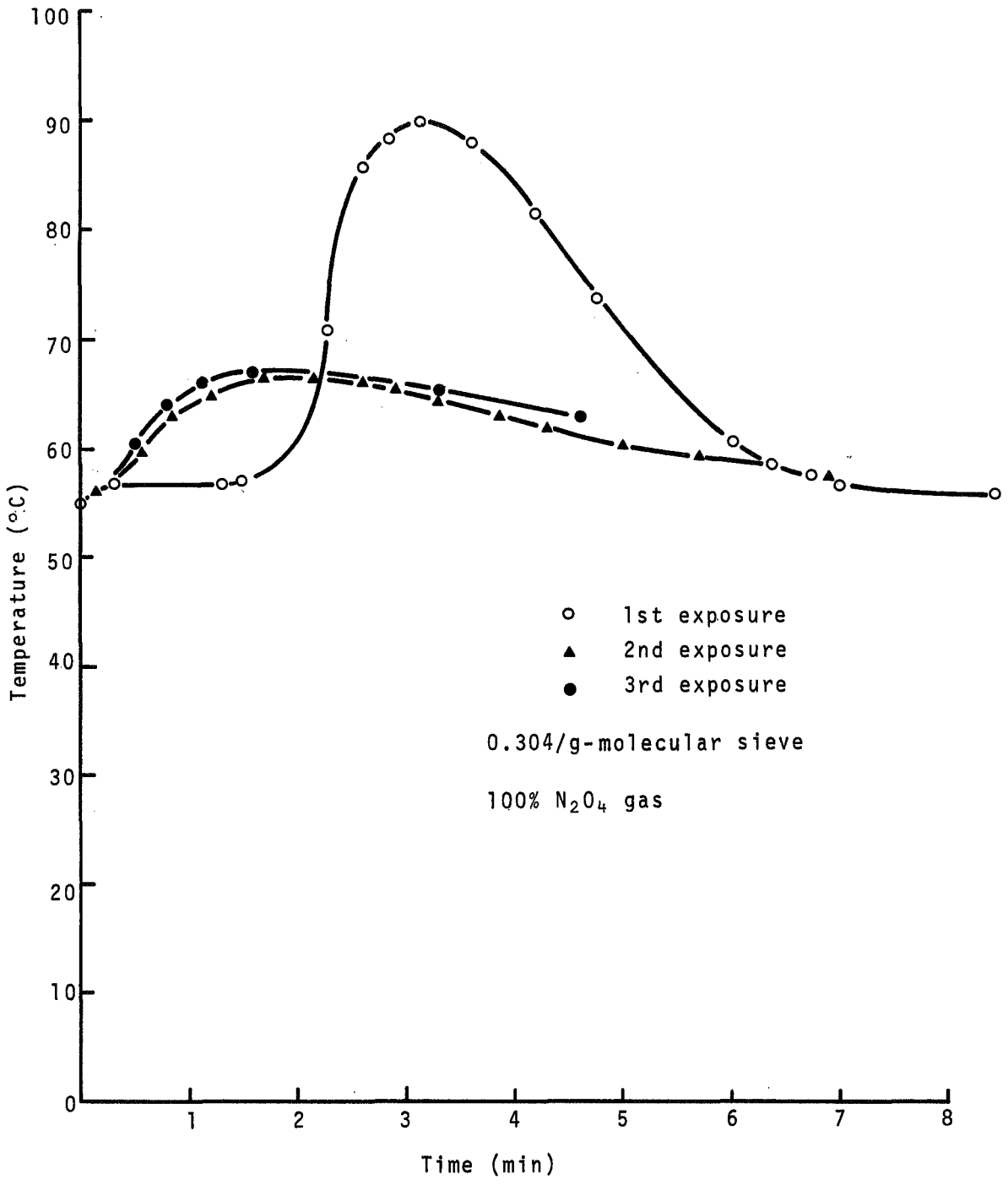

Figure 33. Exposure Effect of N_2O_4 on 13X Molecular Sieve

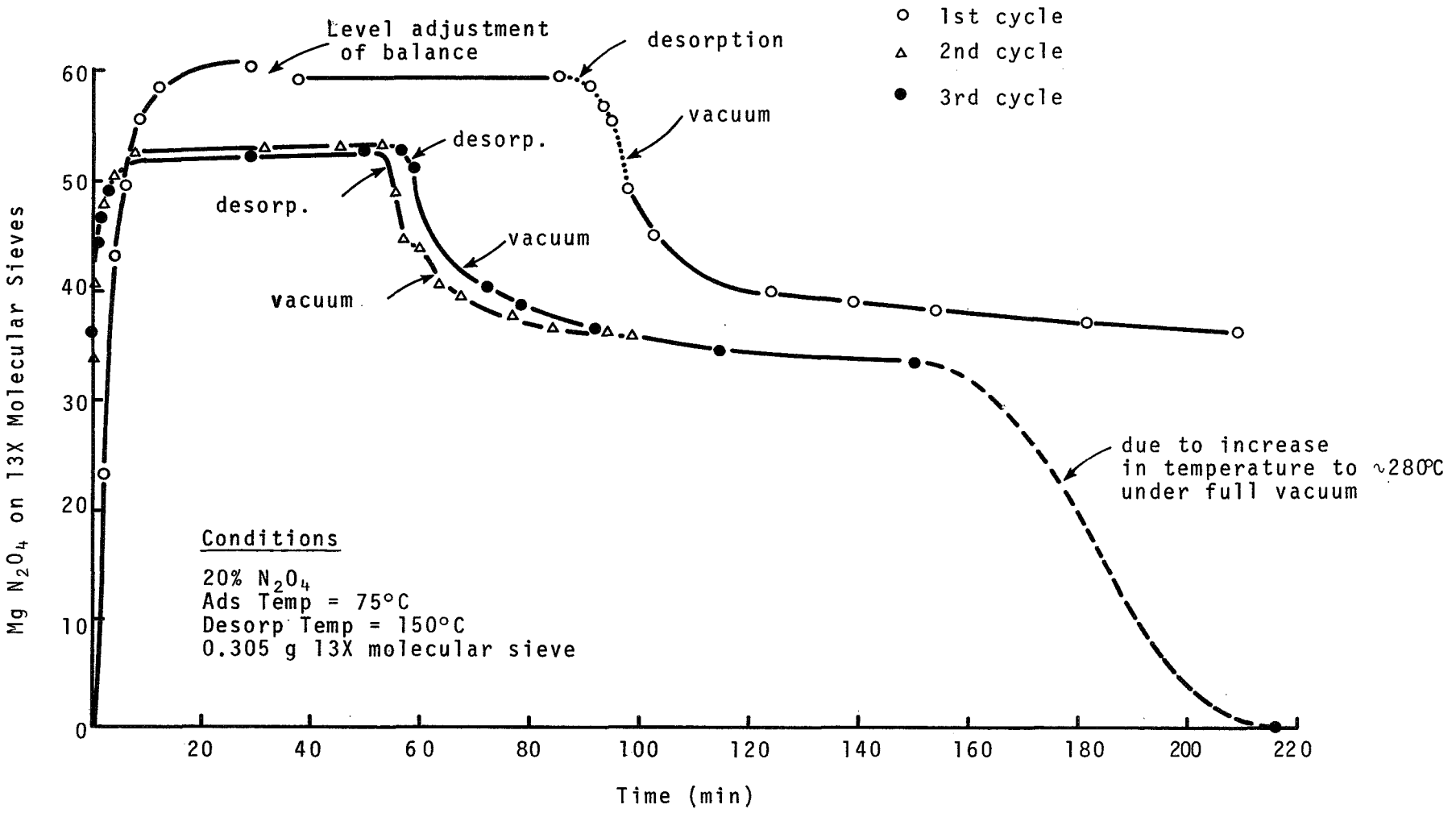

Figure 34. Initial Exposure Effects on Adsorption

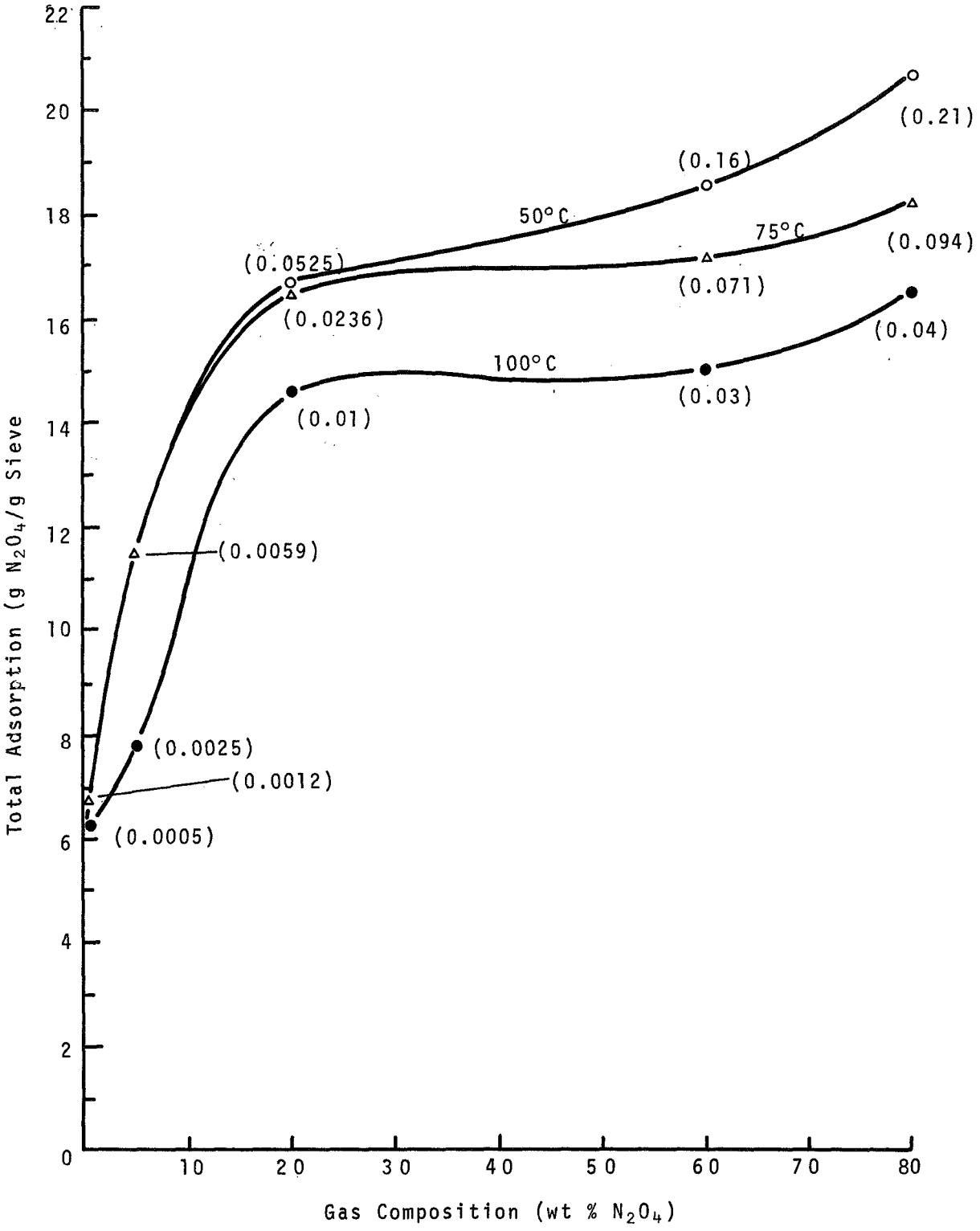

Figure 35. Total Adsorption of N_2O_4 on 13X Molecular Sieve

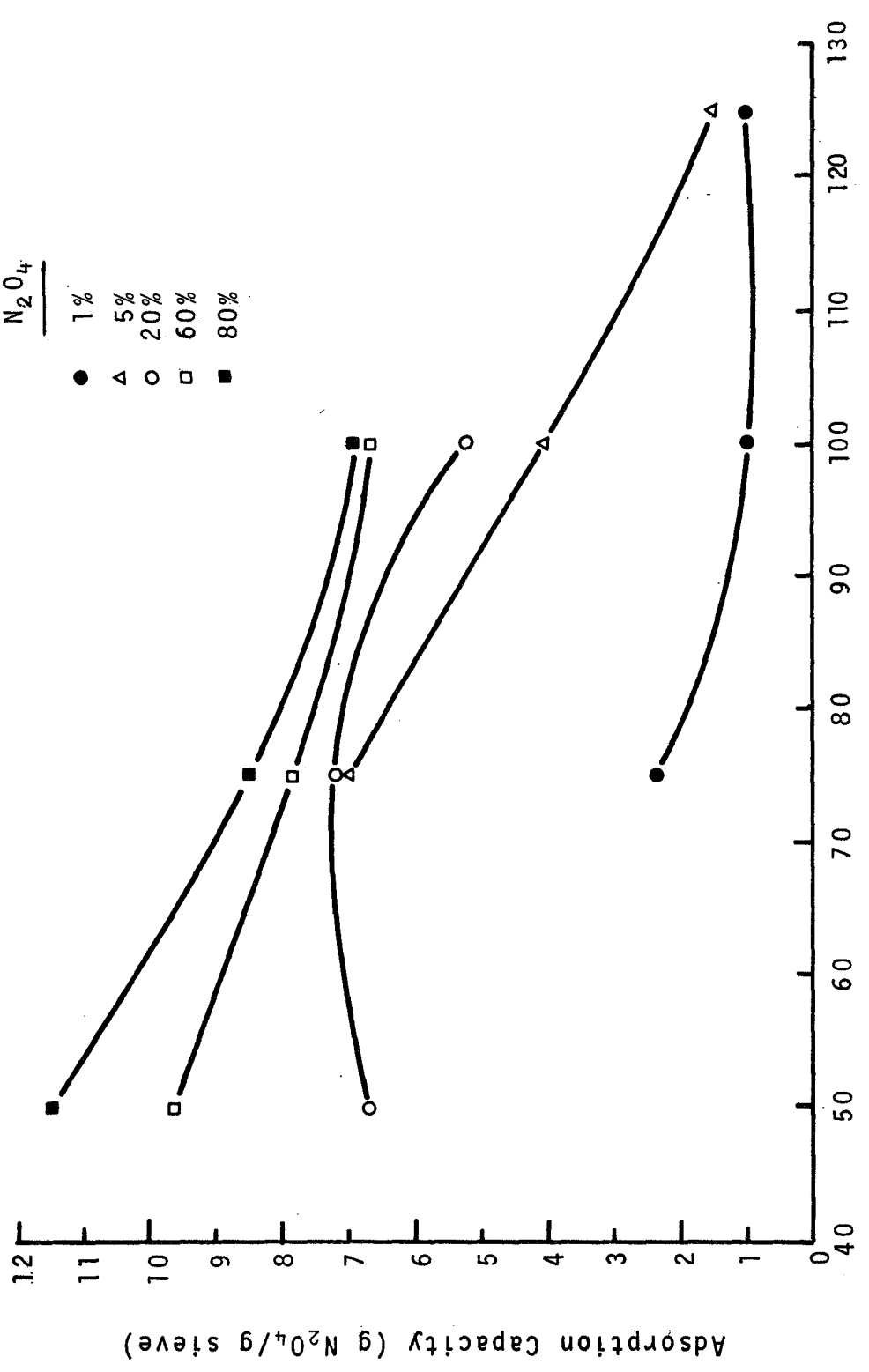

Figure 36. Adsorption Capacity of 13X Molecular Sieve for N_2O_4

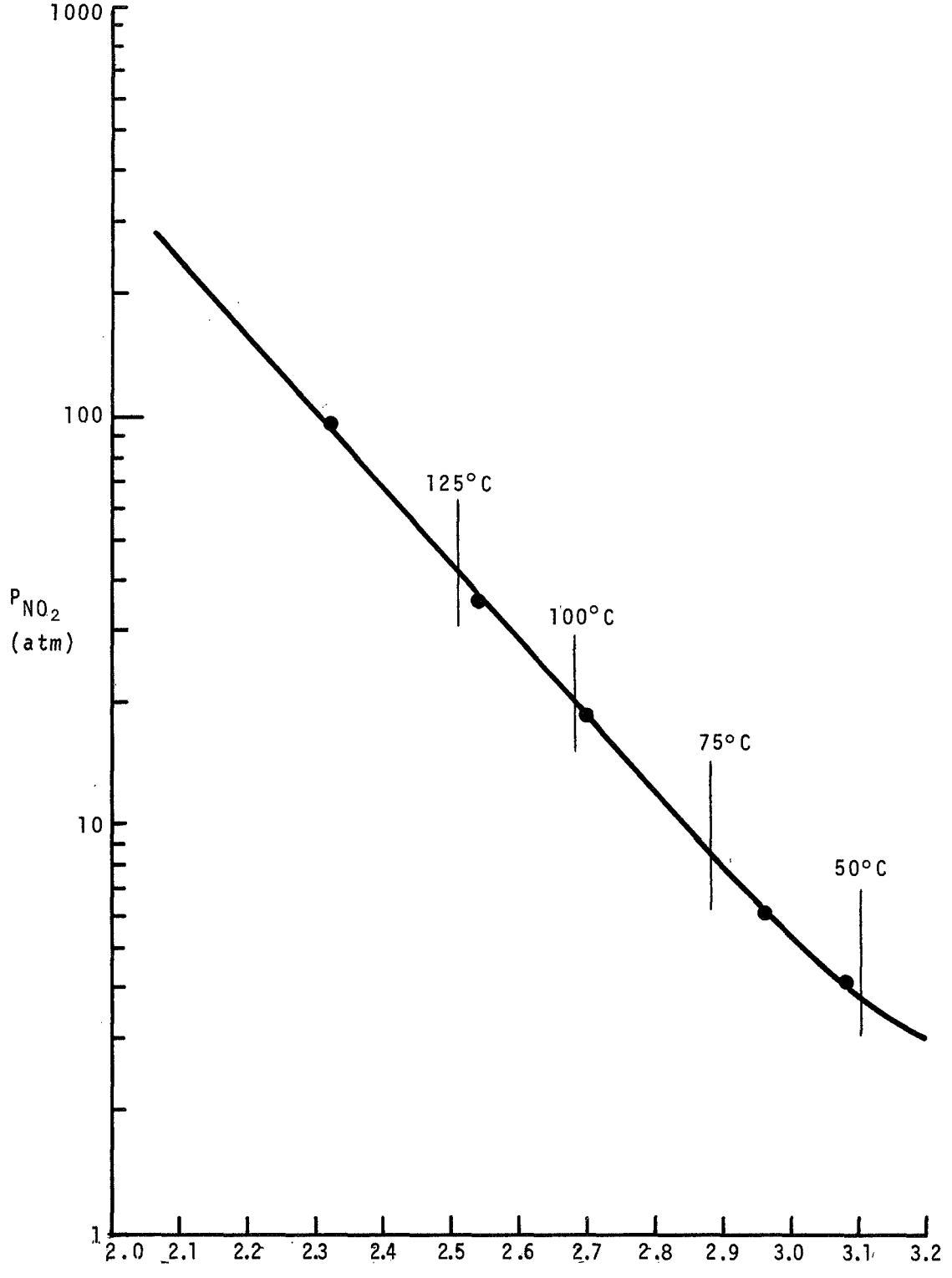

Figure 37. Vapor Pressure of NO_2

As read from this plot, values of P_O corresponding to several temperatures of interest are as follows:

T (°C)	P_O (atm)
50	3.8
75	8.5
100	20.0
125	43.0

Figure 35 shows isotherms for the three temperature levels of 50, 75, and 100°C. The number in parentheses beside each point is the corresponding value of P/P_O. The shapes of these curves can now be readily interpreted and shown to be consistent with the type of adsorption behavior observed by other gases and vapors on molecular sieves.

At a specified temperature the amount of N_2O_4 adsorbed increases rapidly with gas composition, reaching a plateau, and then increases moderately with further increase in partial pressure of N_2O_4. The first two portions of the curve are a Type I adsorption isotherm, in the Brunauer classification, also known as a Langmuir isotherm, and is typically found with molecular sieves. The left-hand portion of the curve represents the partial filling of the fine pores in the sieve itself, and the plateau region represents that range of vapor composition at which the pores are completely filled, but with negligible extraneous effects (see below). The onset of the plateau region typically occurs at P/P_O values in the range of 0.01 to 0.05, as here. As the value of P/P_O is increased beyond the plateau region, capillary condensation into larger pores and multilayer adsorption onto the outer surfaces of the molecular sieve material occurs. As used commercially, molecular sieve pellets are typically composed of single crystals approximately 1 micron in diameter held together by clay binder. Thus, the passageways around the original particles in the pellet and the somewhat larger pores in the clay account for the increase of adsorption of N_2O_4 at the high values of P/P_O.

E. CALORIMETRIC STUDY OF N_2O_4 ADSORPTION

1. Test Plan

The objective of this test was to determine directly the heat produced when N_2O_4 was adsorbed onto 13X molecular sieve. The studies were to be made with flowing gas streams containing relatively large amounts of N_2O_4, and with relatively large amounts of molecular

sieve (~1 g) at both 50°C and 100°C. The objective was to simulate operating conditions as closely as possible.

2. Equipment and Procedure

The basic calorimeter design is shown in Figure 38. Essentially, the design was a jacketed adiabatic calorimeter in which the jacket temperature was maintained close to the calorimeter fluid temperature to reduce cooling corrections. The design was adapted to accommodate a flowing gas stream from which the N_2O_4 content was to be adsorbed onto 13X molecular sieve contained in a coiled stainless steel adsorption tube. In operation, the gas stream containing a known amount of N_2O_4 was temperature equilibrated with the jacket fluid through a coiled tube heat exchanger and then fed to the adsorption tube containing a known amount of molecular sieve. The outlet from the adsorption tube was fed to an analysis unit consisting of a parallel array of gas bubblers containing alkaline/peroxide that could be individually bypassed, and then to a precision wet test meter. The heat effects, i.e., the temperature rise of the calorimeter fluid, were determined as a function of time by continuously measuring the resistivity of a precision thermistor via a wheatstone bridge circuit. The N_2O_4 content of the outlet stream was determined periodically by switching to different gas bubblers for known amounts of time and titrating the remaining caustic. The wet test meter completed the mass balance by determining inert gas.

During a run the gas was continuously admitted and data were taken until outlet and inlet N_2O_4 contents were the same, at which point the sieve was saturated for that particular gas composition and temperature. Heat effects were integrated up to saturation and heats of adsorption in cal/g calculated after mass balances were obtained.

Two sources of error were considered in the design: the sensible heat load (+ or -) imposed on the calorimeter by the flowing gas stream, and the fact that heat effects may be small (100-200 cal/g N_2O_4 adsorbed) compared to the combined heat capacities of the calorimeter fluid, adsorption tube plus sieve, stirrer, thermistor, and heat calibration resistor (which must remain in the calorimeter during the run), necessitating very accurate temperature measurements.

The first problem was approached by providing for continuous measurement of the temperatures of the inlet and outlet streams close to the adsorption tube via thermistor probes in the stainless steel lines. Knowing the mass flow rates, gas compositions, and heat capacities, calculated corrections could then be made to the measured calorimeter heat effects. Calculations showed that at

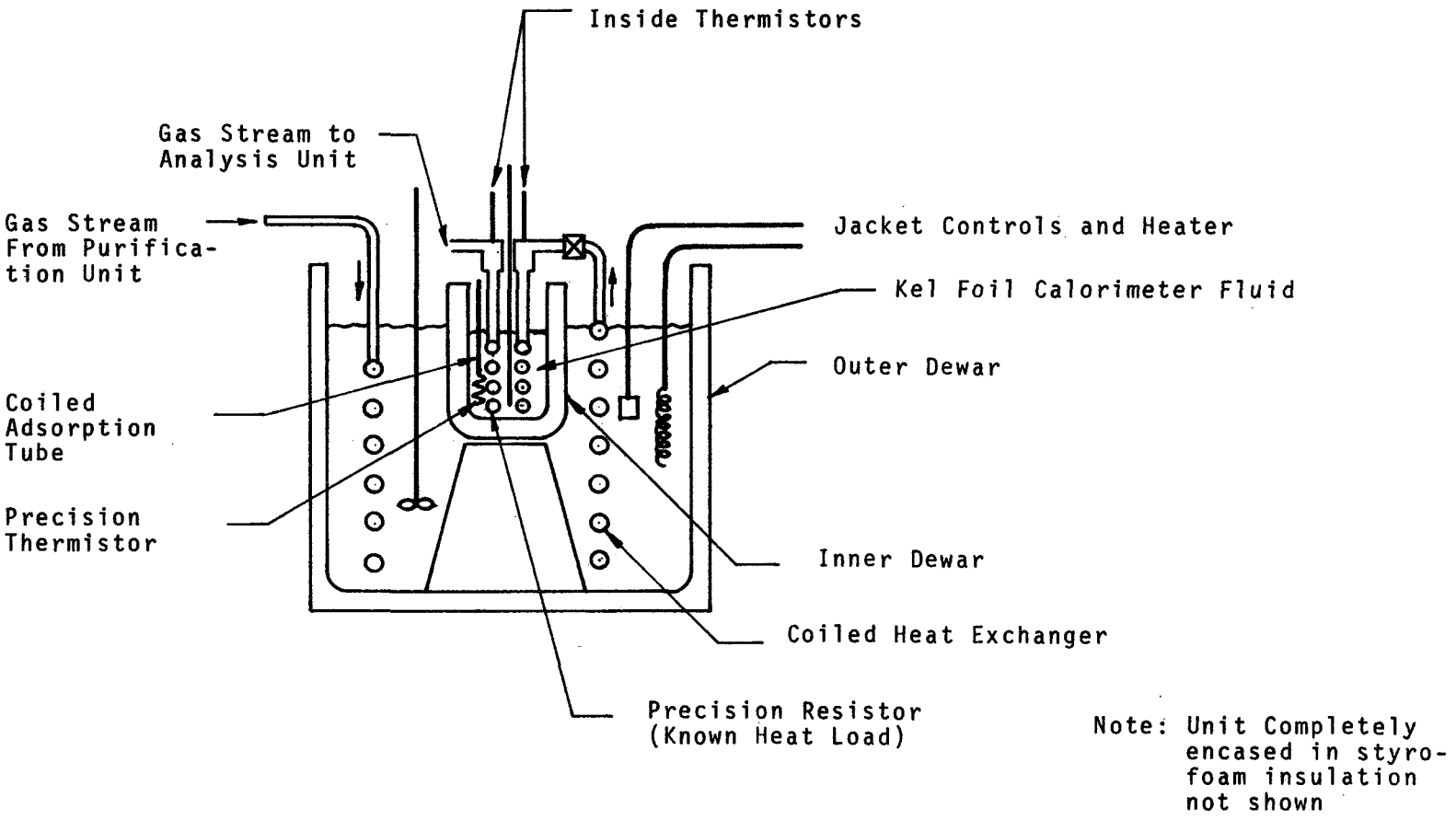

Figure 38. Adsorption Calorimeter Design

nominal conditions of flow and adsorption, temperature differences of 1 to 2°C could be tolerated with <1% error in measured heat effects even if the corrections were not made.

The second problem, i.e., accurate temperature measurement, was approached by utilizing thermistors with a high temperature/resistance coefficient (in the temperature range of interest) coupled with a precision wheat-stone bridge circuit with a high impedance electrometer null indicator. Temperature differences (as indicated by a Beckman precision calorimeter mercury thermometer used for calibration) down to 0.01°C were easily measurable. A calibration curve over the range 47°C to 53°C was obtained with a standard deviation of 0.9%, indicating the inherent precision of the system. The measured slopes were -280 ohm/°C for the 50°C thermistor, and -187 ohm/°C for the 100°C thermistor.

On initial tests there were problems with excessive cooling and subsequent nonsteady temperatures in the inner calorimeter chamber. Experimentation indicated that the temperature excursions were directly related to room temperature variations.

The system was modified by enclosing the whole calorimeter assembly in an "air thermostat", consisting of a large Lucite box that surrounded the calorimeter. No provision for maintaining constant air temperature inside the box was necessary; the box simply shielded the calorimeter from room air currents. In addition, the top of the calorimeter assembly, including the "Christmas Tree" of piping and valves, was packed with glass wool to reduce heat transfer.

Tests with the modified system were quite satisfactory. Constant temperature was maintained overnight in both the outer jacket and the inner Dewar without a continual heat input to the inner Dewar as was necessary previously.

3. Results

Heat calibration curves were obtained on the complete system by admittance of a known amount of electrical energy to a wound Nichrome wire heater element immersed in the inner Dewar (Table XLIV). The linear least squares slope over the range 10 to 60 calories was 0.0065 °C/cal. The standard deviation of the measured points varied from 0.01°C at the low end (10 calories) to 0.05°C at the high end (60 calories). This precision was adequate.

Table XLIV

STANDARDIZATION OF CALORIMETER

Electrical Heat Input (cal)	ΔT (°C)					
	Run 1	Run 2	Run 3	Run 4	Run 5	Run 6
10	0.03	0.01	0.02	0.01	0.03	0.03
30	0.19	0.15	0.12	0.10	0.13	0.14
60	0.41	0.35	0.31	0.26	0.34	0.34

Average Values

at 10 cal, Q = 0.00183°C/cal
30 " Q = 0.00480°C/cal
60 " Q = 0.00553°C/cal

Data for adsorption on 1.00 g 13X molecular sieve utilizing an 80% N_2O_4 gas composition is compiled for both 50°C and 100°C in Table XLV. Actual runs are plotted in Figures 39 and 40. The molecular sieve had been preconditioned by heating overnight at 350°C in a dry argon stream, then exposed to 100% N_2O_4 with subsequent exposure to 200°C, at 29 in. vacuum. Between each run, the sieve was desorbed at 200°C, 29 in. vacuum for 2-3 hours to ensure a reproducible starting point that corresponds to the adsorption measurements made with the spring balance.

The data are reasonably consistent (except for two anomalously high results for the 100°C runs). Cooling/heating corrections were necessary, as indicated.

The data reportedly in a previous section for adsorption at 80% gas composition at the two temperature were:

50°C - 0.115 g NO_2/g sieve

100°C - 0.069 g NO_2/g sieve

Using these values, the average heat of adsorption measured in these runs calculates to be:

50°C - 1009 cal/g NO_2 adsorbed

100°C - 1323 cal/g NO_2 adsorbed

Grand Average = 1180 cal/g NO_2 adsorbed
(all runs)

4. Discussion

The heats of adsorption of nitrogen oxides on 13X sieve as found here amount to about 1000 calories/gram or 46 kcal/gram-mole of NO_2. These values are exceptionally high and invite comparison with data reported for other sorbates on 13X sieve. Considerable information has been reported by A. V. Kiselev and R. M. Barrer (ref. 22) and by others (ref. 23). Very high heats of adsorption on molecular sieves would be expected to occur when the isotherm shows a sharp rise to saturation at low values of P/P_O, as occurs here. For comparison to other systems, it is useful to consider (1) the ratio of the heat of adsorption to the heat of vaporization of the sorbate by itself and (2) the heat of adsorption on 13X sieve as reported for other species. There seem to be no other data for nitrogen oxides on any form of molecular sieve. However, the following comparisons can be made.

Table XLV

MEASURED HEAT EFFECTS FOR ADSORPTION OF N_2O_4 ON 13X MOLECULAR SIEVE

Conditions: 80% N_2O_4 gas composition
1.00 g 13X Molecular Sieve

Run No.	Temp. (Start) (°C)	Heating Correction (°C/min)	ΔT_{meas} (°C)	Time (min)	ΔT_{corr} (°C)	Q_{ads} (cal)
1	48.00	+0.048	0.90	2.0	0.80	123
2	48.00	+0.078	1.01	1.8	0.87	134
3	48.00	+0.045	0.71	1.3	0.65	100
4	48.00	+0.002	0.71	1.0	0.74	114
5	48.00	+0.022	0.74	1.5	0.71	109
6	98.10	-0.024	0.85	4.0	0.95	146
7	98.10	-0.044	0.25	2.5	0.36	55
8	99.30	+0.014	0.94	5.0	0.87	134
9	98.99	-0.020	0.31	1.0	0.33	51
10	98.10	-0.060	0.31	1.0	0.37	57
11	98.32	-0.060	0.27	1.0	0.33	51

Average Values for Qads

50°C - 116 calories
100°C - 82 calories

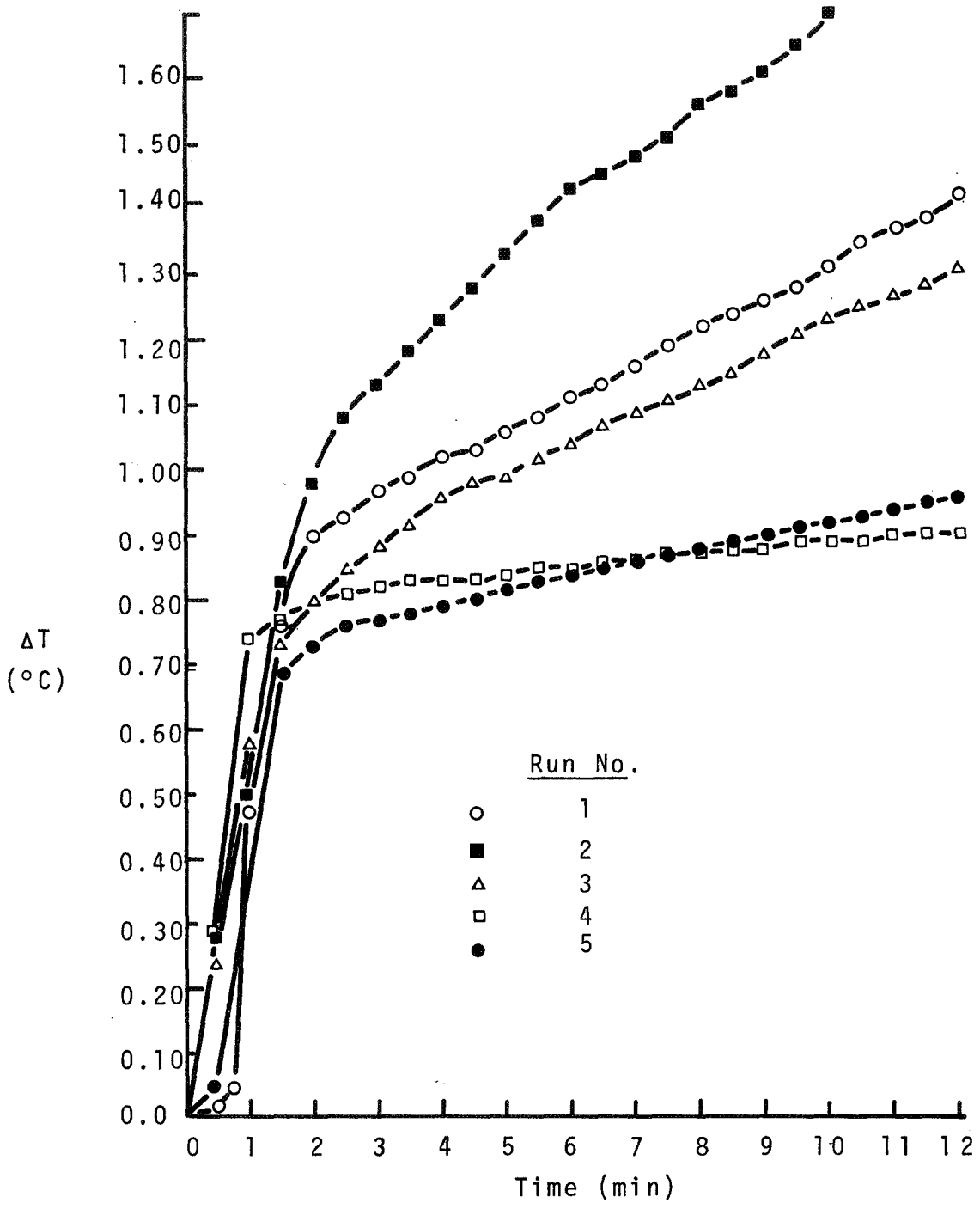

Figure 39. 50°C Calorimetry Runs

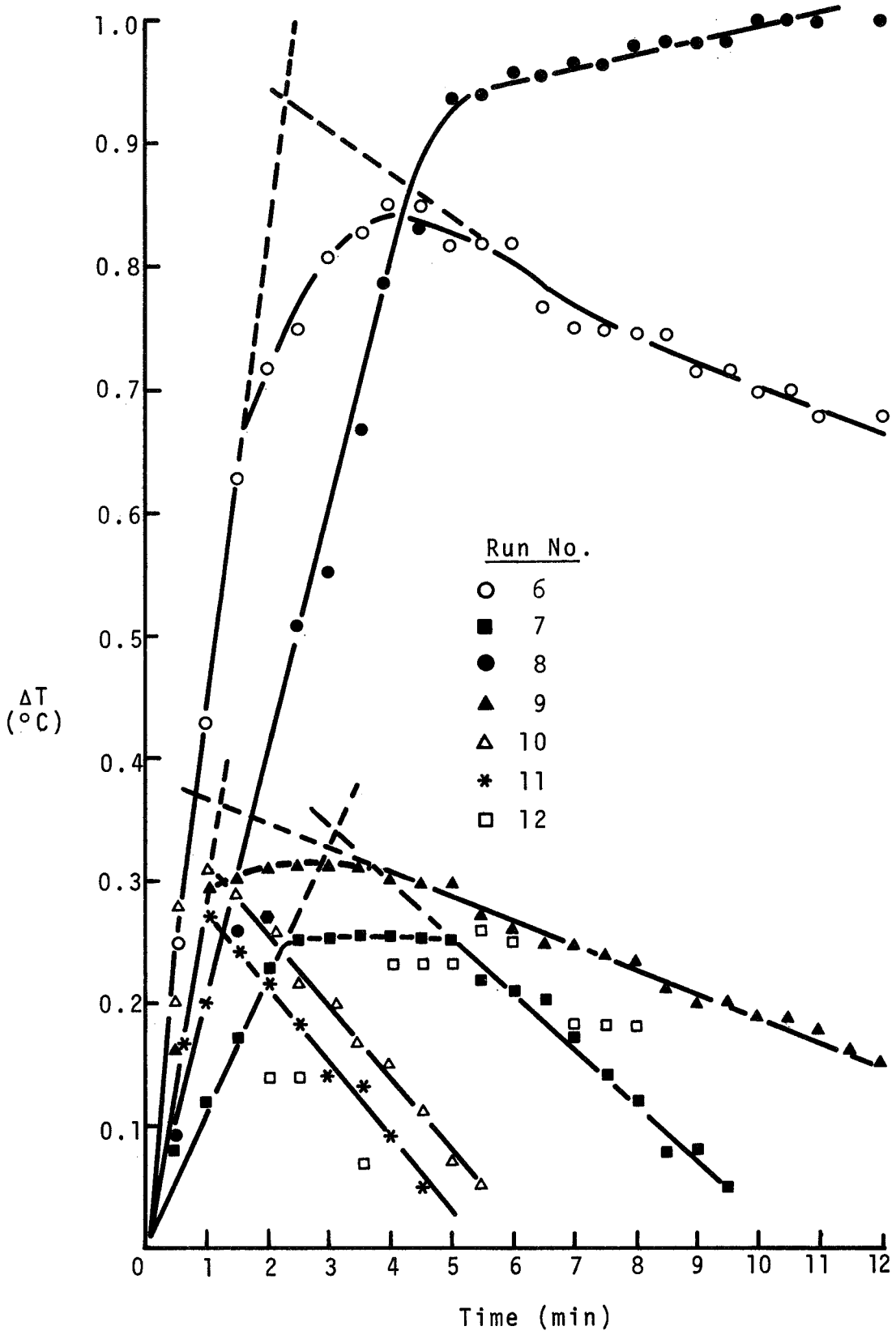

Figure 40. 100°C Calorimetry Runs

The heat of adsorption of NO_2 is about 10 times the heat of vaporization, which is about 4.5 kcal/mole NO_2. For carbon dioxide on the Na-X form of faujasite molecular sieve, the integral heat of adsorption is about 11.2 kcal/mole, which is about four times the heat of vaporization of liquid CO_2 at 30°C. The heat of adsorption of water vapor on Na-X sieve has an integral value of about 1 kcal/gram, which is approximately double the heat of vaporization of water as such. For methyl nitrate the integral heat of adsorption is about 18 kcal/mole compared to a heat of vaporization of about 9.1 kcal/gram-mole. For adsorption of ammonia on Na-X, the integral heat of adsorption is about 13 kcal/mole or about 750 calories/gram and this amounts to about 2.5 times the heat of vaporization.

On the basis of ratio of heat of adsorption to heat of vaporization, no other system comes close to the values found here. However, on the basis of heat of adsorption expressed as calories/gram, the value for nitrogen oxides is comparable to that of water and of ammonia. Molecules having a high permanent electric moment, e.g., a high dipole moment or high quadruple moment, such as water, ammonia, and nitrogen oxides, would be expected to have a high heat of adsorption on molecular sieves. A further contributing effect may be associated with the fact that the gas mixture consists of both NO_2 and N_2O_4 molecules. The 13X sieve consists of cavities, about 20 or so angstroms in diameter, interconnected by portholes of approximately 8 to 10 angstroms in diameter. In view of these very narrow passageways, it is possible that the NO_2 molecules diffuse into the sieve much more rapidly than do the N_2O_4 molecules, and then react in the large cavities to form N_2O_4. The heat of formation of N_2O_4 from NO_2 is 10.204 kcal/mole and this effect, if indeed it occurs, could also contribute to the effective heat of adsorption.

VII. REFERENCES

1. J. O. Smith, et al., "Study of Fuel Cells Using Storable Rocket Propellants," Final Report, Contract NAS3-2791, 11 May 1964.

2. J. C. Orth, et al., "Study of Fuel Cells Using Storable Rocket Propellants," Final Report, Contract NAS3-4175, NASA CR-54640, 9 March 1965.

3. (a) R. F. Drake, et al., "Study of Fuel Cells Using Storable Rocket Propellants," Quarterly Report No. 1, Contract NAS3-6476, NASA CR-54428, 20 July 1965.

   (b) *Ibid*, Quarterly Report, No. 2, NASA CR-54742, 29 October 1965.

   (c) *Ibid*, Quarterly Report No.3, NASA CR-54875, 15 March 1966.

   (d) *Ibid*, Quarterly Report No.4, NASA CR-54921, 27 April 1966.

   (e) *Ibid*, Quarterly Report No.5, NASA CR-54988, 19 July 1966.

4. N. P. Keier, G. K. Boreskov, V. V. Rode, A. P. Terent'ev, and E. G. Rukhadze, "Catalytic Activity of Organic Emiconductors," *Kinetika i Kataliz*, 2:4, 509 (1961).

5. A. P. Terent'ev, Y. G. Rukhadze, and V. V. Rode, *Vysokomolekulyarnye Soyedineniya*, 4:6, 821 (1962).

6. H. L. Klopping and G.J.M. Vander Kerk, *Rec Trav chim*, 70, 941-961 (1951).

7. J. C. Orth, "Research to Improve Electrochemical Catalysts," Final Report, Contract DA-49-186-AMC-166(S), USAERDL, Fort Belvoir, Va., 15 November 1965.

8. K. A. Kobe and R. E. Pennington, "Thermochemistry for the Petrochemical Industry," Part XII, *Petrol. Refiner* 29:7 (1950).

9. L. L. Wikstrom and K. Nobe, "Catalytic Decomposition of Nitrogen Dioxide," *Ind. Eng. Chem., Process Design Develop.*, 4:2, 191 (1956).

10. S. Souriraian and J. L. Blumenthal, "Catalytic Decomposition of Nitric Oxide Present in Low Concentrations," *Actes Du Deuxieme Congres International De Catalyse, Tome II, Technip*, Paris (1960).

11. F. Kaufman and J. R. Kelso, "Thermal Decomposition of Nitric Oxide," *J. Chem. Phys.*, 23:9, 1702 (1955).

12. J. M. Fraser, F. Daniels, "The Heterogeneous Decomposition of Nitric Oxide with Oxide Catalysts," *J. Phys. Chem.*, 62, 215 (1958).

13. J. C. Treacy and F. Daniels, "Kinetic Study of Oxidation of Nitric Oxide with Oxygen in the Pressure Range 1 to 20 mm," *J. Amer. Chem. Soc.*, 77:8, 2033 (1955).

14. M. S. Peters and J. L. Holman, "Vapor and Liquid Phase Reactions Between Nitrogen Dioxide and Water," *Ind. Eng. Chem.*, 47:12, 2536 (1955).

15. F. Fiegl, *J. Chem. Ed.*, March 1943, 139 (1943).

16. K. J. Vetter, "Electrochemical Kinetics. Theoretical and Experimental Aspects," Academic Press, N.Y. (1967) p. 490.

17. R. R. Liberta, Titan II Handbook, Bell Aerosystems Co., Contract AF04(694)-72, Report 8192-933004, March 1962.

18. T. Vermeulen, "Separation by Adsorption Methods," in *Advances in Chemical Engineering*, Vol 2, Academic Press, N.Y. (1958).

19. K. Denbigh, *Chemical Reactor Theory*, Cambridge University Press (1965).

20. M. C. Sneed and R. C. Brasted, *Comprehensive Inorganic Chemistry*, Vol V, D. van Nostrand, (1956) p.83.

21. Gmelin, *Handbuch der Anorganische Chemie*, 8, Teil 4, p. 789-790.

22. A. U. Kiselev, R. M. Barrer, in Molecular Sieves, a symposium, Society of Chemical Industry, London, 1968.

23. C. K. Hersh, Molecular Sieves, Reinhold Publishing Corp., New York (1961).

APPENDIX I

LIQUID PHASE DECOMPOSITION OF ANHYDROUS N_2H_4

The hydrazine decomposition unit described in Section IIIB was modified for the 1000-hour run with a higher hydrazine feed rate of 19.7 g per hour. A new reactor of 1 in. I.D. and 16 in. long was constructed and a new liquid reservoir was installed. The catalyst used was a chopped up MRD laminate membrane made by applying a layer of Englehard rhodium black catalyst on Monsanto Research Coporation standard carbon-PTFE substrate by a proprietary procedure.

The hydrazine feed rate for the decomposer and the decomposer dimensions were calculated from our previous data with the following assumptions:

Fuel cell power output	= 24 watts
Fuel cell voltage	= 0.9 volt
Fuel cell efficiency	= 95%
Decomposer efficiency	= 50%
Diffuser efficiency	= 85%

Under these conditions the required hydrazine feed rate is 19.7 g per hour.

Test runs revealed that it was difficult to maintain a steady hydrazine flow rate because gas was slowly generated inside the feed pump. The formation of gas in the feeding system was due to the slight decomposition of hydrazine by stainless steel 316. For this reason, the pump was dismantled and all parts made of stainless steel 316 were replaced with parts of stainless steel 304. After this was done, the unit was started up again. The pressure in the system was found to be slowly dropping whenever the pump was not in operation. This indicated leakage in the check valves of the pump. These parts were also replaced.

The modified reactor was operated successfully and most of the metering pump problems apparently were solved.

It was planned to start the tests with an H_2O moderator for the reaction to prevent excessive reaction and damaging heat effects as had been noticed previously. The H_2O content of the stream was to be gradually reduced.

The effects of hydrazine/H_2O feed composition and feed rate on hydrogen production efficiency were studied. Illustrative results are shown in Table XLVI. The H_2 efficiency is calculated from the N_2H_4 content of the feed stream assuming the reaction:

$$N_2H_4 \rightarrow N_2 + 2H_2$$

The results are discouraging: our minimum goal of 50% efficiency was obtained only at the lowest feed rate and, within the limits of these data, feed stock composition has little effect on the situation. It should be noted that between runs 1 and 2 a sudden pressure buildup in the reactor caused a rupture disc to blow, with the apparent effect that the efficiency of the reactor was cut approximately in half. If the over-pressure was caused by an initial "run-away" reaction with consequent local high temperature transients, it is apparent that the new start up procedures (N_2 flush, H_2O saturation at start) have not been successful.

Table XLVI

N_2H_4 DECOMPOSITION REACTOR DATA

Reactor Size: 12.6 $in.^3$ internal volume
Temperature for all runs: 30 ± 1°C
Catalyst: 19.2g total Rh metal, carbon-Teflon support

Run No.	Feed Composition, Wt-% N_2H_4/Wt-% H_2O	Average Total Feed Rate ml/hr	Duration of Measured Run hr	Measured Gas Production Rate SCFH	Theoretical Gas Production Rate for 100% Decomposition SCFH[1]	Hydrogen Efficiency % of Theory
1	75/25	26.0	5	0.65	1.60	40[2]
2	75/25	19.5	2 1/2	0.30	1.18	26
3	75/25	10.0	10 1/2	0.32	0.61	52
4	85/15	19.0	4 1/2	0.36	1.30	28

[1] Based on $N_2H_4 \rightarrow N_2 + 2\ H_2$
[2] Rupture disc blown

APPENDIX II

DESIGN OF N_2O_4 SCRUBBER SYSTEMS

A. BASIC SYSTEM CONSIDERATIONS

In the systems detailed here, a delay chamber has been included in the reactor product stream. This delay chamber receives the product stream at 100°C from the heat exchanger and is sized to provide sufficient time for the unreacted NO to combine with oxygen before passing into the adsorbers.

Two of the systems for which heat and material balances were calculated use two adsorber chambers, one of which is being heated and vented to space vacuum, while the other is adsorbing N_2O_4 from the reactor product stream. The third system calculated uses three adsorber chambers, one of which is being heated and vented to space vacuum, while the other two are adsorbing. In all three systems, sufficient heating and cooling capacity was available in the feed and product streams to heat and cool the adsorber chambers during the desorption part of the cycle. All calculations were based on a 90% efficient, 2 kW fuel cell oxygen requirement and 80% efficiency in the N_2O_4 reactor.

Estimates were made for the adsorber container weight and the heat exchanger weight which would be required in each container. These are noted in separate calculations.

The schematic of the system operation for two adsorber chambers is given in Figure 41. The three adsorber chamber system is shown in Figure 42.

B. CALCULATION DETAILS

1. Thermodynamic Constants

Component	Heat Capacity Cal/gm/°C
Stainless Steel	0.12
13X Molecular Sieve	0.20 (est)
N_2O_4 Vapor	0.23
Product Stream from Reactor	8 Cal/g mole/°C
ΔH_{vap} N_2O_4	99 Cal/g

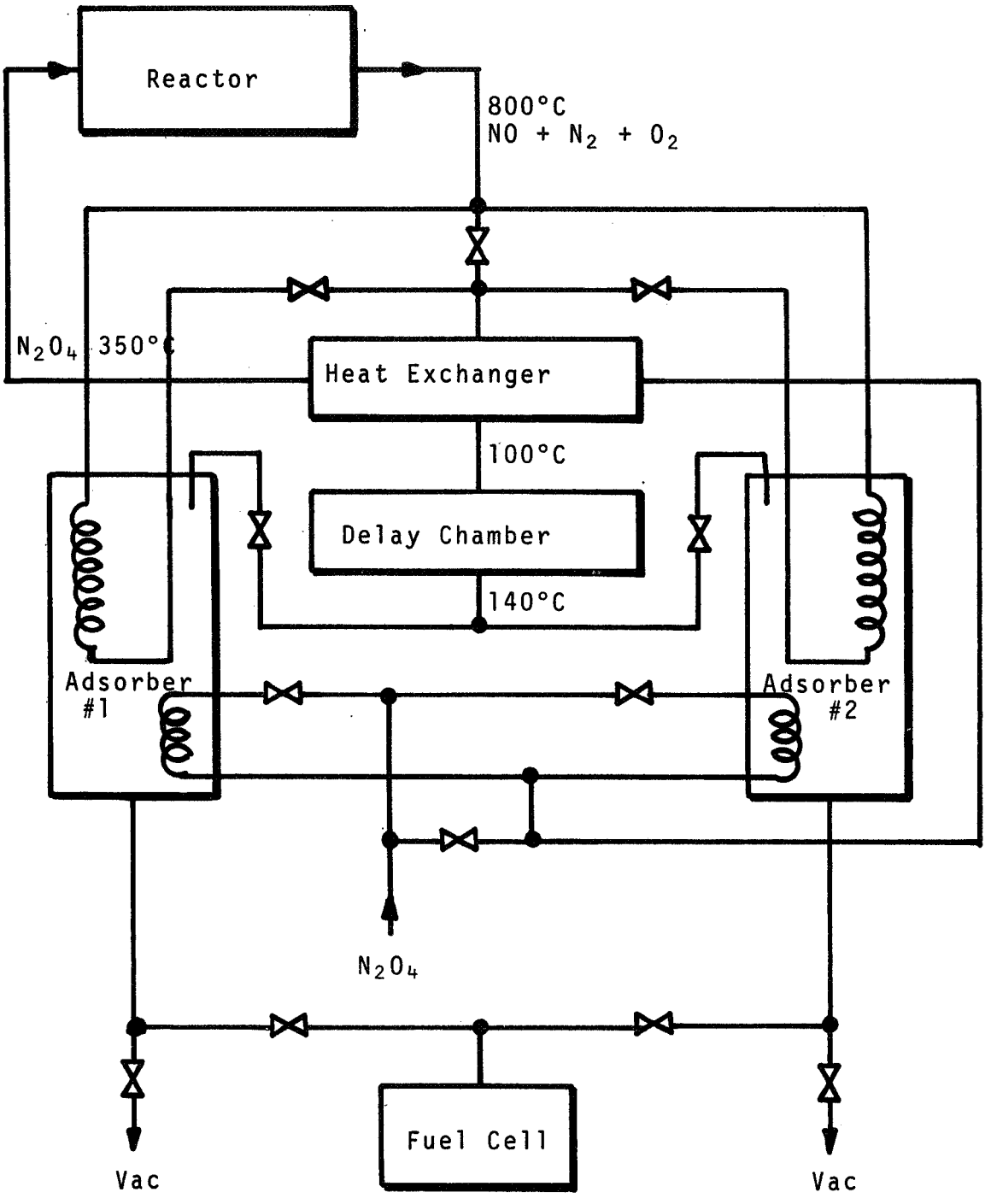

Figure 41. Two Column Adsorber with Delay Chamber.

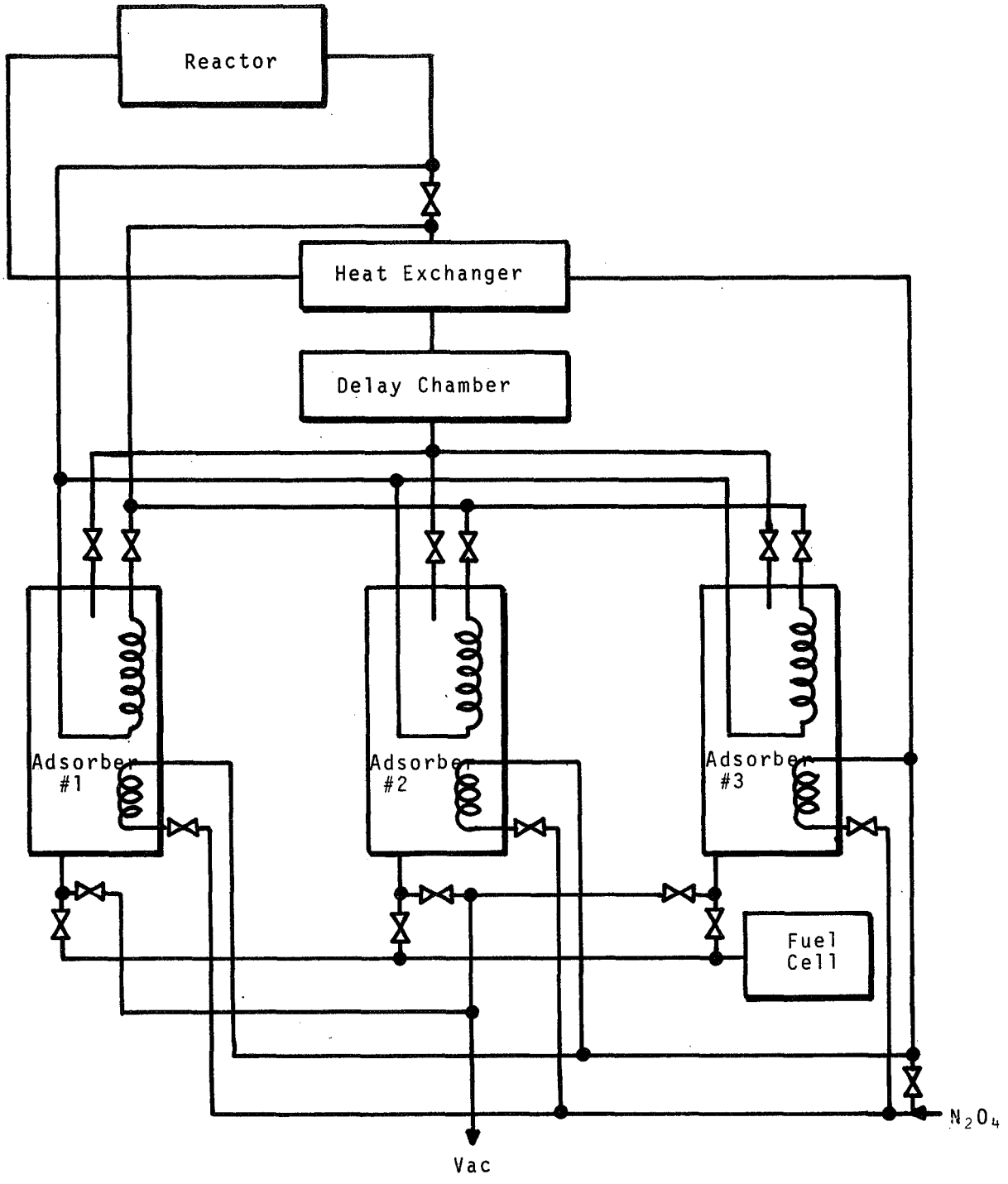

Figure 42. Three Column System

2. System I: Two Columns with Delay Chamber

Column Structure 1.2 lb stainless/lb sieve
Adsorbed State 0.20 lb N_2O_4/lb sieve or g/g
Desorbed State 0.12 lb N_2O_4/lb sieve or g/g
C_p sieve = 0.2 + 1.2(.12) + (.2 x .23) + 0.38 Cal/g/°C

ΔH Desorb

desorb 0.08 g N_2O_4/g sieve
0.08 g x 99 Cal/g N_2O_4 = 7.95 Cal

$$\Delta T = \frac{7.9 \text{ Cal/g sieve}}{0.38 \text{ Cal/g/°C}} = 21°C$$

Adsorb Temp 70°C - Desorb Temp 91°C

Desorption Time (from 0.2g/g to 0.12 g/g
Start desorb at 91°C

$$T_{desorb} = \frac{0.08}{(10-2)x10-3} \ln \frac{10}{2} = 16.1 \text{ min}^*$$

Desorb Preheat (1 lb basis)
Q = 0.38 Cal/gm/°C x 453 x 21°C = 3620 Cal/lb

Reactor Product Stream Heat Content

ΔH = 36.8 moles/hr x 8 Cal/g mole ΔT = Cal/hr

Assume ΔT = 700°C

36.8 x 8 x 700 = 206,000 Cal/hr

$$\frac{206,000}{60} = 3434 \text{ Cal/min}$$

Preheat Time

$$T_{ph} = \frac{453 \text{ x } 0.1 \text{ x } 99 \text{ Cal/g}}{3434} = 1.3 \text{ min/lb sieve}$$

---

* from data, Monthly Report No. 14, p.8

Desorb Time

$$\text{lb sieve} = 16.1 + (1.3 \times \text{lb sieve}) \times \frac{(0.6 \text{ lb } N_2O_4/1\mu)}{60 \times 0.8} = 2.86$$

$$T_{desorb} = 16.1 + (1.3 \times 2.86) = 22.9 \text{ minutes}$$

Column Weights

Sieve	3.0 lb
Stainless Container	3.6 lb
Heat Exchanger	0.5 lb

Heat Required for Heat Up of Columns

$$Q = (3 \times 0.2 \times 453 + (4.1 \times 0.12 \times 453) + (0.2 \times 3 \times 453 \times .23)\ \Delta T$$

$$Q = 11{,}700 \text{ Cal}$$

The columns are heated from the reactor product stream.

Reactor Product Stream Heat Content

$$Q = (800\text{-To} \times 36.8 \times 8.0(\frac{T}{60}) = 11{,}700 \text{ Cal}$$

Assume product stream cooled to 250°C coming out of adsorber
$\Delta T = 550°C$

Heat Up Time

$$T = \frac{11{,}700}{162{,}000 \times 60} = 4.25 \text{ minutes}$$

Desorption Cooling

Heat removed on desorption

$$3 \times 0.08 \times 453 \times 99 \text{ Cal/g } N_2O_4 = 10{,}700 \text{ Cal}$$

$$\Delta H \text{ cool} = 11{,}700 \left(\frac{91 - T_f}{91 - 70}\right) = 10{,}700$$

Final Temp - T_f = 72.8°C

Some cooling will be required using N_2O_4 to bring the column back to 70°C before the adsorb cycle starts and to hold the column temperature during the adsorption part of the cycle. The adsorber column feed temperature is 140°C, from the delay chamber. The

40°C rise is a result of the reaction $NO + O_2 \rightarrow NO_2$.

Cycle Time		(min)
desorption	-	23
heat up	-	4.5
cycle		27.5 min

3. System II: Two Columns, Fast Cycle

This system differs from the first one in that a smaller amount of N_2O_4 is adsorbed on each cycle and the desorption rate is much higher than that found earlier*.

Adsorbed state - 0.20 lb N_2O_4/lb sieve or (g/g)
Desorbed State - 0.15 lb N_2O_4/lb sieve or (g/g)
Approx. C_p of Column = 0.38 Cal/g/°C

ΔH Desorb

0.05 g N_2O_4/gm sieve x 99 Cal/g = 4.95 Cal/g sieve

ΔT Desorb

$$\frac{4.95 \text{ Cal/g}}{0.38 \text{ Cal/g/°C}} = 13°C$$

Desorption Time

desorp from 0.20 to 0.15 g N_2O_4/g sieve
start desorb at 91°C

$$T_{desorb} = \frac{0.05}{(10-5) \times 10^{-3}} 1\mu \frac{10}{5} = 6.94 \text{ min}^*$$

Desorber Preheat (1 lb bases)

Cp = 0.38 cal/g/°C (adsorber)

Q = (0.38)(453)(13°C) = 2220 Cal/lb

---

* Figure 2, Monthly Report No.14

Some cooling is required to complete the cycle:

Cycle time -	Desorption	6.9 min
	Heat Up	1.2 min
	Total	8.1 min

4. System III: Three Columns

This system uses three adsorber chambers and is shown in Figure 42. The same assumptions are made for this system as for the previous two systems except as noted in the calculations.

Adsorber Heat Up Requirements

$$C_p = 0.38 \text{ Cal/g/°C}$$

Product Stream Heating Value

$$Q = \frac{36.8 \times 8 \times \Delta T/\text{min}}{60}$$

Assuming $\Delta T = 600°C$
$Q = 2950$ Cal/min

Basis 1 lb adsorber
Temperature rise

$$0.38 \text{ Cal/mg} \times 453 \times \Delta T = 2950 \text{ Cal/min}$$
$$\Delta T = 17.2°C/\text{min}$$

Assume adsorbers can be cooled at 35°C for adsorb and heated to 100°C for desorb

$$\Delta T = 65°C$$

$$T_{heat} = \frac{65°C}{17.2°C/\text{min/lb}} = 3.78 \text{ minutes/lb sieve}$$

Desorption Time

$$T_{desorb} = \frac{0.07}{(16-8) \times 10^{-3}} \times \text{ln} \frac{16}{8} = 6.05 \text{ minutes}^*$$

N_2O_4 in Product Stream

$$\frac{0.6 \text{ lb/lb}}{60} = 0.01 \text{ lb } N_2O_4/\text{min}$$

* Data, Monthly Report No.14, p.8

Reactor Product Stream Heat Content

Assume cooling to 100°C - ΔT = 700°C

$$\Delta H = \frac{36.8 \text{ moles/l}\mu \times 8 \text{ cal/g mole}}{60} = 3434 \text{ cal/min}$$

Preheat Time

$$T_{ph} = \frac{2220}{3434} = 0.65 \text{ min/lb sieve}$$

Desorb Time

$$\text{lb sieve} = [6.94 + 0.65 \text{ (lb sieve)}]\left(\frac{0.6\#N_2O_4/l\mu}{60 \times 0.05 \text{ g/g}}\right)$$

lb sieve = 1.62

$$T_{desorb} = 6.94 + 0.65 \text{ (1.62 lb sieve)}$$

$$T_{desorb} = 7.99 \text{ minutes}$$

Adsorber container approximately 2.0 lb s.s.
Heat exchanger " 2.5 lb s.s.

Heat Required for Heat Up

$$Q = (1.6 \text{ lb sieve} \times 0.2 \text{ cal/g} \times 453) + (2.5 \times 453 \times 0.12) + (0.2 \times 1.6 \times 453 \times 0.23)\ \Delta T$$

$$Q = (314)\ 13°C = 4080 \text{ Cal}$$

Heating time from reactor product stream

$$T_{heating} = \frac{4080 \text{ Cal}}{3434 \text{ Cal/min}} = 1.19 \text{ minutes}$$

Desorption Cooling

Heat removed on desorption

1.6 lb sieve x 0.05 lb N_2O_4 x 453 x 99 Cal/g (N_2O_4) - 3590 Cal

Final Temperature

$$4080\ \frac{91 - T_f}{91 - 78} = 3590$$

$$T_f = 80°C$$

Sieve loading in adsorbed state 0.07 lb N_2O_4/lb

Assume: 1.20 lb sieve/unit
1.44 lb s.s./unit
2.64 lb Total

$T_{heat\ up}$ = 2.64 lb x 3.78 min/lb = 10.0 min
T_{desorb} = = 6.1 min
16.1 min

The two sieves on the adsorb cycle contain 1.8 lb molecular sieve.

The 2.4 lb sieve in two adsorbers has the capacity for 16.8 min adsorption on product stream.

The adsorption rate data used in these calculations were obtained using tubular absorbers where the path length to the vacuum was much longer than optimum. The configuration suggested for highest desorption rates is a cylinder with a porous tube up the center through which the desorption takes place. This type of design could make the desorption path length very short.

The heat exchanger estimates were conservative, but no attention was given to possible scale formation or other difficulties which may occur at 800°C.